

INFORMATION TO USERS

This manuscript has been reproduced from the microfilm master. UMI films the text directly from the original or copy submitted. Thus, some thesis and dissertation copies are in typewriter face, while others may be from any type of computer printer.

The quality of this reproduction is dependent upon the quality of the copy submitted. Broken or indistinct print, colored or poor quality illustrations and photographs, print bleedthrough, substandard margins, and improper alignment can adversely affect reproduction.

In the unlikely event that the author did not send UMI a complete manuscript and there are missing pages, these will be noted. Also, if unauthorized copyright material had to be removed, a note will indicate the deletion.

Oversize materials (e.g., maps, drawings, charts) are reproduced by sectioning the original, beginning at the upper left-hand corner and continuing from left to right in equal sections with small overlaps.

Photographs included in the original manuscript have been reproduced xerographically in this copy. Higher quality 6" x 9" black and white photographic prints are available for any photographs or illustrations appearing in this copy for an additional charge. Contact UMI directly to order.

ProQuest Information and Learning
300 North Zeeb Road, Ann Arbor, MI 48106-1346 USA
800-521-0600

UMI[®]

UNIVERSITY OF ALBERTA

**The Structure and Composition of an Electroplated Gold-Tin Solder
Alloy Co-deposited by Pulse Plating from Solutions Containing
Ethylenediamine as a Stabilizer.**

by

Jacobus Cornelis Doesburg



A thesis submitted to the Faculty of Graduate Studies and Research in partial fulfillment
of the requirement for the degree of Master of Science

in

MATERIALS ENGINEERING

DEPARTMENT OF CHEMICAL AND MATERIALS ENGINEERING

Edmonton, Alberta

Spring, 2000



National Library
of Canada

Acquisitions and
Bibliographic Services

395 Wellington Street
Ottawa ON K1A 0N4
Canada

Bibliothèque nationale
du Canada

Acquisitions et
services bibliographiques

395, rue Wellington
Ottawa ON K1A 0N4
Canada

Your file *Votre référence*

Our file *Notre référence*

The author has granted a non-exclusive licence allowing the National Library of Canada to reproduce, loan, distribute or sell copies of this thesis in microform, paper or electronic formats.

The author retains ownership of the copyright in this thesis. Neither the thesis nor substantial extracts from it may be printed or otherwise reproduced without the author's permission.

L'auteur a accordé une licence non exclusive permettant à la Bibliothèque nationale du Canada de reproduire, prêter, distribuer ou vendre des copies de cette thèse sous la forme de microfiche/film, de reproduction sur papier ou sur format électronique.

L'auteur conserve la propriété du droit d'auteur qui protège cette thèse. Ni la thèse ni des extraits substantiels de celle-ci ne doivent être imprimés ou autrement reproduits sans son autorisation.

0-612-60116-1

Canada


UNIVERSITY OF ALBERTA

LIBRARY RELEASE FORM

NAME OF AUTHOR: **Jacobus Cornelis Doesburg**
TITLE OF THESIS: **The Structure and Composition of an Electroplated Gold-Tin Solder Alloy Co-deposited by Pulse Plating from Solutions Containing Ethylenediamine as a Stabilizer**
DEGREE: **Master of Science**
YEAR THIS DEGREE GRANTED: **2000**

Permission is hereby granted to the University of Alberta Library to reproduce single copies of this thesis and to lend or sell such copies for private, scholarly or scientific research purposes only.

The author reserves all other publication and other rights in association with the copyright in the thesis, and except as herein before provided, neither the thesis nor any substantial portion thereof may be printed or otherwise reproduced in any material form whatever without the author's prior written permission.


Jacobus Cornelis Doesburg

11034-129 St.
Edmonton, Alberta
T5M - 0Y3

Date: Feb 22/2000


UNIVERSITY OF ALBERTA

FACULTY OF GRADUATE STUDIES AND RESEARCH

The undersigned certify that they have read, and recommend to the Faculty of Graduate Studies and Research for acceptance, a thesis entitled **The Structure and Composition of an Electroplated Gold-Tin Solder Alloy Co-deposited by Pulse Plating from Solutions Containing Ethylenediamine as a Stabilizer** submitted by Jacobus Cornelis Doesburg in partial fulfillment of the requirements for the degree of Master of Science in Materials Engineering.




Dr. M. L. Wayman, Examining Committee Chairman



Dr. D. G. Ivey, Supervisor



Dr. J. Luo, Examining Committee Member



Dr. R. P. W. Lawson, External Examining Committee Member

Date: Feb. 17, 2000

Abstract

Au-30at.%Sn eutectic solder is used in optoelectronic applications, particularly to join InP devices to the submount. The solder can be applied using solder preforms, paste, electron-beam evaporation or electrodeposition. Co-deposition of the solder by electroplating offers advantages over the other methods as a simple, cost effective technique. In this study, pulsed current electrodeposits were formed using a solution based on: 200 g/l ammonium citrate, 5 g/l KAuCl_4 , 2-5 g/l $\text{SnCl}_2 \cdot 2\text{H}_2\text{O}$, 60 g/l sodium sulfite, 15 g/l L-ascorbic acid, and 0.01-0.11M ethylenediamine.

The effects of changing the ethylenediamine and $\text{SnCl}_2 \cdot 2\text{H}_2\text{O}$ concentrations on the structure of the deposits were observed using scanning electron microscopy and x-ray diffraction. Increasing the ethylenediamine concentration in the Au/Sn plating solution results in increased solution stability, an increased deposition rate, and a coarser grain structure. Decreasing the Sn content in the solution leads to a lower Sn content in the resulting deposit and a coarser structure. Increasing the average current density during plating affects the homogeneity of the structure in the electroplated deposit, with a loss of preferred orientation.

Acknowledgments

Firstly, I would like to thank Dr. Doug Ivey for his supervision and immeasurable guidance over the past two and a half years, in addition to letting me satisfy my constant urge to travel while working on my thesis. I have never learned as much from one person about fairness, respect and hard work.

I also wish to thank my family and friends who always seem to be there at the right time and the girls who made my life interesting, Wendy Benbow and Lesley Clements.

Special thanks go out to Heather Welling-Gauld for conducting stability tests and to Andrew Duncan for his x-ray diffraction work. Thanks to Tina Barker for teaching me how to operate a SEM, George Braybrook for the pretty SEM pictures, and Shiraz Merali for help with using the x-ray diffraction equipment.

I would also like to thank the other members of the research group for their help and support, Wenzhen Sun, Udit Sharma, Eric Tang, Barbara Djurfors, Cheryl Steer and Adebayo Badmos.

Finally, I wish to thank Nortel Networks and the Natural Science and Engineering Council of Canada for funding this project.

Table of Contents

1	Introduction.....	1
2	Au-Sn Solder Materials.....	3
2.1	Optoelectronic Packaging.	3
2.2	Solders Used for Optoelectronic Packaging.	6
2.3	Au-Sn Phase Diagram.	6
2.3.1	The δ (AuSn) Phase.	8
2.3.2	The ζ' (Au_5Sn) Phase.....	9
2.3.3	The ζ Phase.	9
2.3.4	The β Phase.....	9
2.3.5	The α -Au Phase.	9
2.4	Deposition Techniques for Au-30at.%Sn Solder.....	10
3	Electrodeposition of Alloys.	11
3.1	Basic Electroplating Theory.....	11
3.1.1	Current and Current Density.	14
3.1.2	Electrode Potential.	16
3.1.3	Polarization.	17
3.1.3.1	Activation Polarization.	17
3.1.3.2	Concentration Polarization.....	18
3.1.3.3	Ohmic Polarization.	19
3.1.4	Effects of Plating Chemicals.....	20

3.2	Alloy Plating.....	21
3.2.1	Brenner's Classification of Codeposition.....	22
3.2.2	Classification of Codeposition by Mixed Potential Theory.....	23
3.2.2.1	Non-interactive Codeposition.....	23
3.2.2.2	Charge Transfer Coupled Codeposition.....	25
3.2.2.3	Mass Transport Coupled Codeposition.....	25
3.3	Pulse Plating.....	25
3.4	Electrodeposition of Au-Sn Alloys.....	28
3.4.1	Cyanide Based Plating Systems.....	28
3.4.2	Non-cyanide Plating Systems.....	30
3.5	Use of Ethylenediamine in Electroplating.....	32
4	Structure of Electrodeposited Coatings.....	34
4.1	Electrodeposition Theory.....	34
4.2	Theory of Electrocrystallization.....	36
4.2.1	Role of Overpotential and Current Density.....	38
4.2.2	Inhibition.....	38
4.3	Structures of Electroplated Deposits.....	40
4.4	Structures of Alloy Plated Electrodeposits.....	43
5	Experimental Methods.....	44
5.1	Solution Preparation.....	44
5.2	Solution Stability.....	45
5.3	Polarization Experiments.....	46
5.4	Electroplating.....	46
5.5	Scanning Electron Microscope Analysis.....	48
5.5.1	Imaging and Thickness Measurements.....	48
5.5.2	Energy Dispersive X-ray Analysis.....	49
5.6	X-ray Diffraction.....	49

6	Results and Discussion.	50
6.1	Polarization Curves and Stability Tests.	50
6.1.1	Stability of Au-Sn Plating Solutions.	50
6.1.2	Polarization Curves for Au-Sn Plating Solutions.	53
6.2	Electroplating Tests.	57
6.2.1	Composition of Au-Sn Deposits.	57
6.2.2	Plating Rate and Current Efficiency.	63
6.3	Deposit Structure.	68
6.3.1	Effects of Varying Ethylenediamine Content.	69
6.3.2	Plating With Reverse Pulse.	80
6.3.3	Varying SnCl ₂ -2H ₂ O Concentration.	83
6.4	X-ray Diffraction.	87
6.5	Summary.	95
7	Conclusions and Recommendations for Future Research.	96
7.1	Conclusions.	96
7.2	Recommendations for Future Research.	97
7.2.1	Solution Development.	97
7.2.2	Deposit Composition and Structure.	98
7.2.3	Miscellaneous.	99
8	References.	100

List of Tables

Table 3-1	Selected Standard Electrode Potentials at 1 M, 25°C and 1 atm.	13
Table 3-2	Standard reduction potentials for selected reactions involving gold. [Stanley87]	21
Table 3-3	Overview of cyanide-based gold electroplating solutions. [Schlodder86]	29
Table 5-1	Mean concentrations and standard deviations for solution components...	45
Table 6-1	Components and compositions of solutions used in the experiments.	50
Table 6-2	Phases and orientation for deposits plated from solutions with varying ethylenediamine concentrations.	89
Table 6-3	Phases and orientation for deposits plated from solution 5 (0.01-0.02 M ethylenediamine) using forward pulse and forward + reverse pulse.....	91
Table 6-4	Phases and orientation for deposits plated from solutions with varying SnCl ₂ -2H ₂ O concentrations.	94

List of Figures

Figure 2-1	Schematic of the self-alignment technique. [Lee94].....	4
Figure 2-2	Four channel laser array positioned using the self-alignment joining technique. [Lee94]	5
Figure 2-3	Schematic of a laser array mounted on a waferboard (a) before, and (b) after the solder reflow process. [Lee94].....	5
Figure 2-4	The Au-Sn phase diagram. [Ciulik93]	7
Figure 2-5	The gold-rich portion of the Au-Sn phase diagram. [Ciulik93].....	8
Figure 3-1	Schematic of the electroplating process.....	14
Figure 3-2	Effects of different polarizations. [Bradford93]	20
Figure 3-3	Polarization diagrams showing situations where metal content in the deposition is related to the metal concentration in solution: (a) Tafel kinetics with equal slopes, (b) diffusion controlled deposition with both components at their limiting current densities. [Landolt94]	24
Figure 3-4	Schematic showing the pulsating diffusion layer.....	27
Figure 4-1	Schematic of electrodeposition: (a) hydrated metal ion in bulk solution, (b) hydrated metal ion enters diffusion layer, and (c) metal ion enters electric double layer. [Tan93].....	35
Figure 4-2	Discharge sites on a growing surface: (1) Surface vacancy, (2) Ledge Vacancy, (3) Ledge Kink, (4) Ledge, and (5) Layer nucleus. [Gabe78]... ..	37
Figure 4-3	Growth screw dislocation with a kinked growth ledge. [Gabe78].....	37
Figure 4-4	Different types of polycrystalline electrodeposits possible as a function of current density and inhibition. [Winand94]	42
Figure 5-1	Electroplating apparatus.....	47
Figure 5-2	Schematic of electroplating setup.	48
Figure 6-1	Solution stability versus ethylenediamine concentration.....	51
Figure 6-2	Polarization curves for solutions containing varying amounts of ethylenediamine and NiCl ₂	54

Figure 6-3	Polarization curves for solutions containing varying amounts of ethylenediamine.	56
Figure 6-4	Sn content vs. average current density for varying ethylenediamine and NiCl ₂ concentration.....	59
Figure 6-5	Sn content vs. average current density for an ethylenediamine concentration of 0.01-0.02 M (solution 5).	61
Figure 6-6	Sn content vs. average current density for varying ethylenediamine concentration.....	61
Figure 6-7	Sn content vs. average current density for varying SnCl ₂ -2H ₂ O concentration and an ethylenediamine concentration of 0.01-0.02 M.	62
Figure 6-8	Plating rate of solutions containing varying amounts of ethylenediamine and NiCl ₂	64
Figure 6-9	Plating rate of solutions containing varying amounts of ethylenediamine.	66
Figure 6-10	Plating rate of solutions containing varying amounts of ethylenediamine.	67
Figure 6-11	Plating rate of solutions containing varying SnCl ₂ -2H ₂ O concentrations and an ethylenediamine concentration of 0.01-0.02 M.....	68
Figure 6-12	SEM plan view images of samples plated from solutions containing no ethylenediamine. (solution 1).....	71
Figure 6-13	SEM cross section images of samples plated from solutions containing no ethylenediamine. (solution 1).....	72
Figure 6-14	SEM plan view images of samples plated from solutions containing 0.01-0.02 M ethylene diamine. (solution 5).....	73
Figure 6-15	SEM cross section images of samples plated from solutions containing 0.01-0.02 M ethylenediamine. (solution 5).....	74
Figure 6-16	SEM plan view images of samples plated from solutions containing 0.05-0.06 M ethylenediamine. (solution 6).....	75
Figure 6-17	SEM cross section images of samples plated from solutions containing 0.05 - 0.06 M ethylenediamine. (solution 6).....	76

Figure 6-18	SEM plan view images of samples plated from solutions containing 0.11 M ethylenediamine. (solution 3)	77
Figure 6-19	SEM cross section images of samples plated from solutions containing 0.11 M ethylenediamine. (solution 3)	78
Figure 6-20	SEM cross section images of samples plated at 2.4 mA/cm ² from solutions with varying ethylenediamine concentrations.....	79
Figure 6-21	SEM plan view images of samples plated from solutions containing 0.01-0.02 M ethylenediamine, 2.4 ms Forw., 0.4 ms Rev., 7.2 ms OFF. (solution 5).....	81
Figure 6-22	SEM cross section images of samples plated from solutions containing 0.01-0.02 M ethylenediamine, 2.4 ms Forw., 0.4 ms Rev., 7.2 ms OFF. (solution 5).....	82
Figure 6-23	SEM plan view images of samples plated from solutions containing 0.01-0.02 M ethylenediamine plated at 2.4 mA/cm ²	84
Figure 6-24	SEM cross section images of samples plated from solutions containing 0.01-0.02 M ethylenediamine plated at 2.4 mA/cm ²	86
Figure 6-25	Normalized intensity ratio of the AuSn phase versus current density for deposits electroplated from solutions with varying ethylenediamine content.....	90
Figure 6-26	Normalized intensity ratio of the AuSn phase versus current density for deposits electroplated from solution 5 (0.01-0.02 M ethylenediamine) using forward pulse and forward + reverse pulse.	92
Figure 6-27	Normalized intensity ratio of the AuSn phase versus current density for deposits electroplated from solutions with varying SnCl ₂ -2H ₂ O content. 93	

List of Symbols

a	- constant in Tafel equation.
a_c	- activity of depositing ion at the cathode.
a_b	- activity of depositing ion in the bulk solution.
A	- atomic weight.
C	- capacitance.
C_b	- bulk concentration of ions in solution.
D_i	- diffusion coefficient of the ions in solution.
E	- potential.
E_c	- electrochemical equivalent weight.
E_{rev}	- equilibrium potential of an ion in solution.
F	- Faraday's constant.
i_a	- exchange current density.
i_c	- current density.
i_C	- capacitive current in pulse plating.
i_F	- Faradic current in pulse plating.
i_L	- limiting current density.
i_{LP}	- pulse limiting current density.
I	- current.
m_a	- actual mass plated.
m_{th}	- theoretical mass of metal plated.
n	- number of electrons taking part in the reaction.
N_p	- number of x-ray counts including background.
N_{p-b}	- number of x-ray counts excluding background.
R	- gas constant.
R_f	- film resistance.
t	- time.
t_i	- transport number of the ions in solution.
T	- absolute temperature.

S_m	- throwing power.
x_a	- actual plated mass.
x_{th}	- theoretical mass of metal plated.
Z	- concentration as a fraction.
δ	- thickness of the diffusion layer.
δ_s	- thickness of stationary diffusion layer.
δ_p	- thickness of pulsating diffusion layer.
ΔG	- free energy.
η	- polarization.
η_a	- activation polarization.
η_c	- concentration polarization.
η_{cr}	- crystallization polarization.
η_r	- ohmic polarization.
ρ	- density.

1 Introduction

Au-30at.%Sn eutectic solder is used in optoelectronic applications, particularly to join InP devices to the submount in a flip-chip assembly. The submount is generally CVD diamond, and the solder serves the purpose of heat dissipation, mechanical support and electrical conduction. The most commonly used solders for bonding in electronic packaging are based on the Pb-Sn system. These alloys have low melting temperatures (183°C - 312°C), and are characterized by high creep rates and stress relaxation, as well as surface and microstructural changes. For optoelectronic devices, higher melting Au eutectic alloys are used, such as Au-Sn (278°C), Au-Ge (361°C) and Au-Si (364°C). The advantages of the higher melting solders include increased thermal stability and long term reliability. The Au-30at.%Sn solder has some advantages over the other Au based solders in that it has the highest strength, lowest elastic modulus and lowest melting temperature of this group of solders. The Au-Sn solder also has a high thermal conductivity compared to other solders, which makes it an attractive choice for packages which run hot, such as laser devices.

Au-30at.%Sn solder can be applied using solder preforms (20-50 μ m in thickness), paste, electron-beam evaporation or electrodeposition. Solder preforms are problematic for flip-chip applications due to alignment trouble and oxidation of the solder prior to bonding. Solder paste also suffers from oxidation prior to bonding, in addition to the possibility of solder contamination during bonding from the organic binder in the paste. Electron-beam evaporation and electrodeposition are advantageous for Au-Sn solder deposition in that the oxide formation prior to bonding can be reduced and the thickness and position of the solder can be closely controlled. The electrodeposition of Au-Sn solder has followed the method of plating Au and Sn layers sequentially from separate Au and Sn solutions. A slightly acidic solution for the co-deposition of Au-Sn solder composed of 200 g/l ammonium citrate, 5 g/l KAuCl₄, 5 g/l SnCl₂-2H₂O, 60 g/l sodium sulfite, 15 g/l L-ascorbic acid, and 1 g/l NiCl₂ for the co-deposition of Au-Sn solder has been developed. The electroplating solution developed for the co-deposition of Au and

Sn is slightly acidic so that it can be used in conjunction with alkaline-developable photoresists. It has been found that the addition of ethylenediamine to the solution resulted in an increase in solution stability.

This thesis studies the effects of the addition of ethylenediamine to the Au-Sn plating solution. The changes in solution stability, plating rate, composition and microstructure resulting from the addition of ethylenediamine are noted. The effects of changing the tin concentration in the solution on plating rate, composition and microstructure are also studied.

The thesis is organized into 8 chapters. Chapters 2-4 give background information relating to the work carried out in this project. The literature review starts with an introduction to the use of Au-Sn solder in optoelectronic packaging, followed by a review of the Au-Sn phase diagram. Next is a chapter on electroplating theory, with a focus on pulse plating and alloy plating, followed by a review of Au-Sn plating solutions as well as the use of ethylenediamine in gold plating. The last chapter in the literature review is about electrocrystallization theory and the resulting structures formed in electrodeposits.

Chapter 5 outlines the experimental method, followed by chapter 6, which describes the results obtained from the experiments. The results are grouped into four parts. The first section relates the ethylenediamine concentration in the solution to the solution stability. The second section studies the effects of ethylenediamine and $\text{SnCl}_2 \cdot 2\text{H}_2\text{O}$ concentration on the composition of the deposit and the plating rate. The next section shows the microstructures formed at various plating conditions while varying the ethylenediamine and $\text{SnCl}_2 \cdot 2\text{H}_2\text{O}$ concentrations. The last section is a x-ray diffraction study on the preferred orientation of the deposits formed under different plating conditions, ethylenediamine and $\text{SnCl}_2 \cdot 2\text{H}_2\text{O}$ concentrations. The results are then summarized and the appropriate conclusions are made, followed by some ideas for future work.

2 Au-Sn Solder Materials

One advantage of using solder to join optical devices is the ability to use the wetting characteristics of the solder to precisely align the devices. The Au-30at.%Sn solder is the preferred alloy for optoelectronic packaging because of its relatively low melting point, low elastic modulus, and high strength compared to other eutectic gold based alloys. There are numerous methods of depositing the solder prior to joining, with electrodeposition offering cost, speed and control advantages over other methods such as evaporation.

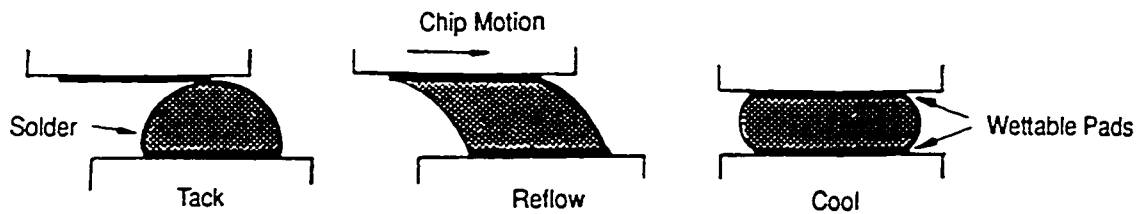
2.1 Optoelectronic Packaging

In optoelectronic packaging, optical fibres or waveguides must be attached to devices such as lasers, light-emitting diodes, or photodetectors. One of the major challenges in optoelectronic packaging is to connect the devices with precision and maintain the alignment during operation. [Lee94] The alignment of these assemblies is crucial to the performance of the package. The two basic methods of aligning the devices in the assembly are active and passive alignment.

Active alignment involves recording the light intensity of different coupling arrangements, and then assembling the package at the optimum condition. This method is both tedious and expensive. Passive alignment on the other hand uses the wetting characteristics of solders to align the device with the submount, allowing a much higher assembly rate compared with using active alignment. The idea of the self-alignment of microelectronic assemblies using solder was introduced by IBM in 1969, with the controlled-collapse chip connection (C4). [Miller69][Goldman69] The self alignment process is based on the fact that the solder will wet the metal bonding pad (usually gold), but not the oxide surrounding the pad. The solders used for joining were Pb-5wt.%Sn and Pb-10wt.%Sn. A schematic of the self alignment process is shown in Figure 2-1.

[Lee94] When the solder is heated beyond its melting point, the solder begins to wet the bonding pad, and the chip begins to move. The movement of the chip is driven by the surface tension of the solder, and the energy of this system is at a minimum when the chip and submount are aligned. The assembly is then cooled, retaining the aligned position. Optical alignments better than $1\mu\text{m}$ have been demonstrated. [Lee94]

Figure 2-1 Schematic of the self-alignment technique. [Lee94]



The advantages of using the self-alignment joining technique include high interconnection density, low cost, high yield (97% in the work by Miller), high strength, efficient heat conduction, batch assembly, and the ability to join multi pad devices of significant size and complexity. Examples of devices joined by the self-alignment process are shown in Figures 2-2 and 2-3. [Lee94]

Figure 2-2 Four channel laser array positioned using the self-alignment joining technique. [Lee94]

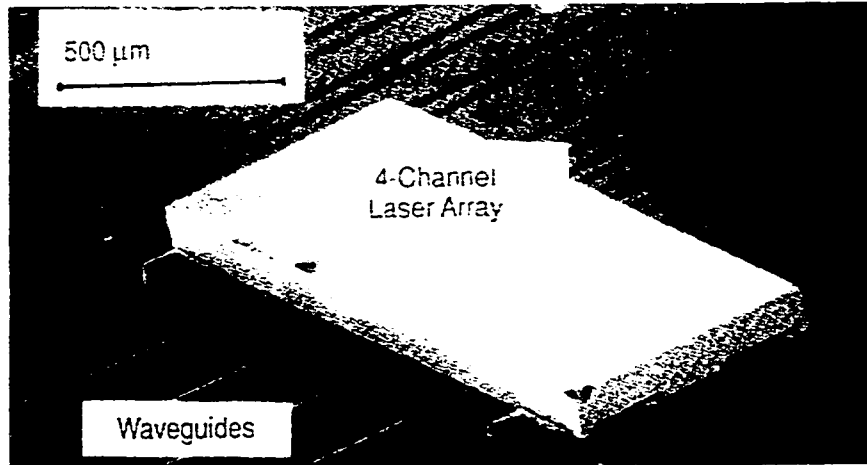
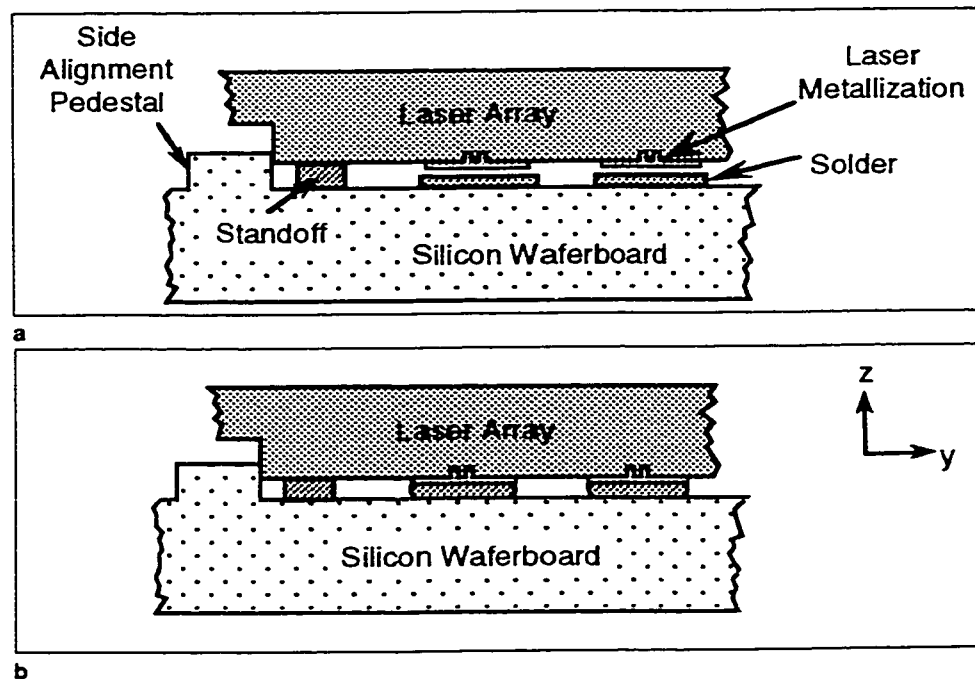


Figure 2-3 Schematic of a laser array mounted on a waferboard (a) before, and (b) after the solder reflow process. [Lee94]



2.2 Solders Used for Optoelectronic Packaging

The most commonly used solders for bonding in electronic packaging are based on the Pb-Sn system. These alloys have low melting temperatures (183°C - 312°C), and are characterized by high creep rates and stress relaxation, as well as surface and microstructural changes. [Plumbridge96] For optoelectronic devices, higher melting Au eutectic alloys are used, such as Au-Sn (278°C), Au-Ge (361°C) and Au-Si (364°C). The advantages of the higher melting solders include increased thermal stability and long term reliability. [Katz94] Au-30at.%Sn eutectic solder is used in optoelectronic applications, particularly to join InP devices to the submount in a flip-chip assembly. The submount is generally CVD diamond, and the solder serves the purpose of heat dissipation, mechanical support and electrical conduction. The Au-30at.%Sn solder has some advantages over the other Au based solders in that it has the highest strength, lowest elastic modulus and lowest melting temperature of this group of solders. The Au-Sn solder also has a high thermal conductivity compared to other solders, which makes it an attractive choice for packages which run hot, such as laser devices.

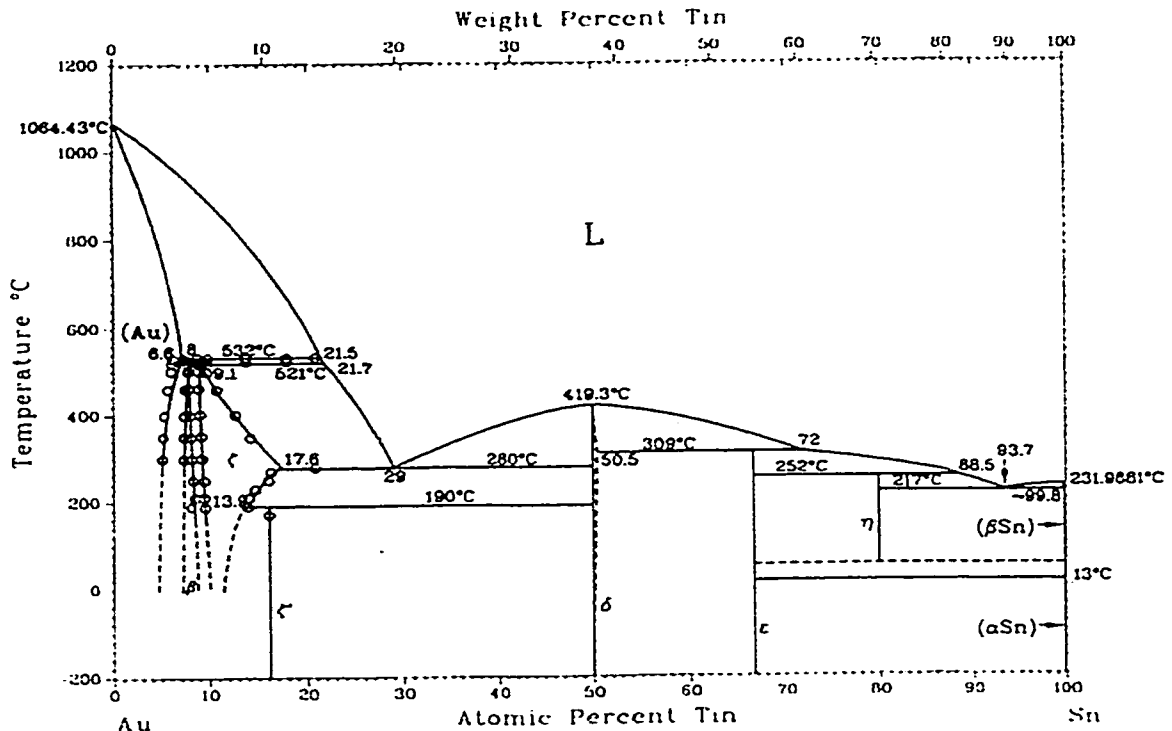
2.3 Au-Sn Phase Diagram

The Au-Sn phase diagram is shown in Figure 2-4. [Ciulik93] The electrochemical characteristics of Au and Sn are quite different, as the electronegativity of Au is 2.3, compared to 1.8 for Sn. Such a difference leads to the formation of stable intermetallic phases as opposed to solid solutions. There are two eutectic reactions in the Au-Sn system. The eutectic point at 93.7 at.% Sn and 217°C ($L \leftrightarrow [\eta + \beta\text{-Sn}]$) has been eliminated as a possible solder for microelectronic applications for three reasons:

- i. The η phase (Au_4Sn) is known to be brittle. [Daebler91]
- ii. The electrical, mechanical and thermal properties of the η phase are unknown. [Matijasevic93]

- iii. There is a reversible transition between β -Sn (metallic b.c.t.) and α -Sn (semiconducting diamond cubic) between 13°C and 20°C. The $\beta \rightarrow \alpha$ transformation is very slow, diffusion controlled, and occurs at 13°C, while the $\alpha \rightarrow \beta$ transformation occurs at 20°C, involves rapid growth, and involves a 21% volume contraction, and is believed to be martensitic. [Smith86]

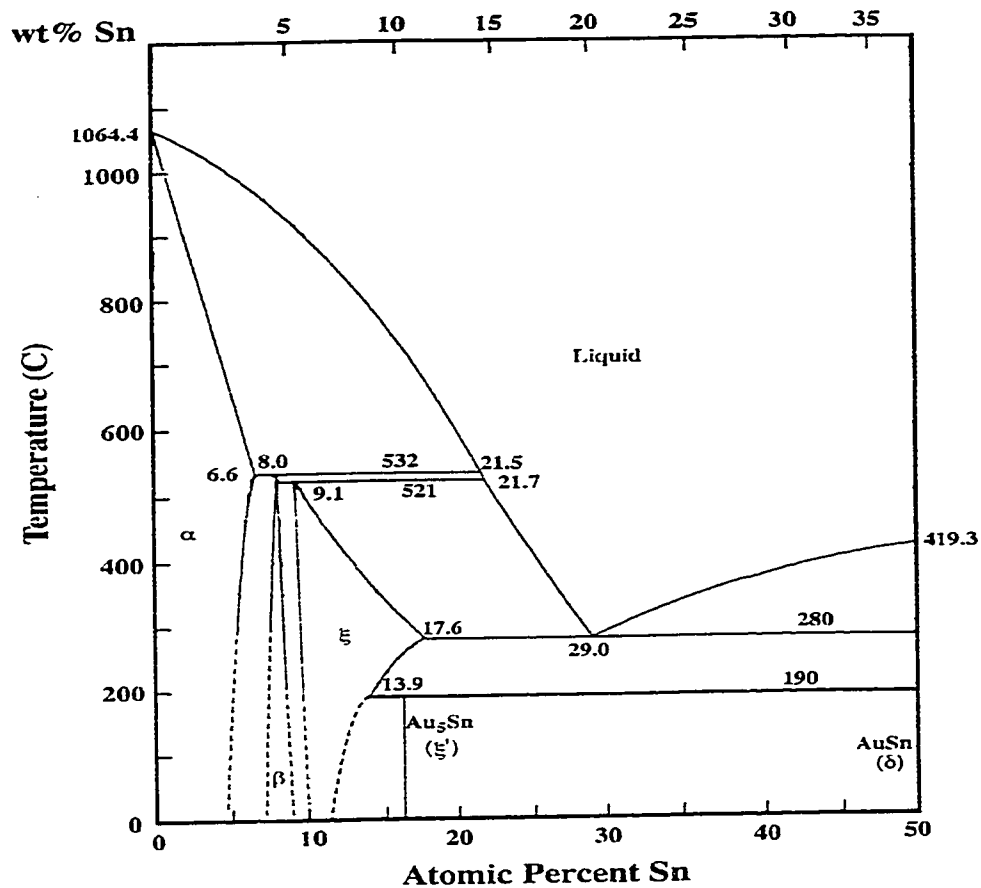
Figure 2-4 The Au-Sn phase diagram. [Ciulik93]



The other eutectic point, at 280°C and 29.5 at.% Sn has the reaction $L \leftrightarrow [\zeta + \delta]$, and is of great interest as a soldering material. At 190°C and 16.0 at.% Sn there is a peritectoid reaction, $\zeta' \leftrightarrow [\zeta + \delta]$, reported by Ciulik & Notis. [Ciulik93][Okamoto93] Prior to this, the reaction was believed to be $\zeta \leftrightarrow [\zeta' + \delta]$ at 190°C and 18.5 at.% Sn. [Yost90] The Au-Sn phases of interest for Au-Sn eutectic solder are ζ' (Au_5Sn), ζ , and δ

(AuSn), which will be described in more detail, along with the other phases found in the gold rich section of the Au-Sn phase diagram. (Figure 2-5) [Ciulik93]

Figure 2-5 The gold-rich portion of the Au-Sn phase diagram. [Ciulik93]



2.3.1 The δ (AuSn) Phase

The δ (AuSn) phase is an intermetallic compound with a melting point of 419.3°C and a NiAs-type (hexagonal) structure. The AuSn phase is a subtractive solid solution containing between 50.0 and 50.5 at.% Sn which can be designated as Au_{1-x}Sn ($0.00 \leq x \leq 0.02$). [Jan63]

2.3.2 The ζ (Au₅Sn) Phase

The ζ (Au₅Sn) phase has a composition of 16.7 at.% Sn, and exists up to 190°C. It has a hexagonal structure, and can be defined by a unit cell containing 15 Au and 3 Sn atoms.

2.3.3 The ζ Phase

The ζ phase exists from the peritectic $\beta + L \leftrightarrow \zeta$ at 9.1 at.% Sn and 521°C to 17.6 at.% Sn at 280°C, and to 13.9 at.% Sn at 190°C. This phase has a Mg-type close packed hexagonal structure, which increases in volume per atom as the Sn concentration increases. The existence of this phase below 190°C has not yet been proven.

2.3.4 The β Phase

The β phase was assumed to be Au₁₀Sn, an intermetallic compound with a Ni₃Ti-type close packed hexagonal structure. [Schubert59] This compound was believed to be stable above 250°C with a composition of 9.1 at.% Sn. [Okamoto84] Work done by Legendre [Legendre87] and Ciulik [Ciulik93] has clarified the peritectic point for the β phase ($\alpha + L \leftrightarrow \beta$), at a composition of 8.0 at.% Sn and 532°C. This phase was found to have a composition ranging between 8.25 at.% and 9.11 at.% Sn at 280°C. It is also not yet known if this phase exists below 190°C.

2.3.5 The α -Au Phase

The α -Au solid solution has the same face centred cubic crystal structure as Au, and is a substitutional solid solution of Sn in Au. The maximum solubility of Sn in this phase is 6.6 at.% at 532°C. The lattice size increases with an increase in tin content.

2.4 Deposition Techniques for Au-30at.%Sn Solder

Au-30at.%Sn solder can be applied using solder preforms (20-50mm in thickness), paste, electron-beam evaporation or electrodeposition. Solder preforms are problematic for flip-chip applications due to alignment trouble and oxidation of the solder prior to bonding. Solder paste also suffers from oxidation prior to bonding, in addition to the possibility of solder contamination during bonding from the organic binder in the paste.

Electron-beam evaporation and electrodeposition are advantageous for Au-Sn solder deposition in that the oxide formation prior to bonding can be reduced and the thickness and position of the solder can be closely controlled. [Lee91] The sequential evaporation of Au and Sn layers to produce a deposit of desired composition has been successfully employed, [Katz94] [Lee91] [Buene80] along with co-evaporation techniques. [Ivey98]

The electrodeposition of Au-Sn solder has followed the method of plating Au and Sn layers sequentially from separate Au and Sn solutions. [Kallmayer96] Recently, Au-Sn solder has been co-deposited by electroplating from both cyanide based [Holmbom98] and chloride based [Sun99-1] solutions. Co-deposition is advantageous in that Sn oxidation is kept to a minimum during the electroplating process, since the wafer does not need to be removed from the solution until plating is complete.

3 Electrodeposition of Alloys

Electroplating is a method of depositing metals in which metal ions are transported to a substrate (cathode) through a conducting solution by the use of an electric current, adsorbed onto the surface, and incorporated into the substrate lattice. There is a potential barrier (polarization) which exists and must be overcome in order for deposition to occur. The potential barrier is introduced by the reaction kinetics and surface conditions at the substrate. The potential barrier can be changed by changing any one of a number of variables in plating, such as metal ion concentration in solution, bath temperature, current density and agitation. The current density affects the deposition by governing the deposition rate, and the amount of polarization affects how the deposit grows.

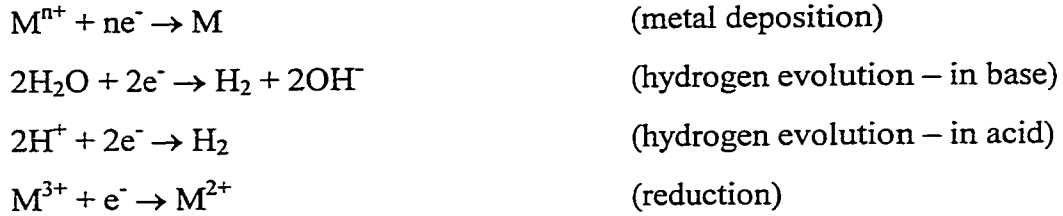
3.1 Basic Electroplating Theory

There are a number of references which contain an excellent background on basic electrochemistry, and most of the information presented in this section comes from books by Tan [Tan93] and Bradford. [Bradford93] Electroplating occurs by passing an electric current through a conducting solution in which metal ions carry the current through the solution between two conducting electrodes. The anode is attached to the positive output of the power supply, while the cathode is attached to the negative output. Reactions occur at each electrode as follows:

Anode:



Cathode:



For electroplating, metal deposition at the cathode is the preferred reaction. Figure 3-1 gives a schematic of the electroplating process. For any type of metal or alloy deposition, the free energy (ΔG) associated with the metal deposition reaction determines whether the reaction will occur. The more negative ΔG is, the more likely the reaction will occur. ΔG is related to the electrode potential (E) by the following equation:

$$\Delta G = -nFE \quad (1)$$

n = the number of moles of electrons taking part in the reaction.

F = Faraday's constant = 96,500 C/mole of electrons.

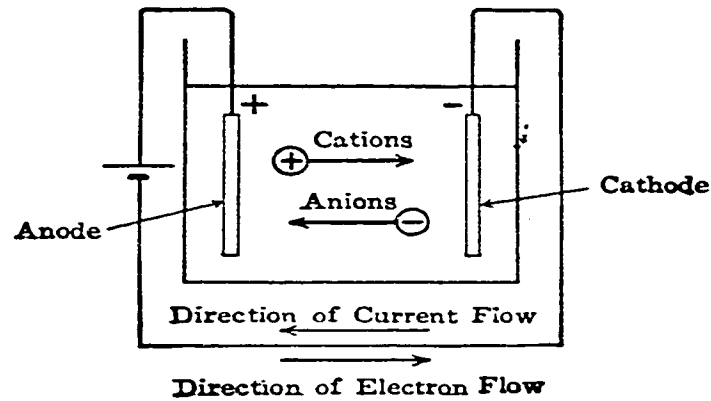
For every metal and a solution of its own ions, an equilibrium is created between dissolution and deposition. The result is that the metal becomes positively or negatively charged with respect to the solution. In this manner a potential exists between the metal and solution, which is called the electrode potential. Each metal/ion system has a particular potential, which is given as a standard electrode potential for the system at standard conditions and is measured relative to the hydrogen electrode. A list of electrode potentials is given in Table 3-1. Metals which are near the top of the list are more likely to donate electrons when coupled with an anode in a solution. This is helpful to understanding alloy plating, as in general the metal with a larger (more positive) standard electrode potential will be preferentially plated. The standard electrode potentials are only a rough guide for electroplating, as metals are almost never found at equilibrium with their ions during plating. The potential during electroplating is heavily

influenced by the concentration of the ions involved, the temperature, and the reaction kinetics.

Table 3-1 Selected Standard Electrode Potentials at 1M, 25°C and 1 atm.

<u>Electrode</u>	<u>E⁰ (V)</u>
$\text{Li}^+ + \text{e}^- = \text{Li}$	-3.045
$\text{K}^+ + \text{e}^- = \text{K}$	-2.925
$\text{Rb}^+ + \text{e}^- = \text{Rb}$	-2.925
$\text{Ba}^+ + 2\text{e}^- = \text{Ba}$	-2.900
$\text{Sr}^{2+} + 2\text{e}^- = \text{Sr}$	-2.890
$\text{Ca}^{2+} + 2\text{e}^- = \text{Ca}$	-2.870
$\text{Na}^+ + \text{e}^- = \text{Na}$	-2.714
$\text{Mg}^{2+} + 2\text{e}^- = \text{Mg}$	-2.370
$\text{Al}^{3+} + 3\text{e}^- = \text{Al}$	-1.660
$\text{Zn}^{2+} + 2\text{e}^- = \text{Zn}$	-0.763
$\text{Fe}^{2+} + 2\text{e}^- = \text{Fe}$	-0.440
$\text{Cd}^{2+} + 2\text{e}^- = \text{Cd}$	-0.403
$\text{Ni}^{2+} + 2\text{e}^- = \text{Ni}$	-0.250
$\text{Sn}^{2+} + 2\text{e}^- = \text{Sn}$	-0.136
$\text{Pb}^{2+} + 2\text{e}^- = \text{Pb}$	-0.126
$\text{H}^+ + \text{e}^- = \frac{1}{2}\text{H}_2$	±0.000
$\text{Sn}^{4+} + 2\text{e}^- = \text{Sn}^{2+}$	+0.150
$\text{AgCl} + \text{e}^- = \text{Ag} + \text{Cl}^-$	+0.222
$\text{Cu}^{2+} + 2\text{e}^- = \text{Cu}$	+0.337
$\text{Ag}^+ + \text{e}^- = \text{Ag}$	+0.799
$\text{Pd}^{2+} + 2\text{e}^- = \text{Pd}$	+1.000
$4\text{H}^+ + \text{O}_2 + 2\text{e}^- = 2\text{H}_2\text{O}$	+1.229
$\text{Au}^{3+} + 3\text{e}^- = \text{Au}$	+1.500
$\text{Au}^+ + \text{e}^- = \text{Au}$	+1.700

Figure 3-1 Schematic of the electroplating process.



3.1.1 Current and Current Density

The amount of metal deposited by a current during electroplating is governed by Faraday's laws of electrolysis, formulated in 1833.

- i. The amount of electricity (charge) passed through a solution is proportional to the amount of any substance deposited or dissolved.
- ii. The amounts of different substances deposited or dissolved by the same amount of electricity (charge) are proportional to their chemical equivalent weights.

The combination of these two laws gives the following equation:

$$m_{th} = E_c It \quad (2)$$

m_{th} = theoretical mass of metal plated.

E_c = electrochemical equivalent weight, in g/coulomb.

I = current in amperes.

t = time in seconds.

The electrochemical equivalent weight is found by:

$$E_c = A / nF \quad (3)$$

A = atomic weight of metal being reduced in g/mole.

n = number moles of electrons participating in the reduction reaction.

F = Faraday's constant (charge of 1 mole of electrons).

The theoretical mass plated during alloy plating can also be found by finding the electrochemical equivalent weight of the alloy from the following equation:

$$E_{c,a} = E_1 E_2 / (f_1 E_2 + f_2 E_1) \quad (4)$$

E_1, f_1 = electrochemical equivalent weight, weight fraction of metal A.

E_2, f_2 = electrochemical equivalent weight, weight fraction of metal B.

The theoretical plating thickness (x_{th}) can be calculated from the theoretical mass by combining the equation $m_{th} = \rho x_{th} A$ with equation 2:

$$x_{th} = 10 E_c i_c t / \rho \quad (5)$$

i_c = current density in mA/cm².

ρ = density of electrodeposit.

One faraday of charge or 96,500 C will then theoretically reduce 1 mole of Au⁺ to Au(s), or 0.5 mole Sn²⁺ to Sn(s). The current passed through the solution is thus directly related to the mass of the deposit. In an ideal situation all of the electrons passed through the solution would combine with the incoming metal ions to deposit at the cathode, but in many cases other cathode reactions such as hydrogen evolution or the reduction of metal ions to a lower valency are present, decreasing the current efficiency. The current

efficiency (ϵ) during electroplating is given by the ratio of the actual mass plated (m_a) divided by the theoretical mass expected from Faraday's law:

$$\epsilon = m_a / m_{th} \times 100 \quad (6)$$

If the plated thickness is known, the current efficiency can also be calculated from the theoretical thickness, assuming the plated thickness (x_a) is constant, by the equation:

$$\epsilon = x_a / x_{th} \times 100 \quad (7)$$

The cathodic current density is given by dividing the current by the surface area of the cathode, while the anodic current density is given by dividing the current by the anode surface area.

3.1.2 Electrode Potential

In addition to the standard electrode potential, there are numerous parameters affecting the potential required for electroplating. These parameters include the concentration of plating ions, the plating solution temperature and effects such as concentration polarization, activation polarization and ohmic polarization. The Nernst equation relates the potential (E) to the ion concentration and temperature in solution for the reaction $M^{n+} + ne^- \rightarrow M$:

$$E = E^0 + (RT / nF) \ln[M^{n+}] \quad (8)$$

R = gas constant.

T = absolute temperature.

From this equation it can be seen that the potential becomes more positive (more noble) with an increase in ion concentration. Since the relationship between potential and

concentration is logarithmic, it is not particularly useful to control composition in alloy plating by the concentration of ions in solution when the reduction potentials are far apart.

3.1.3 Polarization

Once an electrochemical reaction begins, the potential starts to change as the current increases. The difference between the electrode potential with and without current is called the electrochemical polarization (η), and is made up of three different types of polarization. These are the activation polarization (η_a), the concentration polarization (η_c) and the ohmic polarization (η_r). These polarizations are additive and combine with the potential drop across the solution to give the total potential required to deposit metal at a specific current density.

3.1.3.1 Activation Polarization

Activation polarization is present because a certain amount of activation energy is required to incorporate adsorbed ions or atoms into the deposit. When no potential is applied to an electrochemical system, there exists a dynamic equilibrium between the reduction and oxidation reactions at the cathode surface. There is no net current flow, but the current of each of the reactions is the same, and is termed the exchange current density (i_o). This current may be extremely small, but is never zero. As the current is increased and with it the rate of deposition, the potential also increases, as the cathode can receive electrons faster if the potential increases. The activation polarization is related to the current (i_a) by the Tafel equation:

$$\eta_a = a + b \log i_a \quad (9)$$

a = constant.

b = Tafel slope of the reaction: slope of the polarization (V vs. log i) curve.

If the cathode is operated in the activation polarization region, the reaction is said to be reaction controlled.

3.1.3.2 Concentration Polarization

When the current is raised further, the voltage-current characteristics begin to change, as the supply of ions to the cathode surface begins to limit the rate of deposition. As the current increases and the deposition rate increases, the supply of incoming ions decreases as the concentration of ions near the cathode surface decreases. At this stage, the reaction becomes controlled by the diffusion of ions through the depleted region near the cathode, and this is known as concentration polarization. The concentration polarization is given by:

$$\eta_c = RT / nF \log a_c / a_b \quad (10)$$

a_c = activity of depositing ion at the cathode.

a_b = activity of depositing ion in the bulk solution.

At a certain point, the diffusion distance becomes so large that a further increase in potential will not draw more ions to the cathode surface, and a limiting current density (i_L) is reached. The limiting current density is related to the diffusion coefficient of the ions (D_i), the concentration of the ions in the bulk solution (C_b), and the thickness of the diffusion layer (δ) by:

$$i_L = D_i n F C_b / (1-t_i) \delta \quad (11)$$

t_i = the transport number of the ions, which is the fraction of the total current carried by each ionic species.

The concentration polarization is related to current density (i_c) and limiting current density (i_L) by the following relation:

$$\eta_c = (RT / nF) \ln (1 - (i_c / i_L)) \quad (12)$$

Since the limiting current density is related to the diffusion coefficient, and the thickness of the diffusion layer, two important plating parameters can be defined:

- i. Increasing temperature increases the diffusivity exponentially, so the limiting current density will increase.
- ii. Increasing the velocity of ions (agitation) over the cathode decreases the thickness of the diffusion layer increasing the limiting current density.

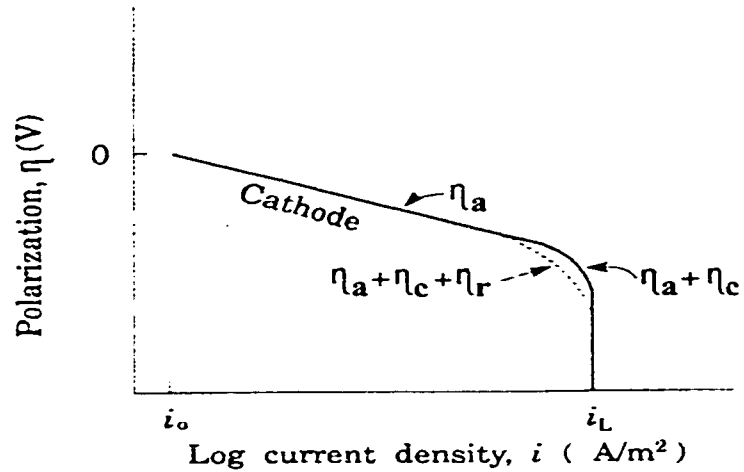
3.1.3.3 Ohmic Polarization

Ohmic polarization is caused by passivating films which form on the surface of certain metals. The resistance of the film (R_f) must be overcome before deposition can occur. Examples of such films are the oxide films on metals such as aluminum, chromium and titanium. The ohmic polarization is given by:

$$\eta_r = IR_f \quad (13)$$

The effects of each type of polarization are additive, and a sample polarization curve is shown in Figure 3-2. [Bradford93]

Figure 3-2 Effects of different polarizations. [Bradford93]



3.1.4 Effects of Plating Chemicals

Metals are rarely deposited from their basic ionic form, and in many cases the metal is complexed with another ion in solution. The reduction potential of a plating reaction is different depending upon the ion complex in which it is present. This can be advantageous for alloy deposition, in that the reduction potential of one metal can be brought closer to the reduction potential of the other metal by complexing one of the metals. Table 3-2 [Stanley87] gives the reduction potentials of some gold complexes. The addition of complexing agents decreases the reduction potentials.

Table 3-2 Standard reduction potentials for selected reactions involving gold.
[Stanley87]

<u>Electrode</u>	<u>E⁰ (V)</u>
$\text{Au}(\text{CN})_2^- + e^- = \text{Au} + 2\text{CN}^-$	-0.57
$\text{Au}(\text{S}_2\text{O}_3)_2^{3-} + e^- = \text{Au} + 2\text{S}_2\text{O}_3^{2-}$	+0.15
$\text{Au}(\text{SCN})_4^- + 3e^- = \text{Au} + 4\text{SCN}^-$	+0.623
$\text{Au}(\text{SCN})_2^- + e^- = 2\text{SCN}^-$	+0.662
$\text{AuCl}_4^- + 2e^- = \text{AuCl}_2^- + 2\text{Cl}^-$	+0.926
$\text{AuCl}_4^- + 3e^- = \text{Au}$	+1.002
$\text{AuCl}_2^- + e^- = \text{Au} + 2\text{Cl}^-$	+1.154
$\text{Au}^{3+} + 2e^- = \text{Au}^-$	+1.40
$\text{Au}^{3+} + 3e^- = \text{Au}$	+1.50
$\text{Au}^+ + e^- = \text{Au}$	+1.69

3.2 Alloy Plating

The basic idea of developing an alloy plating bath is to find ways to bring the reduction potentials of the desired ions to be reduced closer together. The main way is by changing the polarization in some manner, such as by the use of complexing agents. The reduction potential of the more noble alloy can be lowered by having it forming a complex. Once a solution is developed, alloy plating can occur in a number of ways when current is applied, and the composition of the deposition is governed by potential, mass transport and any interactions between the cations during plating.

3.2.1 Brenner's Classification of Codeposition

Brenner [Brenner63] originally categorized alloy plating into 5 groups. The first three types, regular, irregular and equilibrium codeposition are known as normal codeposition, in which the proportion of the more noble metal in the deposition is equal to or greater than its proportion in the solution. The last two types of deposition, anomalous and irregular codeposition, are known as abnormal codeposition. In abnormal codeposition, the proportions of metals in the deposit would not be expected on the basis of the equilibrium potentials of the metals in solution. A brief description of each of the codeposition types is given below.

- i. **Regular Codeposition** - Plating is under diffusion control, and the percentage of noble metal in the deposit is increased by factors which increase the metal content in the diffusion layer. This type of deposition is most likely in simple ion plating baths.
- ii. **Irregular Codeposition** - Plating is affected by the potentials of the metals in the solution, as the potentials have been changed by the use of a complex ion bath.
- iii. **Equilibrium Codeposition** - Plating is carried out in a solution which is in chemical equilibrium with both metals. The ratio of metals in the deposit is the same as the ratio in the solution at most current densities. This is a rare type, and copper-bismuth and lead-tin plated from acid baths are examples.
- iv. **Anomalous Codeposition** - The less noble metal is plated preferentially.
- v. **Induced Codeposition** - Metals, which cannot be deposited by themselves, such as molybdenum, tungsten or germanium, are codeposited with other metals. The metals which stimulate the deposition are called the inducing metal, while the metals which do not deposit alone are called the reluctant metals.

This method of classification is quite vague, and any one plating system can fall into a number of different classifications, depending on the operating conditions. A more recent classification system, based on mixed potential theory as well as kinetics has been proposed by Landolt [Landolt94], and is described in the next section.

3.2.2 Classification of Codeposition by Mixed Potential Theory

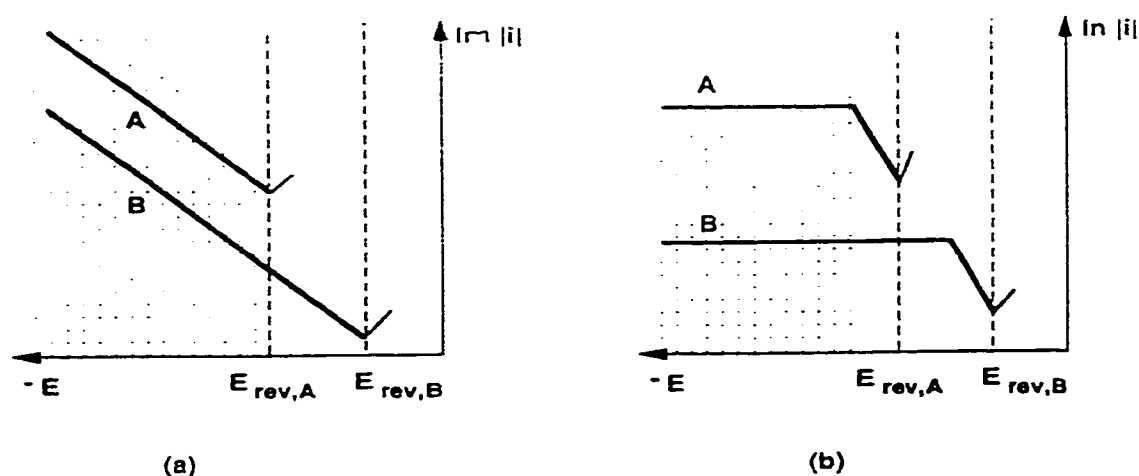
Mixed potential theory was developed for corrosion by Wagner and Traud [Wagner38], and is based on the idea that the measured current in an electrochemical system is the sum of all the partial anodic and cathodic currents. In binary alloy plating there will be at least two and usually three or more partial reactions taking place, one for each metal and the hydrogen reduction reaction. Three types of codeposition behavior have been proposed by Landolt [Landolt94], non-interactive, charge transferred coupled and mass transport coupled codeposition.

3.2.2.1 Non-interactive Codeposition

In a large number of plating systems, the partial currents of the metals taking part in the deposition are independent of each other, so the alloy composition can be predicted from the partial currents since the current is proportional to the deposition rate. By studying the polarization characteristics of each metal, the potentials at which each alloy are preferentially plated can be found. Anomalous codeposition can be predicted in this manner, for example in the case where the more noble metal reaches its limiting current density (diffusion controlled) while the deposition of the less noble metal is still reaction controlled. A further increase in overpotential will cause the less noble metal to be preferentially plated. Examples of non-interactive codeposition are nickel-copper plating [Ying88] and tin-lead alloy plating [Pesco88].

There are two special cases where the metal content in the deposit will be the same as the metal ion content in solution. A diagram of these situations is shown in Figure 3-3, where $E_{rev,A}$ and $E_{rev,B}$ are the equilibrium potentials of each of the metal ions in the solution, and the shaded region denotes the potentials at which the metal content in the deposit is the same as the metal ion concentration in the solution. The first case is when the deposition of both metals is reaction controlled and their Tafel constants (b) from equation (9) are equal. The second case is when the deposition of both metals is diffusion controlled, or plated at the limiting current density. The second case is usually avoided in electroplating, as very rough or dendritic structures are plated. With pulse plating however, electroplating can be carried out at the limiting current density while still producing smooth deposits. Polarization diagrams of the partial currents for each metal in the two cases mentioned are shown in Figure 3-3.

Figure 3-3 Polarization diagrams showing situations where metal content in the deposition is related to the metal concentration in solution: (a) Tafel kinetics with equal slopes, (b) diffusion controlled deposition with both components at their limiting current densities. [Landolt94]



3.2.2.2 Charge Transfer Coupled Codeposition

In this type of codeposition, the partial current of one of the metals is different in the alloy plating solution than if it were in the solution by itself. In some cases, the deposition rate of one metal will be decreased by the presence of the other metal. It is proposed that in this case one metal inhibits the deposition of the second metal by forming intermediate reaction products which are adsorbed on the cathode. [Matlosz93] In other cases, such as in the deposition of the reluctant metals, the presence of one metal has a catalytic effect on the deposition of the other metal. In nickel-molybdenum electroplating, the presence of nickel catalyzes the deposition of molybdenum. For this case it is proposed that the formation of a Ni-Mo oxide forms as an intermediate reaction product allowing the molybdenum to be deposited. [Chassaing89]

3.2.2.3 Mass Transport Coupled Codeposition

This type of deposition occurs when the mass transport of a species being consumed or created at the cathode by one metal affects the deposition of the second metal. An example of this would be when an alloy is being plated in conjunction with hydrogen evolution. The formation of hydrogen can cause a pH increase in the diffusion layer which can change the stability between the metal ions and their anions, possibly decreasing the number of metal ions which make it to the cathode.

3.3 Pulse Plating

In electroplating, the activation polarization must be present for current to flow and for deposition to begin. The cathode potential is thus slightly raised with respect to the solution, and this sets up a situation at the cathode which represents a parallel plate capacitor, known as the electrical double layer. The double layer at the cathode consists of positively charged ions adsorbed onto the cathode surface and a region of ions of mixed positive and negative charge extending into the solution. The net negative charge

of the region extending into the solution is equal to the net positive charge adsorbed onto the cathode surface. So in addition to a voltage-current relationship at the cathode, there is also a voltage/current-time relationship. A certain amount of time is needed to charge the double layer when current is applied, and a certain time is also needed to discharge the double layer when the current is stopped. Pulse plating takes advantage of this phenomenon by allowing a wide range of potentials to be effectively produced at a single average current density by changing the pulse height and width. Since the potential applied affects the alloy composition and structure, pulse plating allows a wider range of plating possibilities over direct current plating.

The ON and OFF times of the current pulse are limited by the charging and discharging times of the electrical double layer. [Puipe86] The current density during plating can be separated into two components, the capacitive current (i_C) which charges the electric double layer, and the faradic current (i_F) which corresponds to the rate of metal deposition. The capacitive current is related to the activation polarization (η_a), capacitance of the electric double layer (C) and time (t) by:

$$i_C = C d\eta_a / dt \quad (14)$$

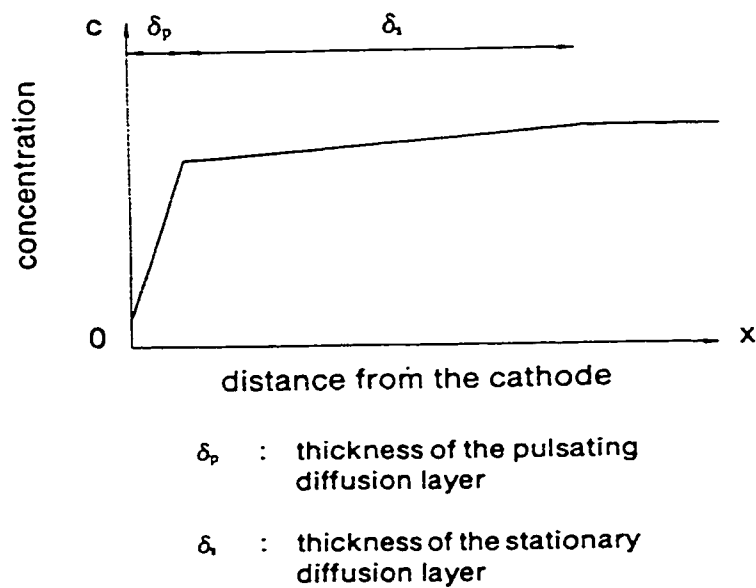
This equation is usually solved for 98-99% of the charging time, and for a system where $C = 50 \mu\text{F}/\text{cm}^2$ and the exchange current density is $5 \text{ mA}/\text{cm}^2$, the charging time varies from $100 \mu\text{s}$ at a pulsed current of $100 \text{ mA}/\text{cm}^2$ to $0.1 \mu\text{s}$ at a pulsed current of $100,000 \text{ mA}/\text{cm}^2$. The capacitance of the electric double layer ranges from 10 to $100 \mu\text{F}/\text{cm}^2$ for various metal/solution interfaces, and is affected by passive layers and organic bath additives. The electrode potential was found to be an important factor on the capacitance, [McMullen59] as the capacitance of the electric double layer has different values on either side of the cell potential.

For pulse plating there is a pulse limiting current density (i_{LP}) which is dependent mostly on the on and off times of the pulse. The average limiting current density (i_L) in pulse plating cannot exceed the average limiting current density in direct current plating.

[Cheh71] The pulse limiting current density is reached when the concentration of ions reaches zero at the cathode surface during the on time. During the off time the ions have time to diffuse to the cathode surface before the next pulse. As the ratio of on/off times becomes larger, i_{LP} increases. The main effect is that a second diffusion layer is created, called the pulsating diffusion layer shown schematically in Figure 3-4. [Puipe86] This diffusion layer is much smaller than the direct current diffusion layer, and the result of this is a smoother deposit, as the pulsating diffusion layer follows the surface topography. An example of this effect is given by Catonne and co-workers [Catonne84], who studied the brilliancy of gold-silver electrodeposits at various on/off times.

One problem with alloy plating is obtaining a uniform composition when using direct current. [Avila86] In plating solder onto printed circuit boards, composition variations lead to differences in melting temperatures which are not desired. Work done on silver-tin pulsed alloy plating [Leidheiser73] showed that the composition of the deposit can be matched to the metal ion composition in the solution by adjusting the pulse parameters.

Figure 3-4 Schematic showing the pulsating diffusion layer.



The main advantages of pulse plating are:

- i. An increase in the throwing power (smoothness of the deposit).
- ii. Improvement of deposit properties (porosity, ductility, hardness).
- iii. Ability to deposit alloy compositions not possible with direct current plating.

Throwing power (S_m) is calculated by taking the minimum thickness of the electrodeposited coating and dividing it by the maximum thickness. It is given as a percentage, and the closer the throwing power is to 100%, the smoother/brighter the deposit is.

3.4 Electrodeposition of Au-Sn Alloys

In electroplating of gold alloys for semiconductor devices, it is important that the plating solution have an acidic pH, as much of the plating is done on circuits covered in alkaline-developable photoresists. Traditionally, most gold and gold alloy plating has been done using cyanide based solutions, but other plating systems, based on sulfide complexes have been developed. Non-cyanide based gold plating systems are becoming more attractive as the disposal and health regulations associated with cyanide become more stringent.

3.4.1 Cyanide Based Plating Systems

Cyanide is the obvious first choice as a gold plating electrolyte, as it has the highest stability of known gold electrolytes. Alkaline cyanide plating systems were introduced by Elkington in 1840, and the development of increasingly acidic cyanide plating solutions has progressed since 1945 to meet the growing needs of the electronic

industry, [Schloder86] since hard, bright gold deposits can be plated from acidic solutions. An overview of cyanide based gold plating solutions is given in Table 3-3.

Table 3-3 Overview of cyanide-based gold electroplating solutions. [Schloder86]

Bath Type	pH Range	Au Complex	Alloying Metals	Conducting and Buffer Salts	Year of Introduction	Main Application
Strong Acid	0.5-2.5	KAu(CN)_4	Co, Ni, In, Sn	Acids, Acid salts	After 1980	Decorative, Electronics
Weak Acid	3-6	KAu(CN)_2	Co, Ni, In, Fe	Phosphates, Weak Organic Acids	After 1955	Electronics
Neutral	6-8	KAu(CN)_2	Cu, Cd, Ag	Phosphates, Citrates	After 1945	Electronics
Alkaline	8-13	KAu(CN)_2	Cu, Cd, Ag, Zn, Pd, Sn	Alkali cyanide, Phosphates, Carbonates	Since 1840	Decorative

Gold and tin have been successfully co-deposited from an alkaline cyanide solution by Holbrom and co-workers. [Holbrom98] The optimized solution is as follows:

- i. Au (in the form Au(CN)_2^-) – 2 g/l
- ii. Sn (in the form SnO_3^{2-}) – 20 g/l
- iii. PO_4^{3-} – 40 g/l
- iv. CO_3^{2-} – 20 g/l
- v. CN^- - 40 g/l
- vi. Proprietary additive – 60 ppm

The solution pH is 10.5, and the operating temperature 45°C. A plating rate of 9 $\mu\text{m/hr}$ is claimed at a current efficiency of 55%, and a current density of 8 mA/cm^2 with agitation. It is possible to plate Au/Sn alloys with compositions close to the eutectic composition using this plating system. The disadvantage of this system for plating electronic components is that the solution is alkaline.

3.4.2 Non-cyanide Plating Systems

Gold plating systems based on sulfite complexes have been known since 1845, and the advantages of plating gold with such systems as opposed to cyanide systems include: [Duffek73]

- i. High purity deposit.
- ii. High throwing power.
- iii. Bright deposits.
- iv. Easier waste disposal.

Unfortunately, alloy plating is difficult with this system, as other metals such as nickel are not easily complexed in this system. Other disadvantages are that the gold precipitates below a pH of 9, in addition to the oxidation of the sulfites into sulfates either by anodic oxidation or by contact with air.

The electrorefining of gold is carried out using gold chloride solutions. [Schalch76] In this process, gold anodes containing impurities and nearly pure cathodes are placed in a solution of HCl. The gold is dissolved at the anodes and deposited in very pure form at the cathodes. Impurities either precipitate, or remain in solution. The potential of the gold in solution is 0.67 V versus a saturated calomel electrode (SCE), so the potential difference between gold and tin in a simple chloride solution is too great to allow alloy plating. Furthermore, gold trichloride (AuCl_3)₂ forms a complex compound with stannic chloride (SnCl_4). [Thorpe50] The trichloroaurate complex will also form a salt with the ammonium ion ($\text{NH}_4\text{AuCl}_4 \cdot 3\text{H}_2\text{O}$).

Laude and co-workers [Laude80] describe a process for taking a gold chloride solution (HAuCl_4) and precipitating it with ammonia. The precipitate is washed, dissolved, and then precipitated a second time using ammonium sulfite. The final precipitate, believed to be $(\text{NH}_4)_3[\text{Au}(\text{SO}_3)_2] \cdot \text{H}_2\text{O}$, is stable in water even at slightly acidic pH. Due to the stability of this compound, alloying metals can easily be added to the solution allowing a wide range of alloy plating possibilities.

A gold-tin alloy electroplating solution based on AuCl_4 , stabilized by sulfite and ammonium complexes was developed recently by Sun.[Sun99-2] The base plating solution has the following composition:

- i. 200 g/l ammonium citrate.
- ii. 5 g/l KAuCl_4 .
- iii. 60 g/l sodium sulfite.
- iv. 15 g/l L-ascorbic acid.
- v. 5 g/l $\text{SnCl}_2 \cdot 2\text{H}_2\text{O}$.

The pH of this solution is 6.5, and the Sn content of the deposits is around 37 at.%. The work in this thesis is based on this plating system, and the effects of the addition of ethylenediamine as a gold complexing addition.

3.5 Use of Ethylenediamine in Electroplating

Another option to increase the stability of plating solutions containing KAuCl_4 is to add the organic base ethylenediamine to form the compound diethylenediaminoauric chloride ($[(\text{H}_2\text{N}-\text{CH}_2-\text{CH}_2-\text{NH}_2)_2\text{AuCl}_3]$). [Thorpe50] In this form auric and 4-covalent gold are part of a complex tetravalent cation, $[(\text{H}_2\text{N}-\text{CH}_2-\text{CH}_2-\text{NH}_2)_2\text{Au}]^{3+}$ or $[(\text{H}_2\text{N}-\text{CH}_2-\text{CH}_2-\text{NH}_2)_2\text{Au}]^{4+}$. Morrissey describes 22 plating solutions, most of which are based on EDTA (ethylenediaminetetraacetic acid), ethylenediamine and sodium sulfite, where gold is added in the form of sodium gold sulfite ($\text{NaAu}(\text{SO}_3)_2$). The base solution is given as: [Morrissey94]

- i. 45 g/l EDTA.
- ii. 8 ml/l ethylenediamine.
- iii. 30 g/l sodium sulfite.
- iv. 1 ml/l nitrobenzene.
- v. 8.2 g/l Au in the form of sodium gold sulfite.

The solution pH was approximately 6.2, and plating was carried out at a solution temperature of 60°C , at current densities up to 5 mA/cm^2 . Binary alloys of gold and arsenic, thallium, silver, copper, iron, cobalt, nickel, cadmium, antimony, lead, tin indium, palladium and platinum are possible with this solution when the pH is adjusted to between 4 and 5.

A gold plating solution based on a gold-sulfite-ethylenediamine complex is reported by Zuntini et al. [Zuntini74] In this system, gold chloride $(\text{AuCl}_3)_2$ is mixed with ethylenediamine and precipitated using sodium sulfite to form crystals of $\text{Na}[(\text{H}_2\text{N}-\text{CH}_2-\text{CH}_2-\text{NH}_2)_2\text{Au}(\text{SO}_3)_2]$. Others forms of this complex can be made using ammonium sulfite or ethylene sulfite. The resulting compound is dissolved in water, and is stable down to a pH of 4.5. The pH can be adjusted by mineral or organic acids and bases. Alloy plating is possible with this solution for binary alloys of gold and zinc, cadmium, lead, iron, nickel, antimony, cobalt, tin, indium, palladium, copper or manganese.

The use of ethylenediamine in other plating systems has also been studied. Zinc-nickel alloys have been plated from solutions with the following composition: [Keshner89]

- i. $\text{NiCl}_2 + \text{ZnCl}_2 - 0.5 \text{ mol/l}$
- ii. Ethylenediamine – 1-2 mol/l
- iii. $\text{KCl} - 0.5 \text{ mol/l}$

Zinc-nickel alloys with compositions ranging between 8 wt.% and 16 wt.% Ni were plated using current densities between 5 and 80 mA/cm². It was found that the ethylenediamine concentration and current density had little effect on the alloy composition. The alloy composition was controlled by the nickel concentration in solution, as an increase in nickel content in solution led to an increase in the concentration in the deposit. The coatings became dark and porous when the pH of the solution was increased from 5 to 7, since the concentration of the nickel and zinc-ethylenediamine complexes decreased. Nickel can also be anodically removed from steel using ethylenediamine and various organic or mineral acids. [Natarajan84]

4 Structure of Electrodeposited Coatings

Electrodeposition or electrocrystallization is the process in electroplating where the incoming metal ions join the metal deposit. The rate of incoming metal ions is the main factor related to the structure formed. In general, a low rate (low current, low polarization) favors the growth of existing nuclei, while a high rate (high current, high polarization) favors the formation of new nuclei. Other factors which affect the structure of the coating are the surface finish of the base metal, and the effects of solution additives which are adsorbed onto the cathode surface and inhibit the growth pattern.

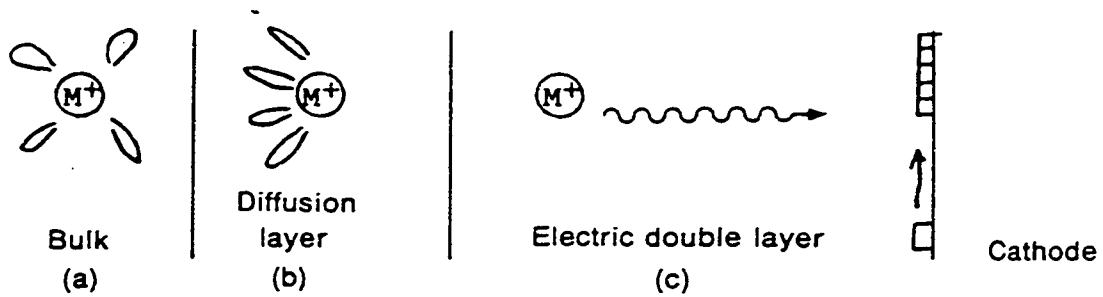
4.1 Electrodeposition Theory

Electrodeposition is the process in electroplating where the incoming metal ions join the metal deposit. This process can be divided into four steps: [Gabe78]

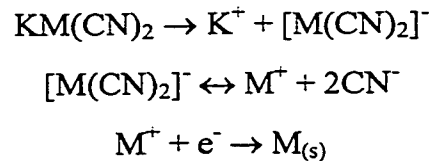
- i. Migration of the ion to the cathode surface through the electrical double layer in which hydration molecules are lost.
- ii. Adsorption of the ion onto the metal surface as an 'adion', or incorporation in an intermediate surface film.
- iii. Diffusion of the adion across the metal surface to a discharge site of minimum surface energy.
- iv. Ionic discharge involving electron transfer (incorporation into crystal lattice).

In simple acid solutions, the metal ion is surrounded by water molecules, and when the ion moves into the diffusion layer, it is believed that the water molecules orient themselves in the direction of the electric field. [Tan93] These water molecules are then lost when the ion reaches the electric double layer, as is shown schematically in Figure 4-1. [Tan93]

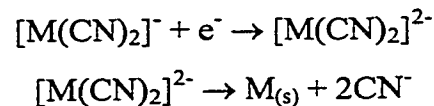
Figure 4-1 Schematic of electrodeposition: (a) hydrated metal ion in bulk solution, (b) hydrated metal ion enters diffusion layer, and (c) metal ion enters electric double layer. [Tan93]



For solutions in which the metal ion is complexed, the metal cation is surrounded by a number of negatively charged anions, and the complex has an overall negative charge. It is not fully understood how the metal ions are discharged from the complex [Lainer70], but it is believed that the deposition proceeds from simple metal ions formed from the dissociation of the complex ion as follows:



The higher polarization for complex ion baths compared to simple ion baths is explained by the low concentration of simple ions in the complex bath. Another explanation for the high polarization is that the complex ions adsorb onto the surface and the subsequent reduction requires a high activation energy. The reduction occurs as follows:



The adsorption of the negatively charged complex ion onto the cathode surface is due to the dipole structure of the complex. The positive end of the complex ion is attracted to the surface, as the complex is deformed by the strong electric field (10^8 V/cm) present in the electric double layer. [Lainer70]

4.2 Theory of Electrocrystallization

Electrocrystallization is the incorporation of the metal atoms into the crystal lattice of the cathode during electroplating. There are two main factors which determine the type of structure which is formed. The first is the current density, which is directly related to the rate of incoming atoms, and the second is the inhibition of the cathode surface by adsorbed substances.

There are various sites on the cathode surface onto which an atom can become attached. The different types of sites are identified in Figure 4-2 [Gabe78] and are numbered in order of increasing free energy. A surface vacancy (1) has minimum energy, but these types of sites are not present in large numbers. Ledge sites (2-4) are favorable for growth because they are repeatable steps. Once an adatom or adion diffuses to a ledge or ledge kink and is incorporated into the lattice, the same ledge structure is present for the next growth step. The nucleation of a new layer (5) requires the most energy.

A screw dislocation mechanism was proposed by Burton [Burton49], and allows growth without the need for nucleation of new layers. In this manner a screw dislocation with the Burgers vector perpendicular to the crystal face grows by the ledge mechanism, winding itself up like a spiral staircase. A diagram of the screw dislocation is given in Figure 4-3. [Gabe78] The screw dislocation mechanism is a rare case in electroplating and operates at low current densities and overpotentials, where there is enough time for the adions or adatoms to diffuse to the growth ledge and the overpotential does not support the formation of new nuclei. This type of growth has been observed for copper plated at low current densities from very pure sulfate solutions. [Pick55]

Figure 4-2 Discharge sites on a growing surface: (1) Surface vacancy, (2) Ledge Vacancy, (3) Ledge Kink, (4) Ledge, and (5) Layer nucleus. [Gabe78]

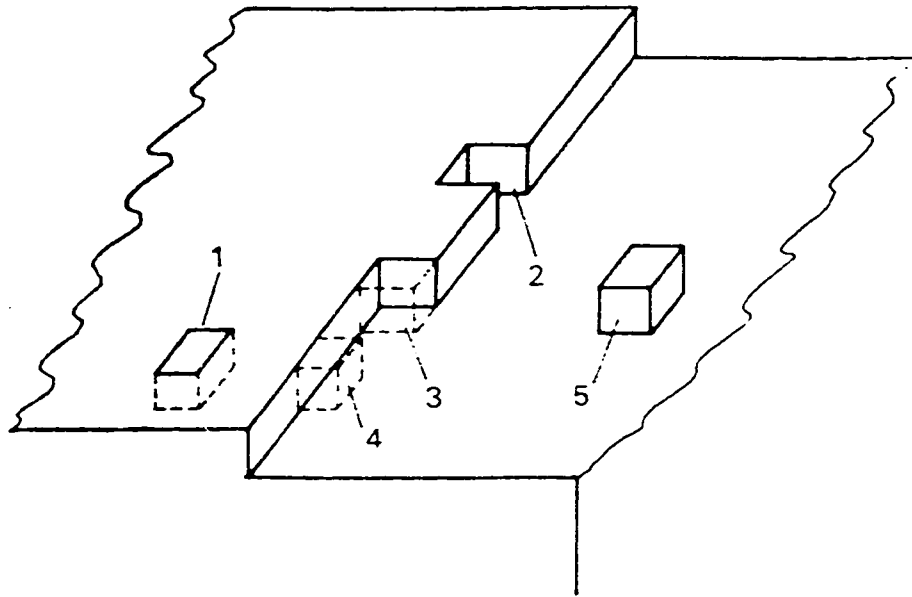


Figure 4-3 Growth screw dislocation with a kinked growth ledge. [Gabe78]



4.2.1 Role of Overpotential and Current Density

The type of structure formed in electroplating is a result of the formation of new nuclei versus the growth of existing nuclei, [Safranek88] as well as the lateral growth versus outward growth. [Winand75][Winand94] It is also known that factors which tend to increase cathode polarization (overpotential) tend to decrease the crystal size. [Safranek88] Polarization increases as the current density increases, so increases in current density also result in a decrease in crystal size. There is a crystallization polarization (η_{cr}) which is part of the total polarization (η), but this polarization is difficult to measure. [Winand94] The use of the total polarization as a single variable does not provide an explanation for the structures observed in electroplating. Winand [Winand75][Winand94] has suggested the use of the following two parameters to explain the structures found in electroplating:

- i. i_c/C_b – the ratio of the current density to the bulk concentration of the metal ions being plated. This parameter can also be given as i_c/i_L – the ratio of the current density to the limiting current density.
- ii. Inhibition intensity – the amount of inhibition due to the presence on the cathode surface of ions other than the ones being plated.

4.2.2 Inhibition

Inhibitors play an important role in determining the structure of electrodeposits, as they are physically or chemically adsorbed on the cathode surface. They usually do not cover the entire surface of the cathode, but favor active sites such as growth ledges. Inhibitors are usually organic, do not usually take part in the reduction reactions at the cathode, but physically impede the pattern of growth.

Additives which are adsorbed at points of high current density (high overpotential) inhibit outward growth and level the deposit surface, while additives which adsorb at points of low current density (low overpotential) inhibit lateral growth, refining the grain structure. [Gabe78] The additive may or may not be absorbed by the growing deposit. Many brightening additives are characterized by the presence of sulfur in the organic molecule, and for nickel deposition two types of additives have been identified: [Gabe 78]

- i. Class I – Additives which produce bright deposits, but without lustre. These additives may reduce stress and are characterized by a =C-SO₂-group. The carbon may be part of an aromatic ring structure or alkylene chain, while the SO₂ part may be sulfonic acid, sulfonate, sulfone or sulfon-amide.
- ii. Class II – Additives which produce lustre in deposits, but often raise internal stress and brittleness. These additives are characterized by unsaturation, e.g. C=O, C=C, N-C=S, N=N.

The mechanism of inhibition in nickel plating has been studied, and it was found that the additives adsorb rapidly and are not affected by the process of nickel deposition. It was found that sulfur is captured in the deposit, but carbon is generally not, which means that the adsorption probably takes place at the sulfur atom and the molecule can be broken during the reduction process, leaving the sulfur in the deposit.

4.3 Structures of Electroplated Deposits

The types of microstructures produced by electroplating single metals have been categorized by Fisher and his co-workers. [Fisher54][Seiter60] Five main growth types have been identified:

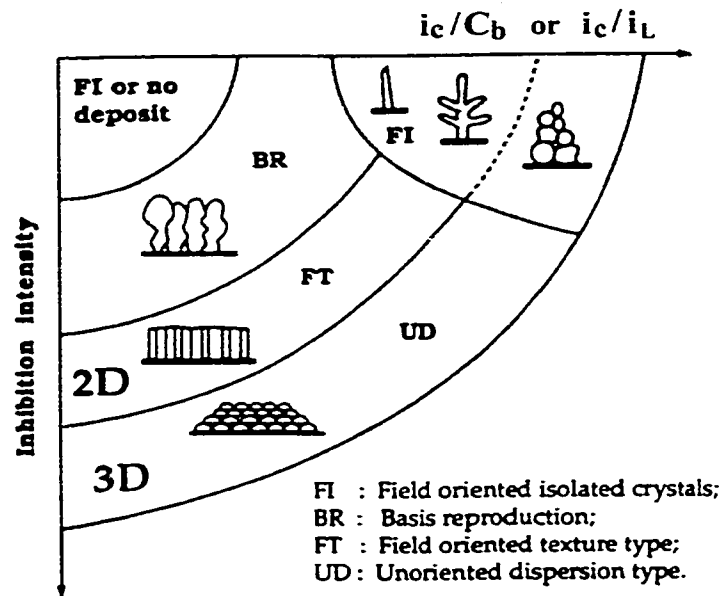
- i. Field oriented isolated crystals (FI) – This type of crystal is observed at low inhibition, and as the current density increases whiskers, prismatic crystals, dendrites and powders are successively formed. These types of deposits are common for silver and tin, metals which have a low inhibition.
- ii. Basis-oriented reproduction (BR) – There is more lateral growth than in the (FI) type, although the crystals may become large enough to trap electrolyte in the deposit. This type of deposit is a coarse columnar structure.
- iii. Twinning intermediate (Z) – This type of structure is considered to be an intermediate between type II (BR) and type IV (FT). Little information is given on this type of structure.
- iv. Field oriented texture (FT) – This type of deposit is formed at fairly strong inhibition and/or high current density. The structure appears as large numbers of grains elongated perpendicular to the cathode surface.
- v. Unoriented dispersion (UD) – This last type of structure is obtained at very high inhibition and/or current density, and is characterized by a large number of fine crystals.

The structure types outlined have been categorized graphically by Winand, and are shown in Figure 4-4. [Winand94] When this study of microstructure was made, the inhibition was related to the exchange current density. Metals such as silver and tin which have a high exchange current density are categorized as having low inhibition, while metals such as nickel and iron which have a low exchange current density are categorized as having a high inhibition. The addition of organic inhibitors to a plating system was found to change the structures to those found at higher inhibitions on the graph.

The structure of copper deposited from sulfate solutions was studied by Barnes and co-workers, and it was found that the structure changes as the current density is changed. [Barnes60][Pick60][Vaughan60] It was found that as the current density was increased the structure changed from the growth of ridges to the formation of platelets, blocks and finally fine polycrystals. It was also noted that impurities in the solution affected the microstructure by lowering the overpotential, resulting in a higher current density necessary to form the same structure compared to a solution which was not 'contaminated'.

The structure of chromium deposited by pulse plating was studied by Tsai, who found that there was a preferred orientation when the α and β chromium phases were electroplated. [Tsai91] Preferred orientation has also been studied by x-ray diffraction in copper deposited from sulfate solutions, [Ye92][O'Keefe78] and the (220) plane was found to have the greatest intensity. It was also noted that the peak intensity of the (220) orientation increased with an increase in polarization to a certain point, after which a further increase in polarization resulted in a more random texture due to the onset of three-dimensional nucleation.

Figure 4-4 Different types of polycrystalline electrodeposits possible as a function of current density and inhibition. [Winand94]



i_c = current density.

C_b = bulk concentration of ions in solution.

I_L = limiting current density.

2D = two-dimensional nucleation.

3D = three-dimensional nucleation.

4.4 Structures of Alloy Plated Electrodeposits

There is presently no general theory permitting the predictions of alloy microstructures formed by electroplating, as impurity and mass transport effects in alloy plating make the reproducibility of results difficult. [Landolt94] In general, the structures produced in alloy plating will follow those found in single metal plating, except that more than one phase may be growing at the same time, and one metal ion may act as an inhibitor for the other metal. Some studies of structure in alloy plating have been made and will be reviewed briefly.

The structures of an 80Sn-20Pb alloy deposited from an organic sulphonate bath by pulsed current electroplating were related to the duty cycle. [Kim96] It was found that as the duty cycle increased (pulse height, pulse current density decreased) the structure observed became more coarse. Preferred orientation was observed in the Sn-rich crystals at high duty cycles, which was lost as the duty cycle was decreased. Similar trends in microstructure were observed in Au-Sn pulsed alloy electroplating, [Sun99-1] where an increase in the duty cycle (ratio of pulse time to overall cycle time) also resulted in a coarsening of the observed microstructure.

The texture of pulse plated Sn-Pb alloys was studied by Chen using x-ray diffraction. [Chen89] In this study, the ratio of peak intensities for the Pb (111) and Pb (200) for samples plated under a range of conditions was made. It was found that this ratio increased with an increase in current density up to 0.75 of the limiting current density, after which an increase in current density resulted in a decrease of the ratio. This result is similar to the findings of Ye [Ye92] for electroplated copper, and is most likely due to the onset of three-dimensional nucleation.

5 Experimental Methods

5.1 Solution Preparation

The solutions for the stability tests, polarization and electroplating experiments were prepared in the following manner:

- i. An empty 250 ml round bottom flask was weighed on a Sartorius Student balance (160 g capacity), and the mass was recorded to the nearest 0.0001 g. After this 6 g of tri-ammonium citrate [$\text{H}_4\text{NO}_2\text{CCH}_2(\text{OH})(\text{CO}_2\text{NH}_4)\text{CH}_2\text{CO}_2\text{NH}_4$] was weighed out, and approximately 20 ml of de-ionized water was added. The ammonium citrate was then dissolved by swirling the flask, resulting in a colourless solution.
- ii. For some of the experiments, between 0.0270 g and 0.1867 g of ethylenediamine ($\text{NH}_2\text{CH}_2\text{CH}_2\text{NH}_2$) was added at this point. The ethylenediamine was added to the solution using an eye dropper, and the solution was again swirled to ensure complete mixing.
- iii. The next addition to the solution was potassium tetrachloroaurate (KAuCl_4). 0.15 g was added to the solution and the solution was then swirled to dissolve the KAuCl_4 , resulting in a colour change from clear to bright yellow.
- iv. 1.8 g of sodium sulfite (Na_2SO_3) was then added to the solution, which was again swirled to ensure mixing. At this point the colour of the solution became a lighter shade of yellow, and the solution was left to stand until it turned colourless. The time for this change to occur varied between 15 minutes and a couple of hours.
- v. 0.45 g of L-ascorbic acid was then dissolved into the solution, changing the colour to very light yellow.
- vi. Tin(IV) chloride ($\text{SnCl}_2 \cdot 2\text{H}_2\text{O}$) was then added to the solution in amounts ranging from 0.06 g to 0.15g.

- vii. For some experiments, 0.03 g of nickel(II) chloride was introduced into the solution at this point. The solution was swirled until the species dissolved, and the colour of the solution changed to light green.
- viii. After the last component of the solution was added and dissolved, the solution was transferred to a 100 ml graduated cylinder, and deionized water was added to give a solution volume of 30 ml.

The mean concentrations and standard deviations of the solution components are given in Table 5-1. It should be noted that the ethylenediamine concentrations are not given in this table, as the concentration of this species was varied in the experiments and will be reported in the next chapter. For some experiments, the tin(IV) chloride concentration was varied, and will also be reported in the next chapter.

Table 5-1 Mean concentrations and standard deviations for solution components.

<u>Solution Component</u>	<u>Mean Concentration (g/l)</u>	<u>Standard Deviation (g/l)</u>
Ammonium Citrate	200.5	1.3
KAuCl ₄	5.1	0.1
Sodium Sulfite	60.1	1.0
L-Ascorbic Acid	15.1	0.2
SnCl ₂ -2H ₂ O	5.1	0.1
NiCl ₂	1.0	0.04

5.2 Solution Stability

A set of solutions was made up in order to determine the affect of ethylenediamine concentration on the stability of the plating solution. The manner of solution preparation was similar to the procedure outlined in section 5-1. Approximately 20 ml of each solution was placed in a clear glass vial and sealed, almost completely filling the vial. The remainder of each solution was placed in another vial, half filling it.

The state of the solutions was monitored each day, and the date at which precipitation occurred was recorded.

5.3 Polarization Experiments

Cathodic polarization tests were carried out on solutions containing varying amounts of ethylene diamine and nickel(II) chloride in order to study the current - voltage relationship of the plating solutions. The polarization tests were performed using an EG&G Model 273 Potentiostat/Galvanostat, scanning at 0.5 mV/s between 0 V and -1.2 V. The cathode was a piece of InP wafer with a 25 nm Ti / 250 nm Au metallization. Stop off lacquer was used to define an area on the front side of the sample, and to cover the backside of the sample. The plating area was calculated using a ruler to measure each side to the nearest $\frac{1}{4}$ mm, and the sample was washed in de-ionized water and dried in air. A piece of platinum foil was used for the anode, and the reference electrode was a saturated calomel electrode.

5.4 Electroplating

Electroplating tests were carried out using a circular polypropylene tank about 6.5 cm in diameter and 5 cm deep. Two polypropylene sample holders were employed, giving a spacing of 37 mm between the anode and the cathode. The cathodes were cleaved pieces of InP or Si wafers coated with a 25 nm Ti / 250 nm Au metallization. The plating area was defined using stop off lacquer, and the backsides of the wafers were protected by stop off lacquer to prevent backside plating.

The plating area ranged between 0.3 cm² and 0.8 cm², and the samples were cleaned in de-ionized water and dried in air. A Dynatronix PR 0.1-10 pulsed current power supply with ON and OFF time ranges of 0 - 9.9 ms was used for the experiments. A pulsed current with an ON time of 2 ms and an OFF time of 8 ms was used for most of the experiments. For the remainder of the experiments a forward pulsed current with an

ON time of 2.4 ms and an OFF time of 6.6 ms followed by a reverse pulsed current with an ON time of 0.4 ms and an OFF time of 0.6 ms was used. The peak current density during plating was measured using an oscilloscope and a 50 Ω resistor connected in parallel with the plating circuit. A picture of the plating circuit is given in Figure 5-1, and a schematic of the plating setup is shown in Figure 5-2. After electroplating, the samples were rinsed with de-ionized water, dried in air, and placed in a sample box, ready for further examination in the scanning electron microscope and x-ray diffractometer.

Figure 5-1 Electroplating apparatus.

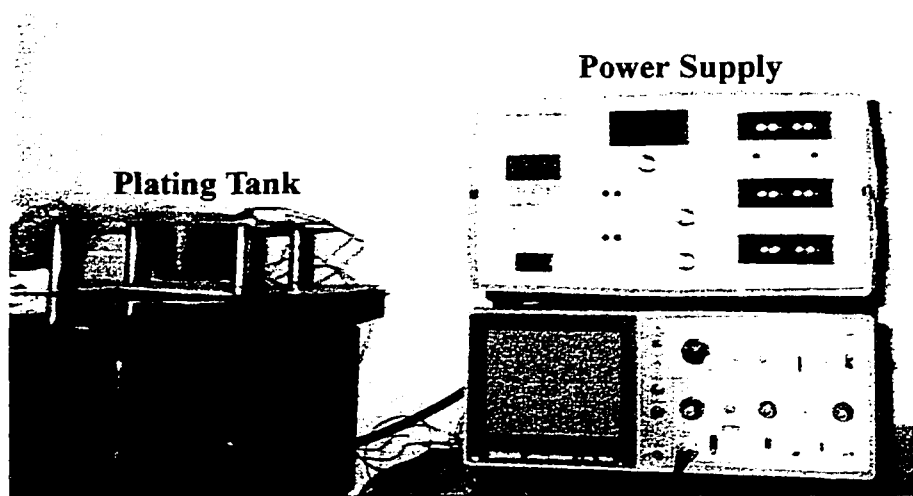
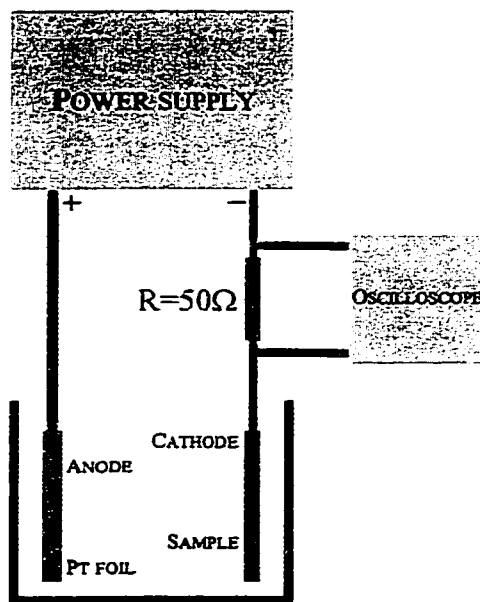


Figure 5-2 Schematic of electroplating setup.



5.5 Scanning Electron Microscope Analysis

5.5.1 Imaging and Thickness Measurements

Imaging of the electroplated coating structure was performed in a JEOL-JSM 6301 FXV field emission scanning electron microscope (FESEM) using an accelerating voltage of 5 kV. Each sample was cleaved so that it could be observed in plan view and in cross section view. The cleaved pieces were attached to aluminum stubs using either copper or carbon tape, and colloidal carbon was applied to ensure electrical connection between the electroplated coating and the stub. The images were collected in secondary electron (SE) mode at working distances between 10 and 15 mm. The aperture size used in the imaging was 50 μm in diameter. For each sample, two plan views were captured, one at 4000X magnification and the other at 15000X magnification.

Each of the cross section samples was imaged in three different places at a magnification of 15000X, and the imaging software was used to measure the coating thickness in three places for each image giving a total of nine measurements. The average and standard deviation of the nine measurements were calculated and are reported in the next chapter.

5.5.2 Energy Dispersive X-ray Analysis

The composition of the electroplated coatings was measured using energy dispersive spectroscopy (EDS) with pure gold and tin standards at an accelerating voltage of 20kV. The samples from the first 63 plating tests were analyzed using the Link eXL (EDS) system and software. With this system, the 70 μm aperture was used with a working distance of 12 mm and a live collection time of 100 s. The beam current was adjusted so that the count rate was between 3000 and 4000 counts per second. For the remainder of the plating experiments, a PGT PRISM IG detector and PGT IMIX software was employed. For this system the 70 μm aperture was again used, but at a working distance of 17 mm. The live collection time remained at 100 s, and the beam current was adjusted so that the count rate was between 3500 and 4500 counts per second. For each sample, 4 areas (1.5 mm by 1.5 mm square) were subjected to EDS analysis, and the average composition of these areas was used in the results.

5.6 X-ray Diffraction

X-ray diffraction was performed on the electroplated samples with a Rigaku RU-200A x-ray diffractometer. The samples were attached to a glass slide using a small amount of grease. The samples were situated so that the x-ray beam was incident on the top of the plated coating. The x-ray detector was rotated between a 2θ range of 10° and 80° at a speed of 1° per minute. The anode used was a rotating copper target, the operating voltage was 40 kV, and the current was 110 mA.

6 Results and Discussion

Table 6-1 gives the composition of the nine solutions which were used for the stability tests, polarization curves and electroplating experiments.

Table 6-1 Components and compositions of solutions used in the experiments.

Solution #	1	2	3	4	5	6	7	8	9
Component	Concentration (g/l) – (mole/l for ethylenediamine)								
Ammonium Citrate	200	200	200	200	200	200	200	200	200
Ethylene-diamine			0.11	0.11	0.01- 0.02	0.05- 0.06	0.01- 0.02	0.01- 0.02	0.01- 0.02
KAuCl₄	5	5	5	5	5	5	5	5	5
Sodium Sulfite	60	60	60	60	60	60	60	60	60
L-Ascorbic Acid	15	15	15	15	15	15	15	15	15
SnCl₂-2H₂O	5	5	5	5	5	5	4	3	2
NiCl₂		1		1					

6.1 Polarization Curves and Stability Tests

6.1.1 Stability of Au-Sn Plating Solutions

Stability tests were performed for solutions containing between 0 and 0.135 M of ethylenediamine in the plating solution. One test was performed for each ethylenediamine concentration, and no NiCl₂ was present in the solutions. The stability

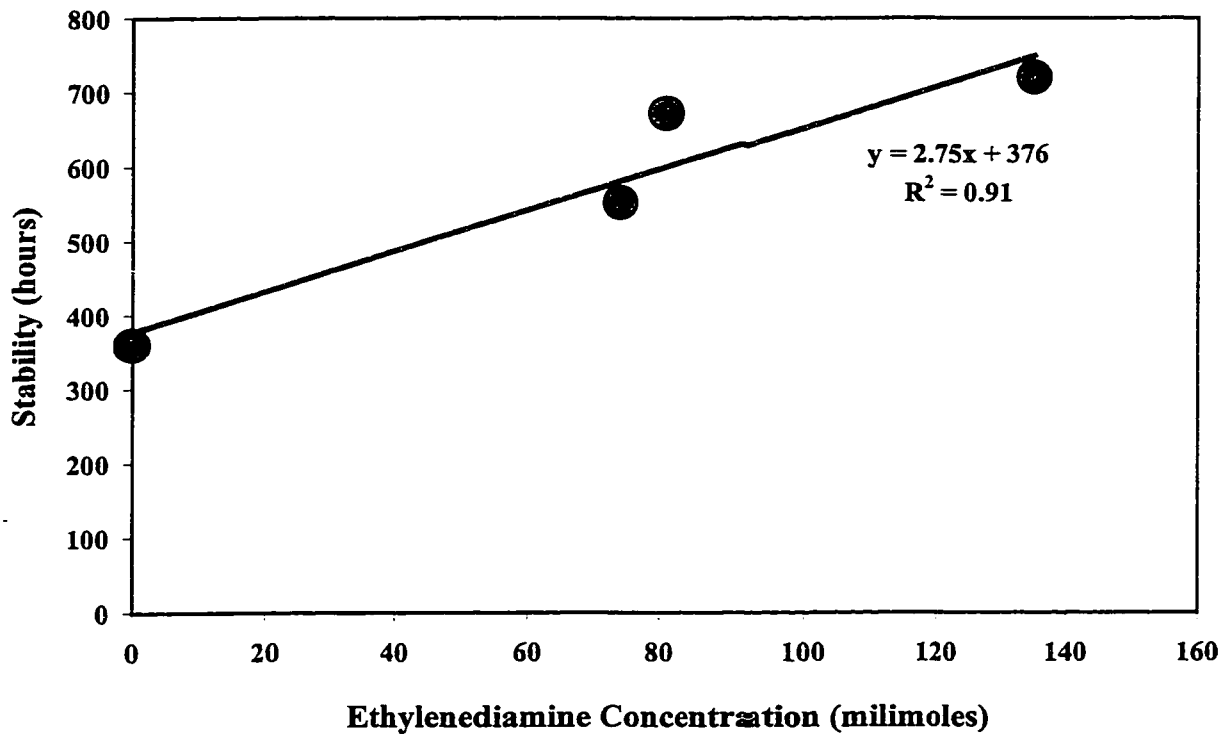
times for solutions containing varying concentrations of ethylenediamine are shown in Figure 6-1, and show an increase in stability time with an increase in ethylenediamine concentration. The stability follows a linear trend for the ethylenediamine concentrations tested, and a stability equation based on a linear regression of the data can be made:

$$\text{Stability} = 2.75C_{\text{EDA}} + 376 \quad (15)$$

C_{EDA} = concentration of ethylenediamine in millimoles.

From the graph, the expected stability for a gold-tin plating solution containing no ethylenediamine (solution 1) is 16 days, while the stability for a solution containing 0.11 M ethylenediamine (solution 3) is 28 days or almost double.

Figure 6-1 Solution stability versus ethylenediamine concentration.



The Au³⁺ concentration in all the solutions was 0.013 M. Two molecules of ethylenediamine are required to form the gold-chloride-ethylenediamine complex [Thorpe50], while one molecule of ethylenediamine is required to form the gold-sulfite-ethylenediamine complex. From this information combined with the stability data it is presumed that not all of the ethylenediamine added to the solution forms complexes with gold in solution, since the solution stability keeps increasing beyond an ethylenediamine concentration of 0.026 M. It is unknown whether the complex formed in the plating solutions is a gold-chloride-ethylenediamine complex or a gold-sulfite-ethylenediamine complex or some combination thereof. It is presumed that the complex formed is a gold-sulfite-ethylenediamine complex, since after the ethylenediamine is added to the solution, sodium sulfite is added resulting in a color change from yellow to clear, signaling a reaction.

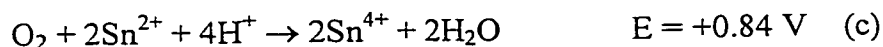
The stability results reported in Figure 6-1 are for the solutions placed in 20 ml glass vials, which were filled about 1/2 full and sealed. The stability of the same solutions in 20 ml glass vials nearly completely filled was much less in all cases but one. This means that the oxygen reduction reaction could be related to the solution stability. For an acidic solution, the oxygen reduction reaction is: (P_{O₂} = 0.211 atm., [H⁺] = 3.16x10⁻⁷ M at a pH of 6.5)



The corresponding oxidation reaction is most likely: ([Sn²⁺] = 2.2x10⁻² M (5g/l SnCl₂-2H₂O), and setting [Sn⁴⁺] = 1x10⁻⁷ M as a reasonable small concentration, since the initial concentration is 0)



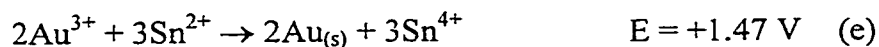
Combining the reactions gives an overall reaction of:



From equation (1) $\Delta G = -324$ kJ/mol, so the reaction products are thermodynamically favored. The stability of the solution is limited by the reduction of the gold ions by the tin in solution. The reduction of gold is given by: ($[\text{Au}^{3+}] = 1.3 \times 10^{-2}$ M (5 g/l KAuCl_4))



Combining reactions (b) and (d) gives:

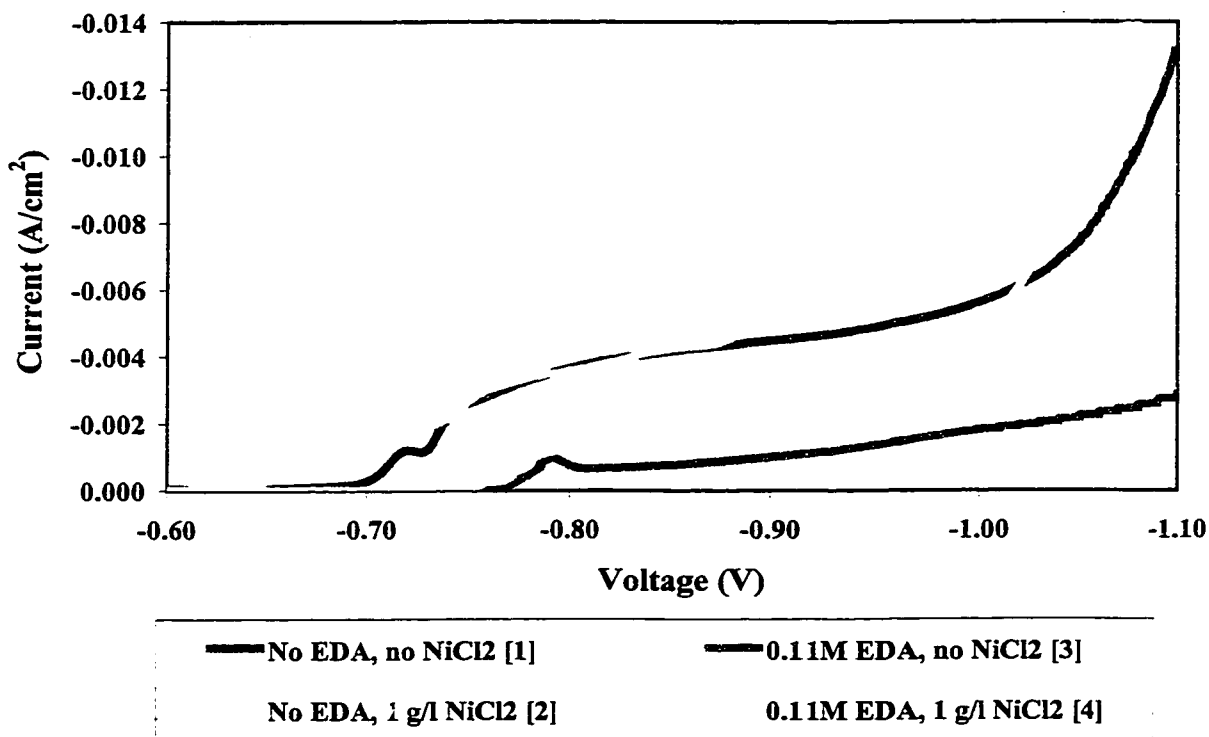


For reaction (e), $\Delta G = -851$ kJ/mol, so that the forward reaction is favored. Reactions (c) and (e) compete with one another in the solution, so when the oxygen concentration in the solution drops low enough, reaction (e) becomes the only reaction possible, leading to precipitation of gold. This would explain the premature precipitation of the solution in the 20 ml glass vials nearly completely filled and sealed. The free energy values given in this analysis serve only as a rough guide, as the potentials of gold and tin are drastically changed by the formation of complexes in the solution.

6.1.2 Polarization Curves for Au-Sn Plating Solutions

The cathodic polarization data is plotted in Figures 6-2 and 6-3 for the solutions used in this study. Figure 6-2 shows the effects of ethylenediamine and NiCl_2 additions to the Au-Sn plating solution. For all of the curves, the initial, gently sloping part corresponds to the potentials at which mostly gold is deposited. At a potential of about -0.70 V, the curve for solution 1, containing neither ethylenediamine nor NiCl_2 , begins to rise sharply until it reaches a current density of 3.0 mA/cm^2 . This rise is related to the tin reduction reaction and its inclusion in the deposit, as was also reported in a previous polarization study of this solution. [Sun99-2]

Figure 6-2 Polarization curves for solutions containing varying amounts of ethylenediamine and NiCl₂.



The curve for solution 2 containing 1 g/l NiCl₂ and no ethylenediamine begins to rise at a potential of -0.65 V, so the addition of NiCl₂ to the solution increases the potential (decreases the polarization) for tin reduction. Both curves are nearly identical between -0.75 and -0.87 V, and the curve for solution 2 shows a second rise at potentials lower than -0.87 V. The reduction reaction for the second rise is not known since the highest current density plated was 3.6 mA/cm², but it is possibly the nickel reduction reaction.

The cathodic polarization curve for solution 3 containing 0.11 M ethylenediamine is much lower than the other curves, as the cathode polarization is increased, most likely because ethylenediamine forms a stable complex with the gold and possibly tin ions. Solution 4 containing 0.11 M ethylenediamine and 1 g/l NiCl₂ shows less polarization for

tin reduction than solution 3, similar to the decrease in polarization observed in solution 2 with the addition of NiCl_2 to solution 1. Natarajan [Natarajan84] reports that nickel acts as a depolarizer, which is in agreement with the results reported here. The addition of ethylenediamine decreases the potential at which the tin reduction begins (increases the polarization), from -0.70 V for solution 1 to -0.77 V for solution 3. The large increase in polarization for solution 3 is detrimental from an electroplating standpoint, as the range of current densities possible for plating is very small, from $0-1$ mA/cm^2 , compared with $0-5$ mA/cm^2 for solution 1.

There is also a second rise in the polarization curve for solution 4 at -0.87 V, although the rise is much smaller than that observed for solution 2. This rise corresponds to the inclusion of nickel in the deposit which is observed at current densities of 1.4 mA/cm^2 and higher. It is possible for solution 4, that ethylenediamine forms a complex with the nickel ions which is reduced to solid nickel at the cathode. Ethylenediamine is known to form a complex with nickel, as it has been used effectively for nickel stripping solutions. [Natarajan84] The addition of both ethylenediamine and NiCl_2 to the Au-Sn plating solution is detrimental to the deposition of Au-Sn solder for two reasons:

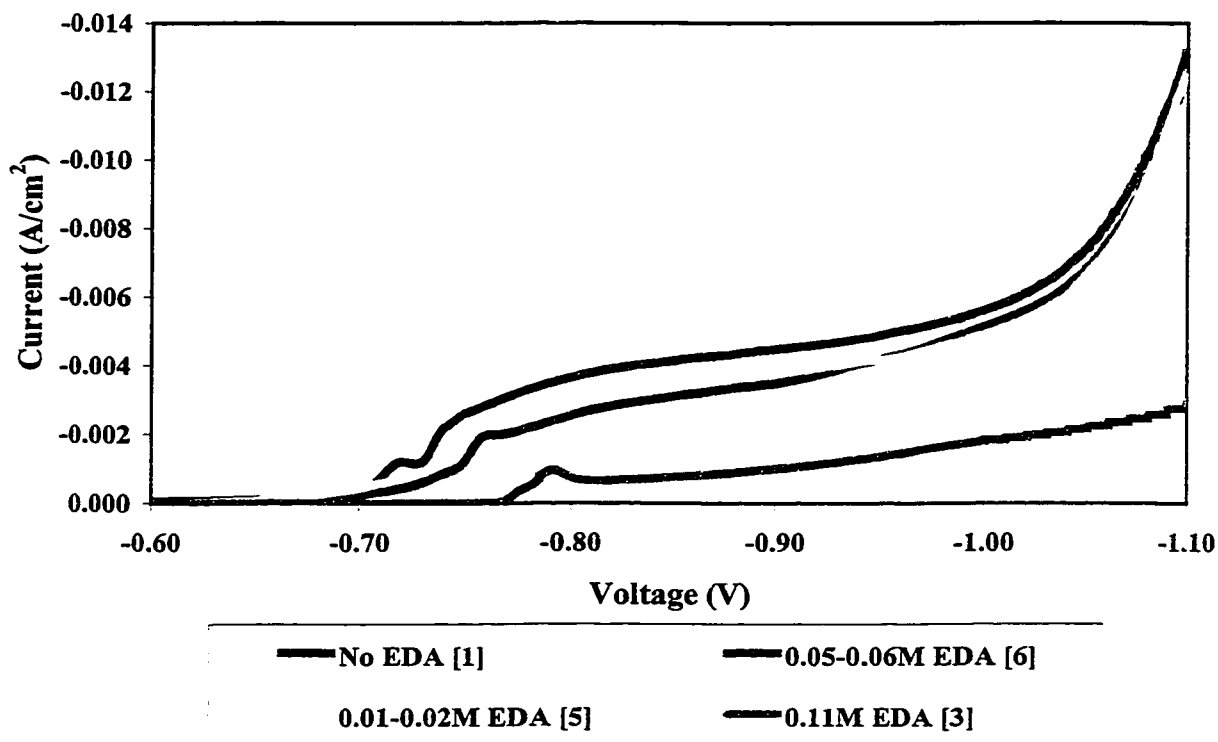
- i. The polarization is increased to the point that electroplating is only possible at current densities below 2 mA/cm^2 , resulting in low deposition rates and low tin contents.
- ii. The inclusion of nickel in the deposit is not desired for this project.

For these reasons, NiCl_2 was not further used in the plating solutions containing ethylene diamine.

Figure 6-3 shows the effects of different concentrations of ethylenediamine on the Au-Sn plating solution. Solutions 1 and 3 from Figure 6-2 are plotted along with two other solutions, solution 5 containing $0.01\text{M}-0.02\text{M}$ ethylenediamine and solution 6 containing $0.05-0.06\text{M}$ ethylenediamine. As the concentration of ethylenediamine in the solution increases, the polarization also increases, while the range of current densities

available for electroplating decreases. For all the polarization curves plotted in Figures 6-2 and 6-3 the sharp rise at potentials less than -1.0 V is due to the hydrogen reduction reaction which is accompanied by hydrogen gas evolution at the cathode and results in a 'burned' deposit. The effects of the change in polarization caused by the addition of ethylenediamine on the composition and structure of the Au-Sn deposit were then studied.

Figure 6-3 Polarization curves for solutions containing varying amounts of ethylenediamine.



6.2 Electroplating Tests

The error in the composition measurements from the energy dispersive x-ray analysis is approximately ± 1 at.% for the Sn content at 50 at.% Sn. The total error in the measurements is made up of the absolute error in the EDS analysis combined with the standard deviation of the Sn composition from four areas measured on each sample. The absolute error (ΔZ) for the EDS analysis is given by:

$$\Delta Z \geq 2.33 Z * 2 N_p^{1/2} / N_{p-b} \quad (19)$$

Z = concentration as a fraction.

N_p = number of counts in peak (including background).

N_{p-b} = number of counts in peak (excluding background).

For a Sn concentration of 50 at.%, the absolute error in the EDS analysis is about 0.5 at.% for the number of x-ray counts collected. As the Sn content decreases, the absolute error decreases slightly. The total error in composition for the data plotted in Figures 6-4 through 6-7 is about the size of the data point. All the electroplating tests were carried out with an ON time of 2 ms and an OFF time of 8 ms unless otherwise noted. The KAuCl_4 concentration in all the solutions was 5 g/l, giving an Au^{3+} concentration of 1.3×10^{-2} M. The $\text{SnCl}_2 \cdot 2\text{H}_2\text{O}$ concentration in the solutions was 5 g/l ($[\text{Sn}^{2+}] = 2.2 \times 10^{-2}$ M) unless otherwise noted.

6.2.1 Composition of Au-Sn Deposits

Figure 6-4 shows the gold and tin composition of the deposits plated from solutions 1-4, and corresponds to the polarization curves in Figure 6-2. For solution 1, the deposit contains between 14 and 17 at.% Sn at current densities ranging from 1.2 – 1.8 mA/cm^2 . The tin content then increases to near 50 at.% between 1.8 and 2.4 mA/cm^2 , and remains at this composition for current densities up to 3.6 mA/cm^2 . Comparison of

the composition results for solution 1 (Figure 6-4) with its polarization curve (Figure 6-2) shows that the gold-rich compositions up to 1.8 mA/cm^2 coincide with the rise in the polarization curve at -0.70 V . As the polarization curve begins to flatten out and approach the limiting current density, the tin concentration in the deposit increases to 50 at.%.

With the addition of 1 g/l NiCl_2 (solution 2), the tin concentration in the deposit rises slightly to 17 at.% at a current density of 1.2 mA/cm^2 . The behavior of the tin concentration with respect to an increase in current density then becomes somewhat erratic between 1.4 and 2.4 mA/cm^2 , ranging between 18 and 50 at.%. It is difficult to correlate the composition to the polarization curve for this solution (Figure 6-2), as the polarization curve rises gently in this range. The tin concentration in the deposit for solution 2 is greater than for solution 1 between 1.2 and 2.0 mA/cm^2 , which can be related to the decreased polarization for solution 2 due to the addition of NiCl_2 .

For solution 3, the addition of 0.11 M ethylenediamine to the plating solution decreases the tin content in the deposit compared to solution 1 at current densities greater than 1.8 mA/cm^2 . This result can be explained by observing the polarization curve (Figure 6-2), which shows a rise in current density between -0.77 and -0.79 V corresponding to the reduction of the tin ions to metal at the cathode, followed by a decrease in current density between -0.79 and -0.81 V . The drop in current density with an increase in cathodic polarization is indicative of a lowered tin deposition rate. The tin content in the deposit never exceeds 20 at.% and 'burned' deposits were observed at current densities above 1.8 mA/cm^2 , where hydrogen reduction is present.

When 1 g/l NiCl_2 and 0.11 M ethylenediamine are present in the solution (solution 4), the tin concentration in the deposit increases with an increase in current density between 1.2 and 2.0 mA/cm^2 . The tin concentration reaches about 28 at.% between 1.6 and 2.0 mA/cm^2 and then declines with a further increase in current density. The tin concentration does not reach 50 at.%, as in solution 2, because nickel is also deposited at a current density of 1.4 mA/cm^2 and higher. The combined total of the tin

and nickel concentrations in the deposits plated at current densities between 1.6 and 2.4 mA/cm² is between 40 and 48 at.%, so the nickel is deposited in place of the tin and not the gold. The nickel deposition begins at 1.4 mA/cm², which is near the second rise of the polarization curve at -0.87 V (Figure 6-2).

Figure 6-4 Sn content vs. average current density for varying ethylenediamine and NiCl₂ concentration.

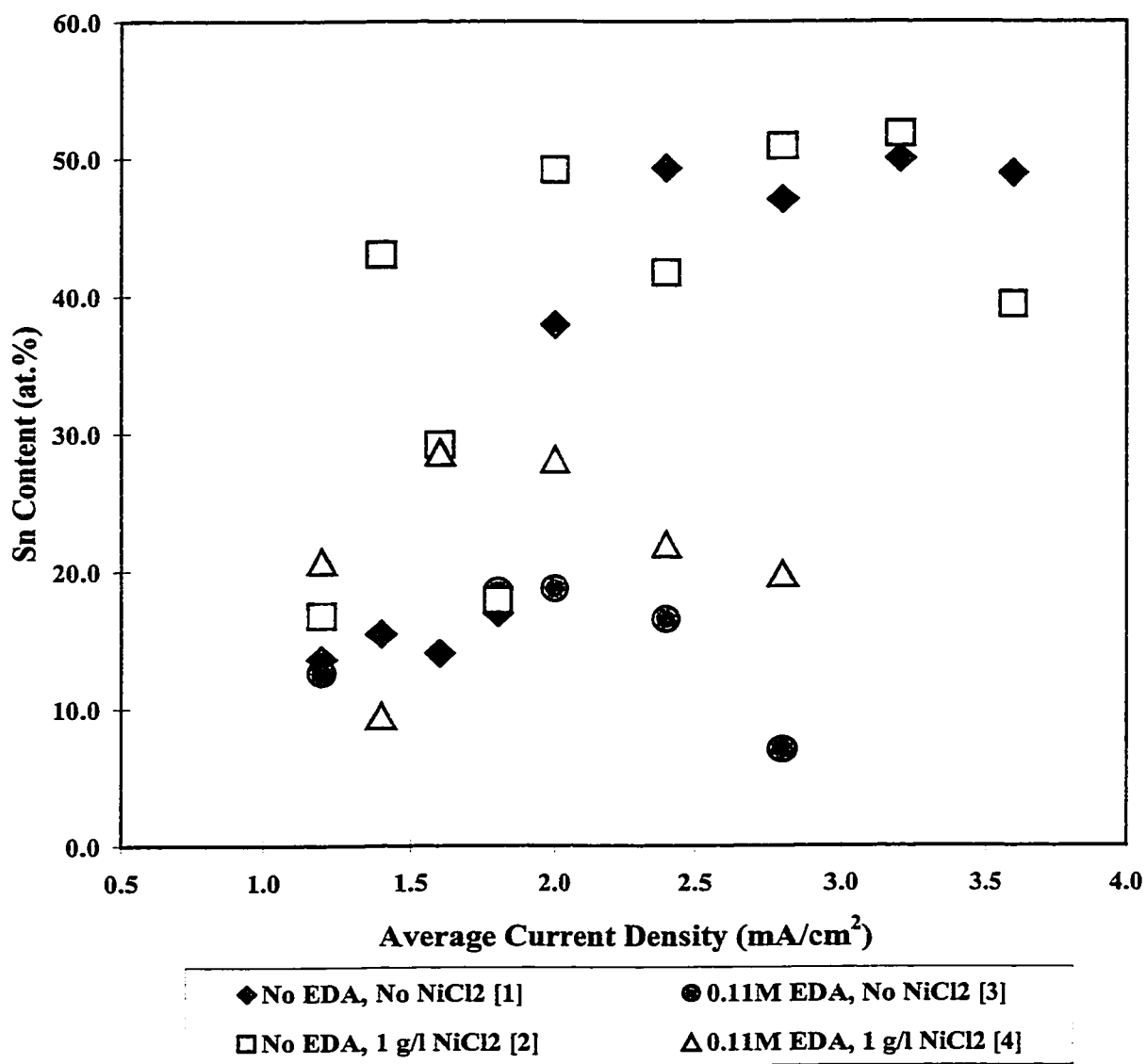


Figure 6-5 shows the gold and tin composition of the deposits plated from solution 5, which contains between 0.01 and 0.02 M ethylenediamine and corresponds to the polarization curve in Figure 6-3. At current densities between 1.0 and 2.2 mA/cm², there is an increase in the tin content in the deposit from 10 to 50 at.% Sn, although there is a large amount of variability in the data. This current range corresponds to the near vertical rise in the polarization curve (Figure 6-3) at -0.74 V. Between 2.2 and 3.2 mA/cm², the tin content remains close to 50 at. % and falls off at current densities greater than 3.2 mA/cm², as hydrogen evolution and a 'burned' deposit are observed. No measurable difference in the composition of the deposit was observed for samples plated with a 2 ms forward pulse and 8 ms OFF time compared to a 2.4 ms forward pulse, 0.4 ms reverse pulse and 7.2 ms OFF time.

Figure 6-6 shows the tin composition plated from solutions 1, 3 and 6, containing concentrations of 0, 0.11 and 0.05-0.06 M of ethylenediamine respectively. When no ethylenediamine is present in the solution (solution 1), the 50 at.% Sn plateau is reached at 2.4 mA/cm², while at a concentration of 0.05-0.06 M ethylenediamine the plateau begins at a current density of 1.4 mA/cm². These results are consistent with the shift of the limiting current density for tin deposition to lower current densities at higher ethylenediamine concentrations in the polarization curves (Figure 6-3). The increase in polarization caused by the addition of ethylenediamine to the gold-tin plating solution favors tin deposition at ethylenediamine concentrations up to 0.05-0.06 M, but not at an ethylenediamine concentration of 0.11 M.

Figure 6-5 Sn content vs. average current density for an ethylenediamine concentration of 0.01-0.02 M (solution 5).

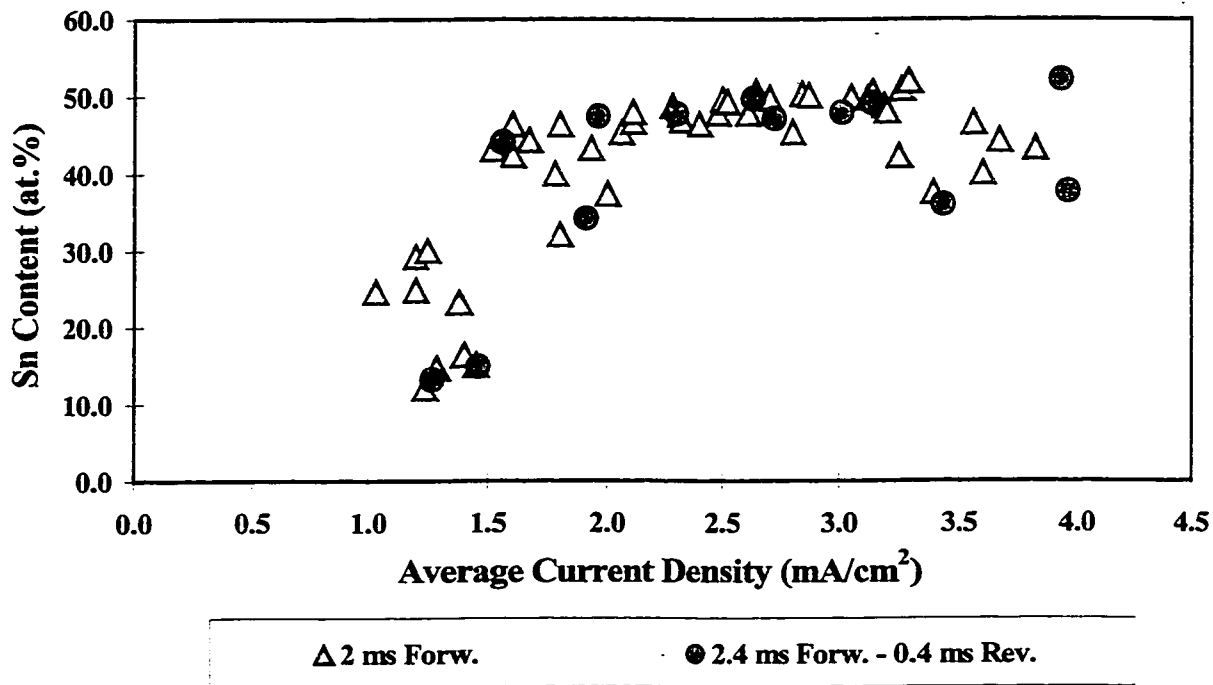


Figure 6-6 Sn content vs. average current density for varying ethylenediamine concentration.

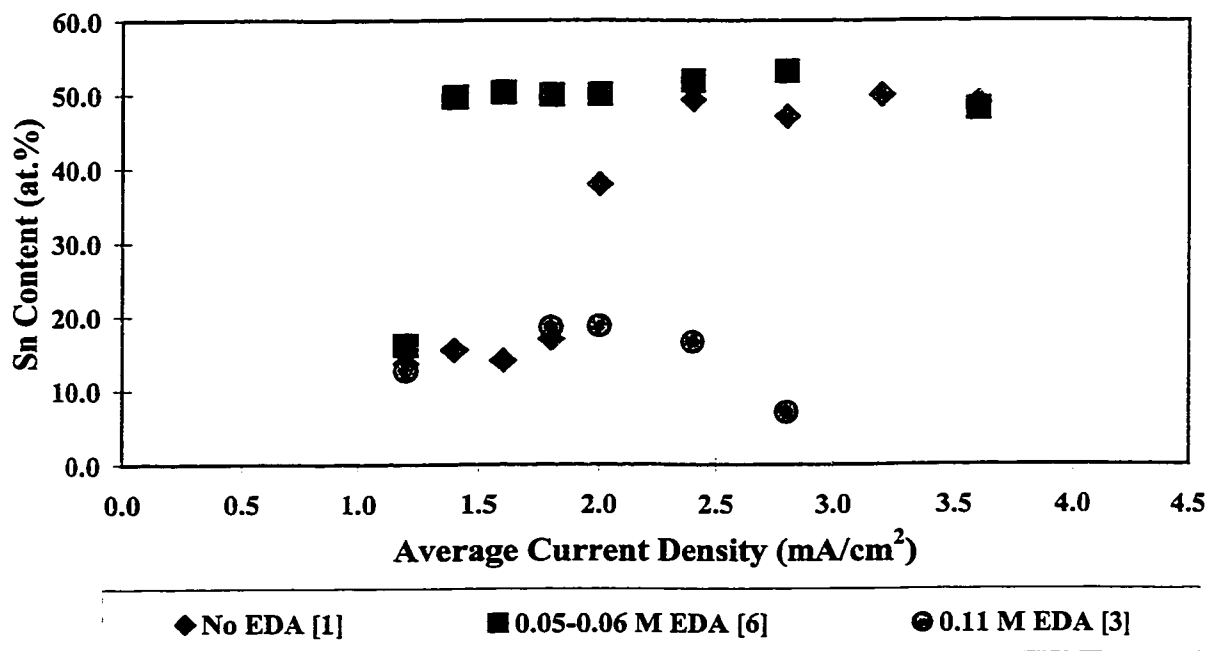
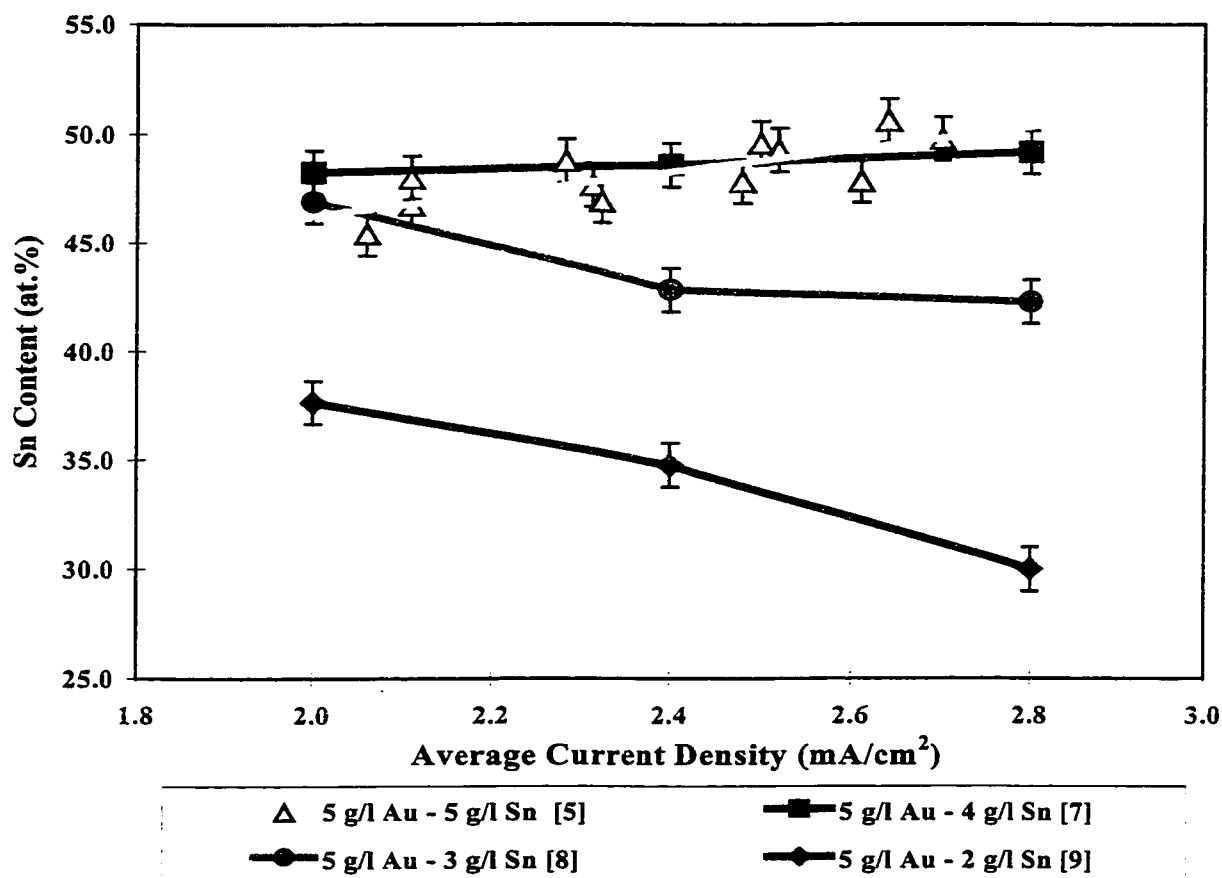


Figure 6-7 shows the effects of changing the $\text{SnCl}_2 \cdot 2\text{H}_2\text{O}$ concentration in the solution on the concentration of tin in the deposit. The $\text{SnCl}_2 \cdot 2\text{H}_2\text{O}$ concentration was varied between 2 and 5 g/l while the ethylenediamine concentration was fixed at 0.01-0.02 M (solutions 5, 7-9). The plating tests were performed at between 2.0 and 2.8 mA/cm^2 , which is the range for the tin plateau in the deposit composition results in Figure 6-5. As the tin content in the solution decreases, the tin content in the deposit also decreases. With pulse plating it is possible to match the concentrations of the metal ions in solution with that of the composition of the deposit. [Leidheiser73] Because the pulsed current is near the limiting current density for tin and gold deposition, the metal content in the deposit should be the same as the metal ion content in the solution. [Landolt94]

Figure 6-7 Sn content vs. average current density for varying $\text{SnCl}_2 \cdot 2\text{H}_2\text{O}$ concentration and an ethylenediamine concentration of 0.01-0.02 M.



The gold ion concentration in a solution containing 5 g/l KAuCl_4 is 0.013 M, while the tin ion concentration in a solution containing 5 g/l $\text{SnCl}_2 \cdot 2\text{H}_2\text{O}$ is 0.022 M. The atomic Sn/Au ratio for this solution is 0.63/0.37, while for a solution containing 5 g/l KAuCl_4 and 2 g/l $\text{SnCl}_2 \cdot 2\text{H}_2\text{O}$ the Sn/Au ratio is 0.41/0.59. For all the solutions, the tin concentration in the deposit is less than the tin ion concentration in the solution. One explanation for this discrepancy could be that some of the Sn^{2+} has been oxidized to Sn^{4+} either by a reaction at the anode ($\text{Sn}^{2+} \rightarrow \text{Sn}^{4+} + 2e^-$), or by the reaction with oxygen ($\text{O}_2 + 2\text{Sn}^{2+} + 4\text{H}^+ \rightarrow 2\text{Sn}^{4+} + 2\text{H}_2\text{O}$). Both Sn^{2+} and Sn^{4+} ions are present at the cathode making up the total Sn ion concentration, but only Sn^{2+} is reduced to metal while the Sn^{4+} ions are reduced to Sn^{2+} . In this manner the tin concentration in the deposit would be less than in the solution as even though both the gold and tin are reduced under diffusion control, not all the tin ions that attach to the deposit surface are plated in one step. A recently reported gold-tin plating solution based on cyanide used Sn^{4+} in the form of SnO_3^{2-} to electroplate gold-tin deposits near the eutectic composition. [Holmbom98]

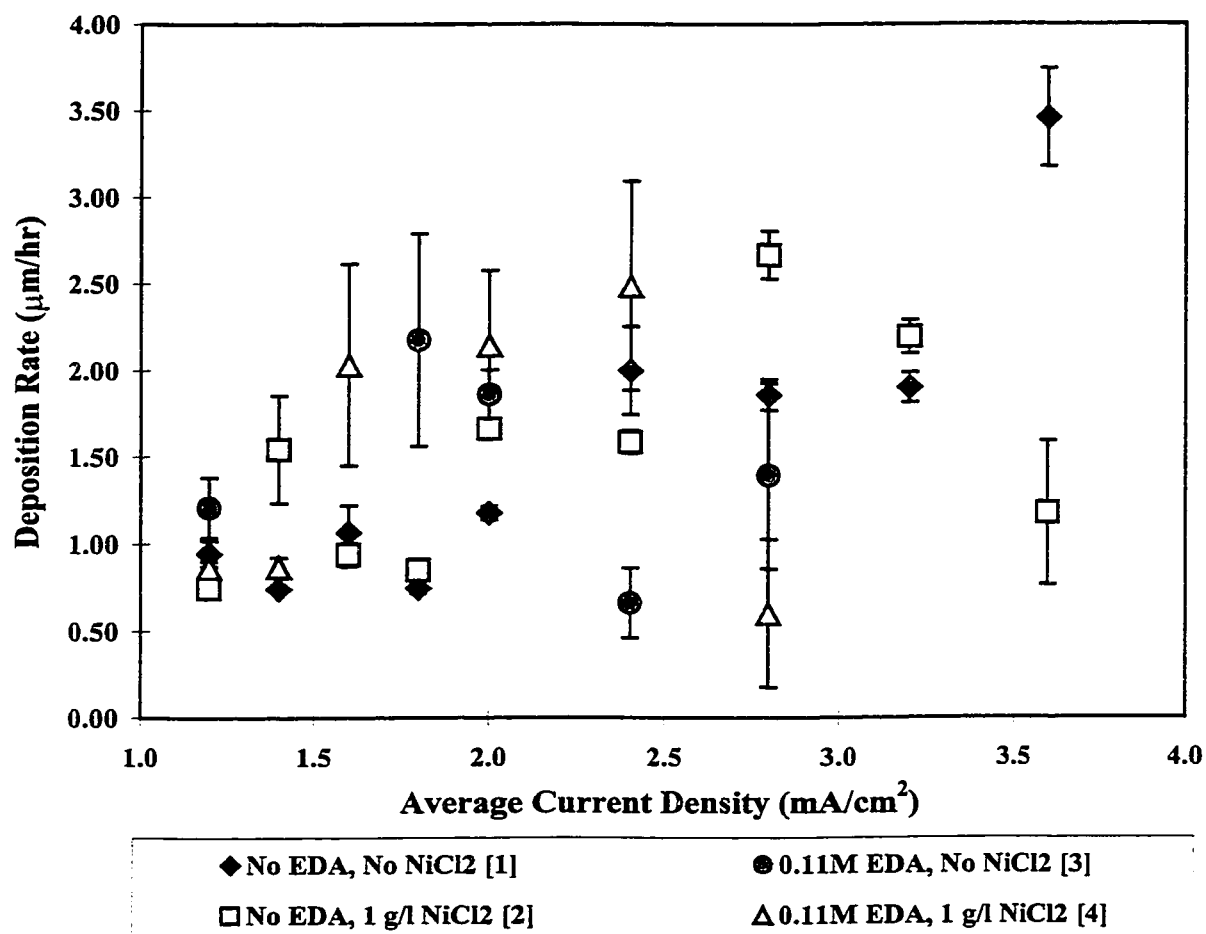
6.2.2 Plating Rate and Current Efficiency

The plating rate was calculated by making thickness measurements on the SEM cross section images of the electroplated deposits. Three images were obtained for each deposit, and three thickness measurements were made on each image for a total of nine. The average thickness and standard deviation were calculated for each deposit and divided by the plating time to give the average plating rate. The error bars in Figures 6-8 through 6-11 represent plus or minus one standard deviation of the plating rate.

The plating rate of solutions 1-4 is shown in Figure 6-8. The addition of 1 g/l NiCl_2 to the base plating solution does not have a discernable effect on the deposition rate when comparing the results from solution 1 (no ethylenediamine, no NiCl_2) and solution 2 (no ethylenediamine, 1 g/l NiCl_2) at current densities between 1.2 and 3.2 mA/cm^2 . At a current density of 3.6 mA/cm^2 , the plating rate for solution 2 is much lower. The

addition of 0.11 M ethylenediamine to these solutions appears to increase the plating rate at current densities between 1.2 and 1.8 mA/cm². The plating rate for solution 3 (0.11 M ethylenediamine, no NiCl₂) decreases sharply above 1.8 mA/cm², and the same drop in deposition rate is observed for solution 4 (0.11 M ethylenediamine, 1 g/l NiCl₂) above 2.4 mA/cm². The drop in plating rate for these solutions is due to the start of the hydrogen reduction reaction. The other effect that the addition of ethylenediamine to the plating solution has on the deposits is that the roughness increases, as noted by the large error bars for these solutions.

Figure 6-8 Plating rate of solutions containing varying amounts of ethylenediamine and NiCl₂.



The effect of ethylenediamine additions on the plating rate is shown in Figure 6-9. The error bars represent the standard deviation of the thickness measurements. An increase in the error represents an increase in deposit roughness. In Figure 6-10, linear regressions were made from the data for solution 1 (no ethylenediamine), solution 5 (0.01-0.02 M ethylenediamine) and solution 6 (0.05-0.06 M ethylenediamine). The equations are given below, and are only a rough guide for measuring the current efficiency since the change in plating rate is minimal with the addition of ethylenediamine and the linear regressions for the data from the solutions containing no ethylenediamine and 0.01-0.02 M ethylenediamine have a poor fit.

$$\text{No ethylenediamine:} \quad R_d = 0.64 i_c \quad (16)$$

$$0.01\text{-}0.02 \text{ M ethylenediamine:} \quad R_d = 0.74 i_c \quad (17)$$

$$0.05\text{-}0.06 \text{ M ethylenediamine:} \quad R_d = 0.91 i_c \quad (18)$$

R_d = plating rate in $\mu\text{m}/\text{hour}$.

i_c = average current density in mA/cm^2 .

The first step in calculating the current efficiency is to calculate the theoretical thickness plated in one hour using equation (5). For this calculation $2.4 \text{ mA}/\text{cm}^2$ is used, as for each of the three solutions AuSn ($\rho = 11.7 \text{ g}/\text{cm}^3$) is plated at this current density, and the electrochemical equivalent ($E_{c,a}$) for AuSn is calculated to be $6.43 \times 10^{-4} \text{ g}/\text{C}$ from equation (4) ($E_c(\text{Au}) = 6.8 \times 10^{-4} \text{ g}/\text{C}$, $E_c(\text{Sn}) = 6.1 \times 10^{-4} \text{ g}/\text{C}$). The theoretical plated thickness after one hour at $2.4 \text{ mA}/\text{cm}^2$ is calculated to be $4.78 \mu\text{m}$. The second step is to find the actual plated thickness at $2.4 \text{ mA}/\text{cm}^2$ from equations (16), (17) and (18), then using equation (7) to find the current efficiency. In this manner, the current efficiencies at an average current density of $2.4 \text{ mA}/\text{cm}^2$ of the solutions containing varying amounts of ethylenediamine are:

No ethylenediamine:	32%
0.01-0.02 M ethylenediamine:	37%
0.05-0.06 M ethylenediamine:	46%

In comparison, the current efficiency from the cyanide based gold-tin plating solution reported by Holmbom [Holmbom98] is 55% at 45°C with agitation, a current density of 8 mA/cm² and a plating rate of 9 μm/hour. The current efficiency increases with an increase in ethylenediamine content up to a concentration 0.05-0.06 M. A decrease in current efficiency is due to competing reduction reactions, such as hydrogen evolution. In the case of the gold-tin plating solution studied here, the competing reduction reaction is likely $\text{Sn}^{4+} + 2e^- \rightarrow \text{Sn}^{2+}$. The addition of ethylenediamine to the plating solution most likely decreases the amount of Sn^{4+} present by stabilizing the Au^{3+} ions by preventing the reaction $2\text{Au}^{3+} + 3\text{Sn}^{2+} \rightarrow 2\text{Au}_{(s)} + 3\text{Sn}^{4+}$, or else by stabilizing the Sn^{2+} ions.

Figure 6-9 Plating rates for solutions containing varying amounts of ethylenediamine.

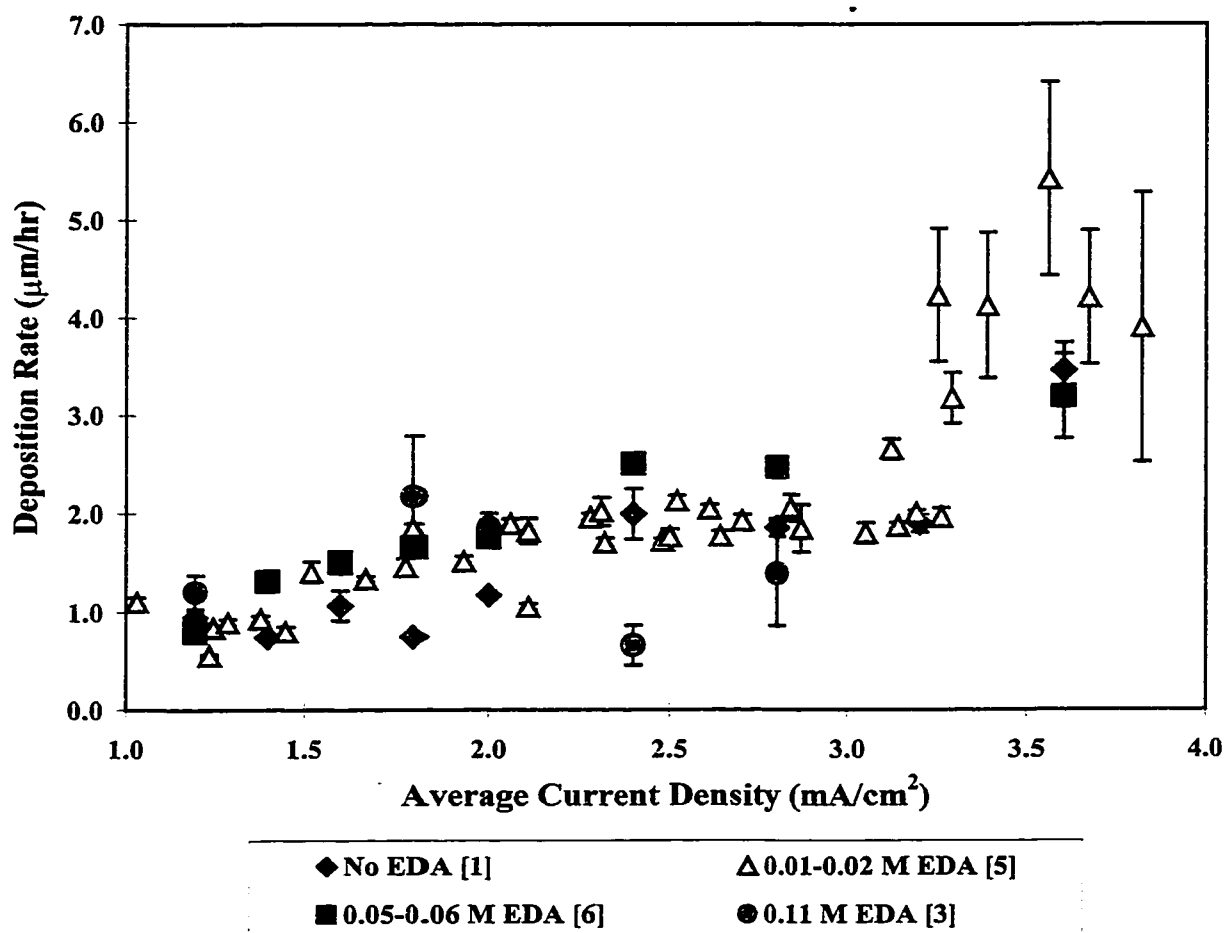


Figure 6-10 Plating rates for solutions containing varying amounts of ethylenediamine.

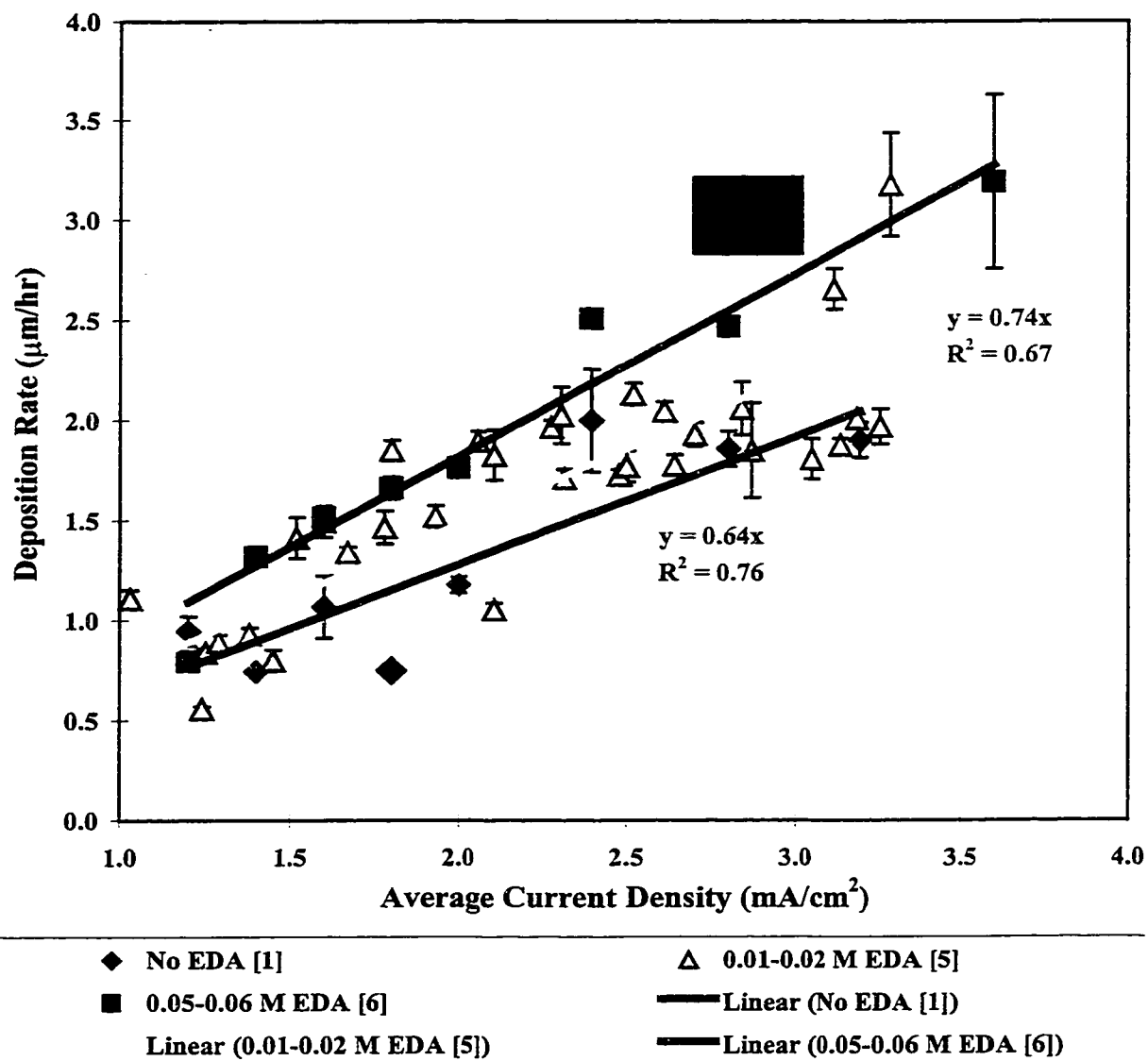
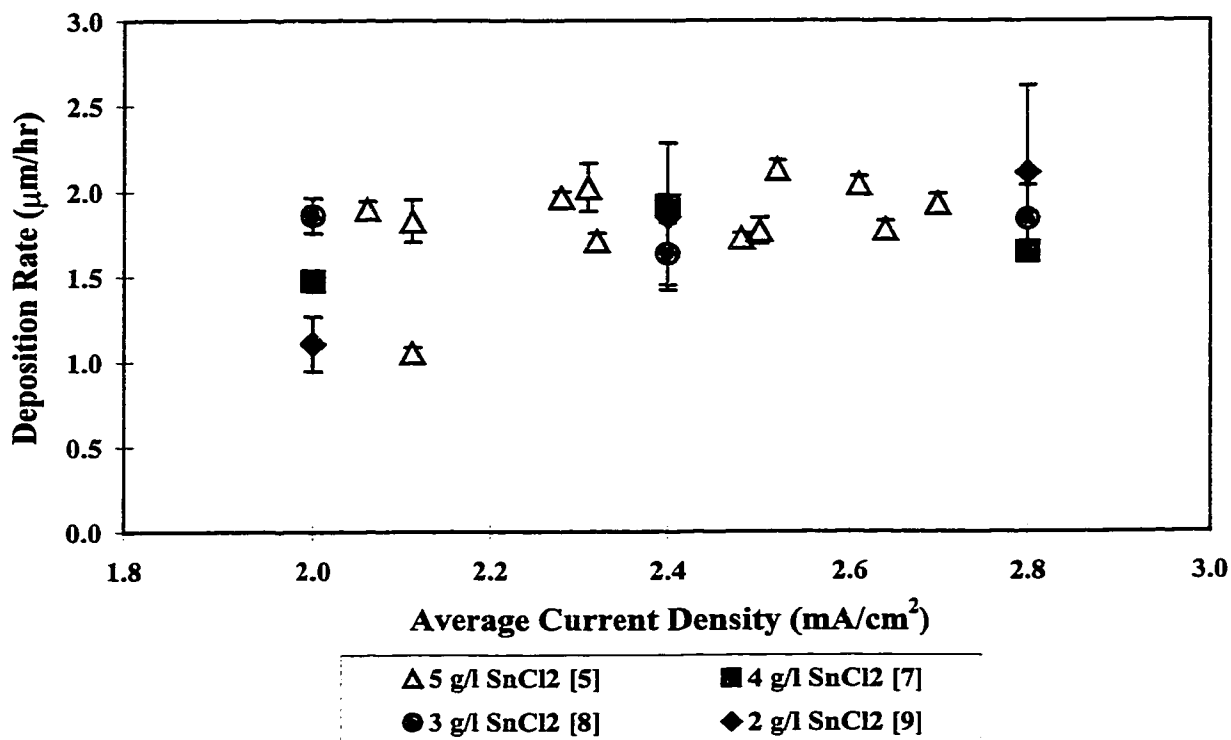


Figure 6-11 shows the effect of the tin concentration in the solution on the deposition rate. There is no observable change in the deposition rate as the $\text{SnCl}_2 \cdot 2\text{H}_2\text{O}$ content of the solution is varied between 2 and 5 g/l. The standard deviation of the data increases with a decrease in tin content signifying an increase in deposit roughness, matching the observations made in the following section from the cross section images.

Figure 6-11 Plating rate of solutions containing varying SnCl₂·2H₂O concentrations and an ethylenediamine concentration of 0.01-0.02 M.



6.3 Deposit Structure

All the electroplating tests were carried out with an ON time of 2 ms and an OFF time of 8 ms unless otherwise noted. The KAuCl₄ concentration in all the solutions was 5 g/l, giving an Au³⁺ concentration of 1.3x10⁻² M. The SnCl₂·2H₂O concentration in the solutions was 5 g/l ([Sn²⁺] = 2.2x10⁻² M) unless otherwise noted. The captions in Figures 6-12 through 6-24 give the current density, the measured Sn concentration from the energy dispersive x-ray analysis and the plating time for each image.

6.3.1 Effects of Varying Ethylenediamine Content

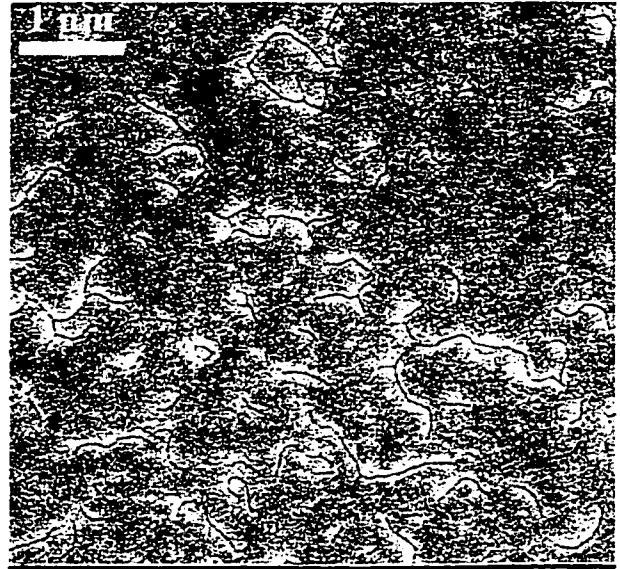
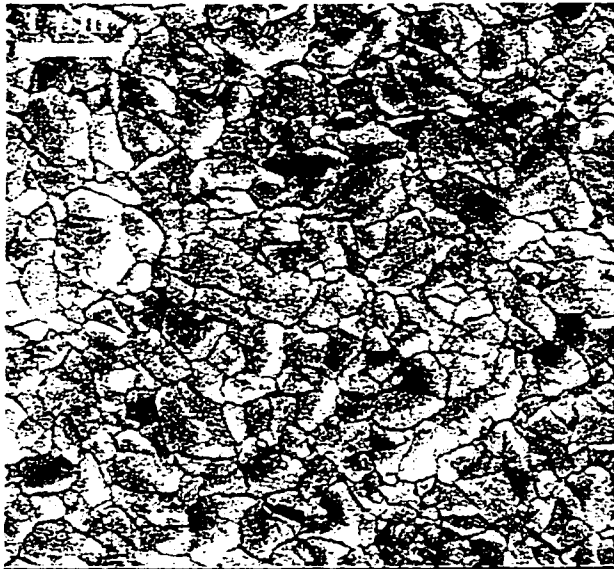
Figures 6-12 through 6-20 show plan view and cross section scanning electron microscope (SEM) images for deposits plated at varying ethylenediamine concentrations. Note that the plating time varies between samples, so the thickness observed is not a direct measure of the plating rate. Figures 6-12 and 6-13 show the change in structure resulting from changes in average current density for solution 1 (no ethylenediamine). The structure is columnar between 1.2 and 3.2 mA/cm². This type of structure is identified as field oriented (FT) by Fisher's growth types [Winand94], and is found in deposits plated at a medium inhibition intensity. This type of structure is a result of two-dimensional nucleation.

In Figures 6-14 and 6-15, the deposits plated from solution 5 (0.01-0.02 M ethylenediamine) are shown. Figure 6-14(a) shows a very fine, feathery structure at a current density of 1.2 mA/cm² (12 at.% Sn) with some larger grains near the bottom-center of the deposit (Figure 5-15(a)). This type of structure is most likely a basis-oriented reproduction type (BR), but this is hard to distinguish because the cross section was made by cleaving the sample, and at low Sn concentrations the deposit is ductile. At current densities of 1.8 and 2.4 mA/cm², the deposit structure switches to a columnar field oriented type, which is similar to the structures observed for solution 1 (Figures 6-13(b,c)). At 3.2 mA/cm², the addition of 0.01-0.02 M ethylenediamine to the plating solution causes a change in structure to a unoriented dispersion type (UD) which is formed by three-dimensional nucleation. This structure is associated with current densities near the limiting current density, and is consistent with the lowered limiting current density observed in the polarization tests (Figure 6-3) due to the addition of ethylenediamine to the plating solution. The bottom 2/3rds of the deposit has the very fine-grained, feathery appearance associated with the UD type structure, while the top 1/3rd of the deposit switches to a columnar structure. The most likely explanation for the change in structure from the bottom to the top of the deposit is that as the surface roughness and total surface area increase due to the formation of the UD type deposit, the

average current density decreases, shifting the growth mode back to two-dimensional nucleation and a FT structure.

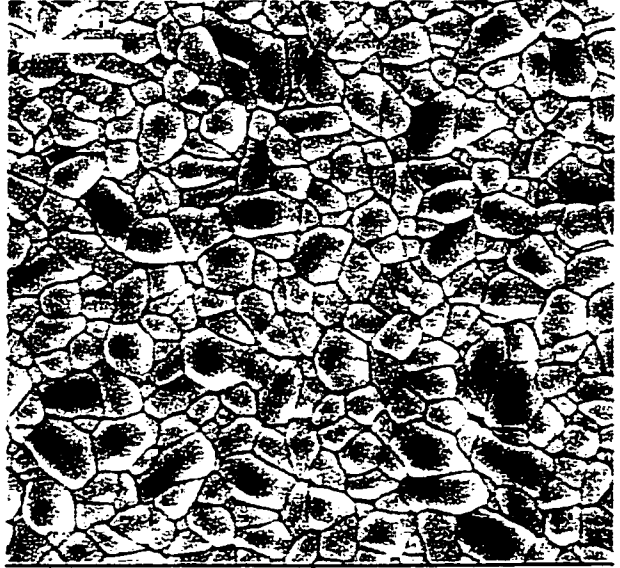
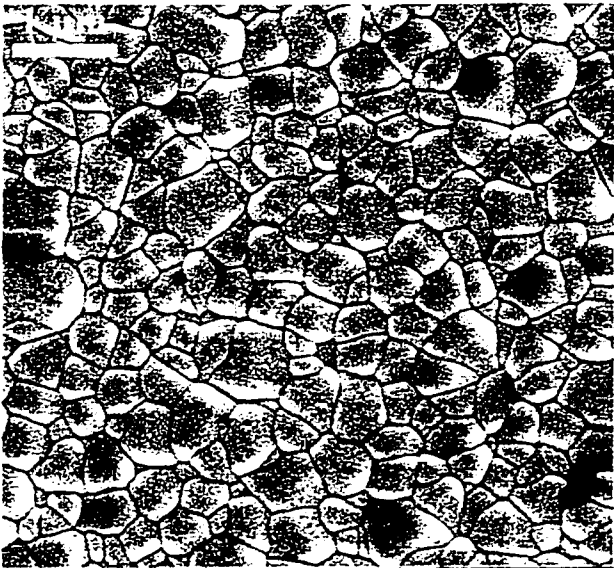
The structures of the deposits plated from solution 6 (0.05-0.06 M ethylenediamine) are shown in Figures 6-16 and 6-17. At a current density of 1.2 mA/cm² (16 at.% Sn) the BR or basis-oriented reproduction type structure is again found, followed by a FT structure at a current density of 1.8 mA/cm². For this solution, the UD structure (three-dimensional nucleation) is found at a current density of 2.4 mA/cm², and degrades to a powdery deposit at higher current densities which is also classified as UD type in Fisher's categorization of electroplating deposits. [Winand94] The tin content of the deposit is unknown, as the deposit is less than 1 μm thick and the gold substrate will be detected in the EDX analysis, giving false results.

Figures 6-18 and 6-19 show the SEM images of the deposits plated from solution 3 (0.11 M ethylenediamine). At a current density of 1.2 mA/cm² the deposit has a UD structure (three-dimensional nucleation), while at a current density of 2.4 mA/cm², the structure is powdery and burnt (UD) as hydrogen reduction competes with the reduction of the metal ions. If the structures formed from solutions 1 (no ethylenediamine), 5 (0.01-0.02 M ethylenediamine), 6 (0.05-0.06 M ethylenediamine) and 3 (0.11 M ethylenediamine) at 2.4 mA/cm² are compared (Figure 6-20), it can be seen that the structure of the deposit plated goes from a columnar (FT) structure, to a fine, feathery (UD) structure and finally to a powdery structure as the concentration of ethylenediamine increases. The reason for this is that the limiting current density decreases as the ethylenediamine concentration increases, which is observed from the polarization tests shown in Figure 6-3. As the ethylenediamine concentration increases in the solution, the structure formed at a current density of 2.4 mA/cm² will become rougher because the ratio of the current density to the limiting current density is increased. It is possible that the addition of ethylenediamine to the plating solution has an effect on the inhibition intensity of the deposition, but this change is likely negligible since the change in limiting current density caused by the ethylenediamine addition accounts for the microstructures observed.



a) 1.2 mA/cm^2 (14at.% Sn – 240 min.)

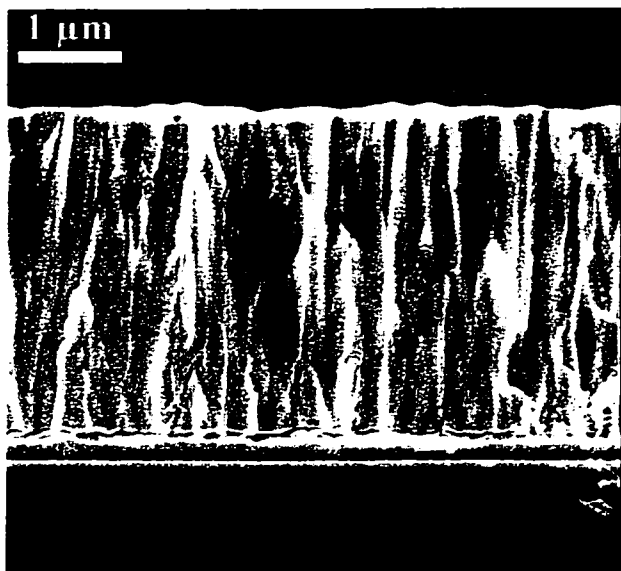
b) 1.8 mA/cm^2 (17at.% Sn – 90 min.)



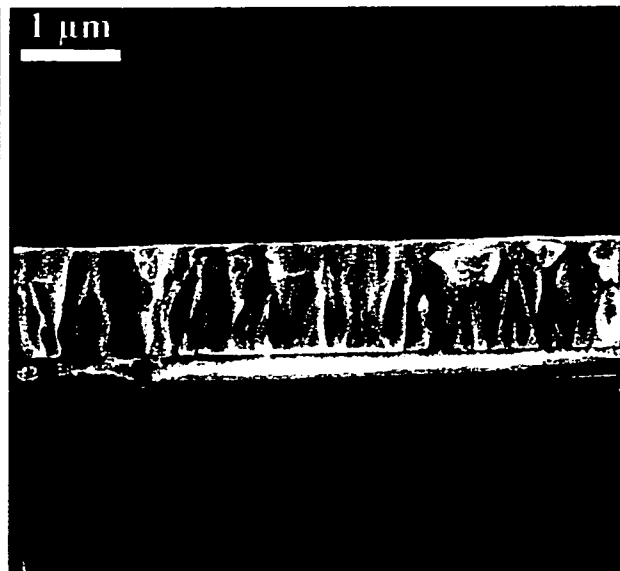
c) 2.4 mA/cm^2 (49at.% Sn – 90 min.)

d) 3.2 mA/cm^2 (50at.% Sn – 60 min.)

Figure 6-12 SEM plan view images of samples plated from solutions containing no ethylenediamine. (solution 1)



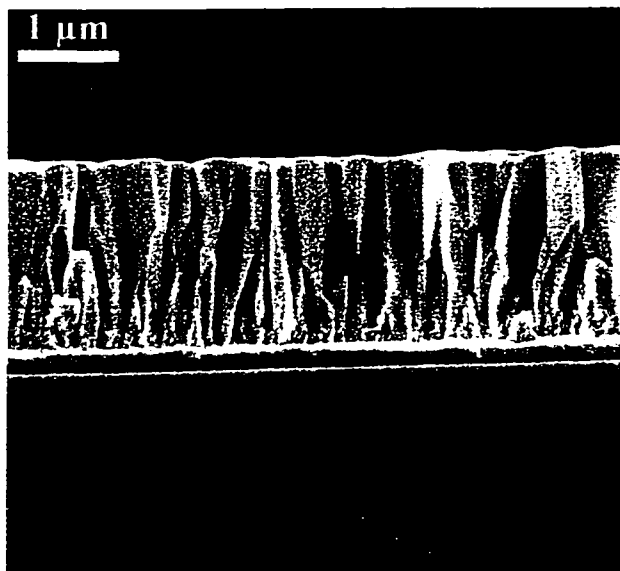
a) 1.2 mA/cm^2 (14at.% Sn – 240 min.)



b) 1.8 mA/cm^2 (17at.% Sn – 90 min.)

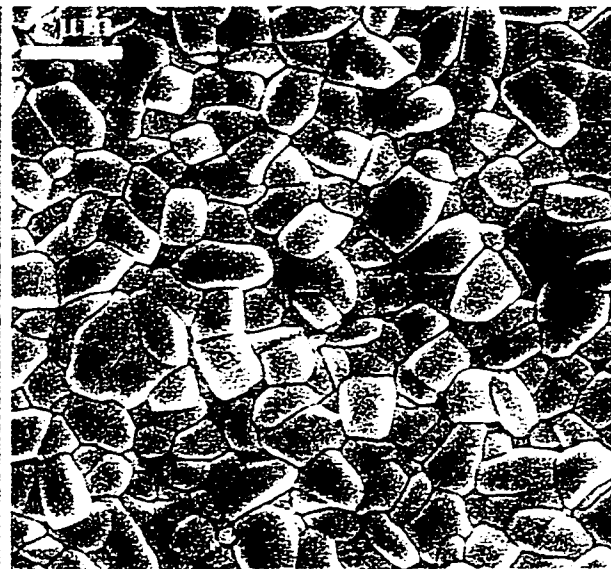
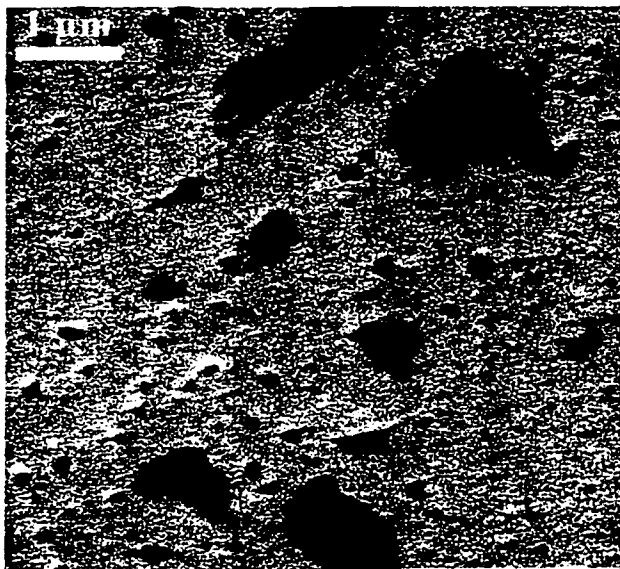


c) 2.4 mA/cm^2 (49at.% Sn – 90 min.)



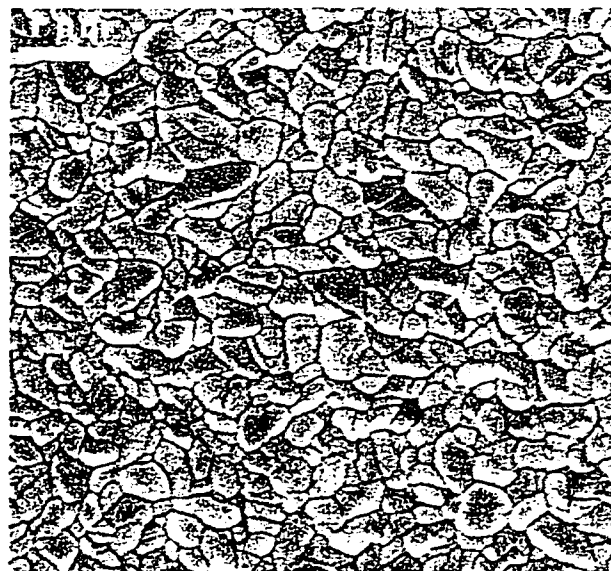
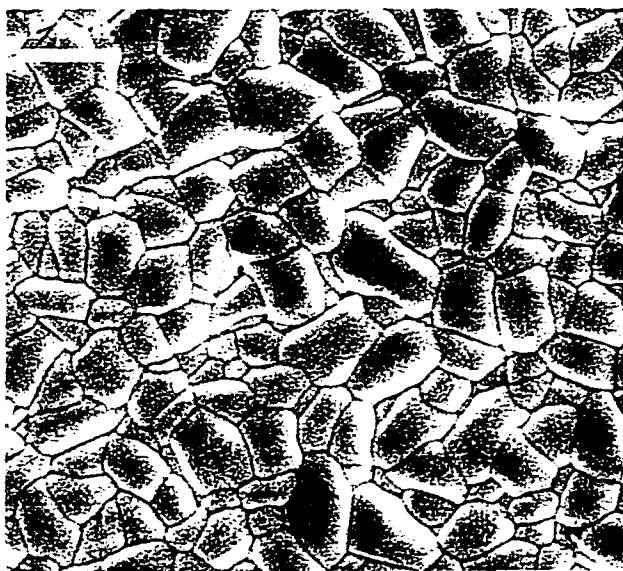
d) 3.2 mA/cm^2 (50at.% Sn – 60 min.)

Figure 6-13 SEM cross section images of samples plated from solutions containing no ethylenediamine. (solution 1)



a) 1.2 mA/cm² (12at.% Sn – 180 min.)

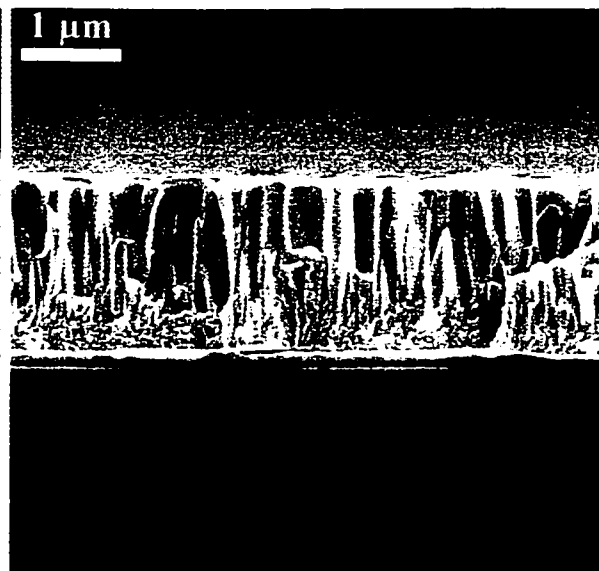
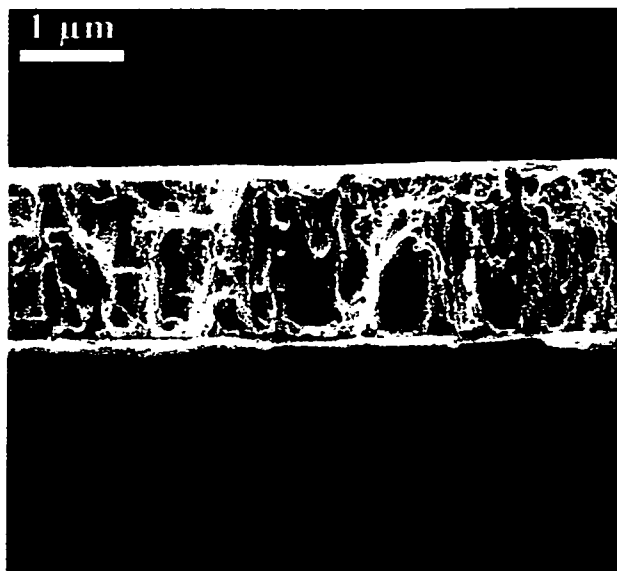
b) 1.8 mA/cm² (46at.% Sn – 90 min.)



c) 2.4 mA/cm² (48at.% Sn – 90 min.)

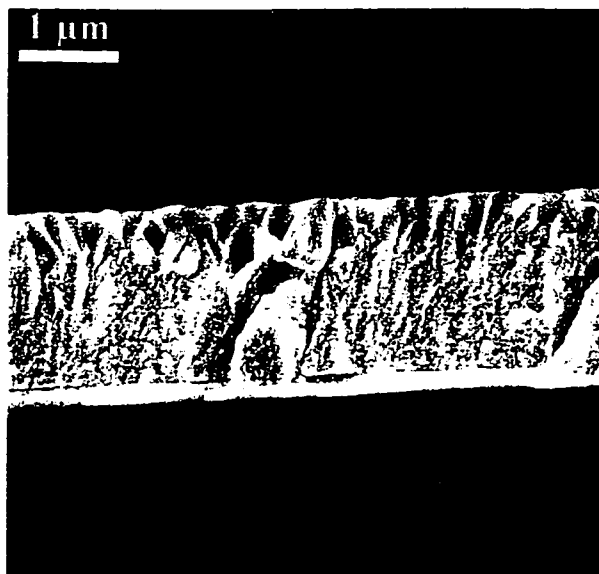
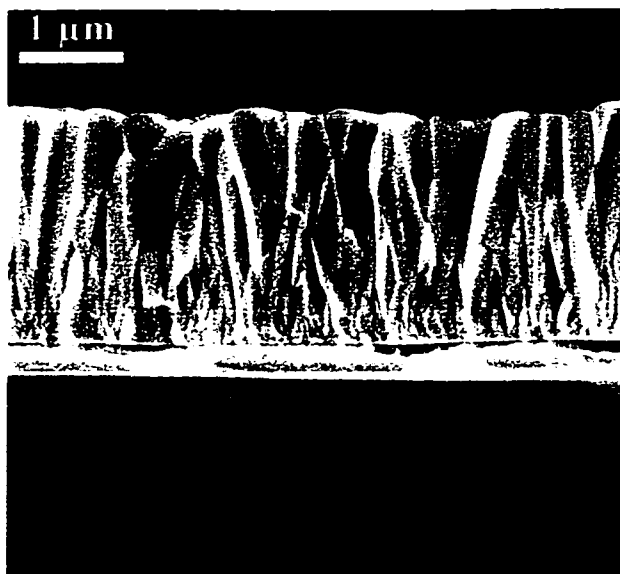
d) 3.2 mA/cm² (49at.% Sn – 60 min.)

Figure 6-14 SEM plan view images of samples plated from solutions containing 0.01-0.02 M ethylenediamine. (solution 5)



a) 1.2 mA/cm² (12at.% Sn – 180 min.)

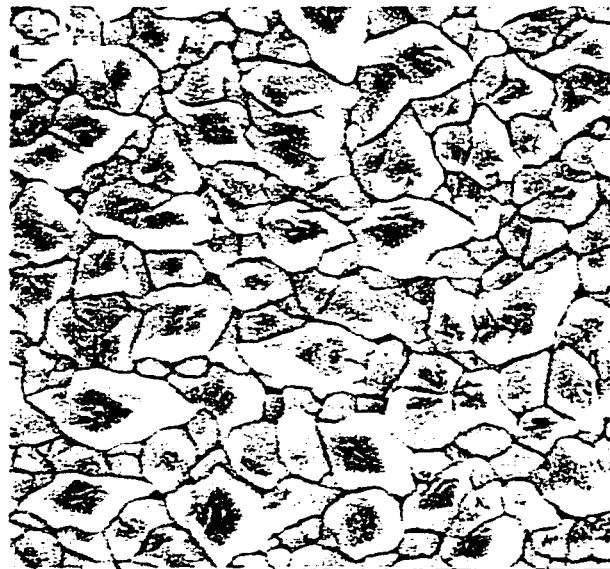
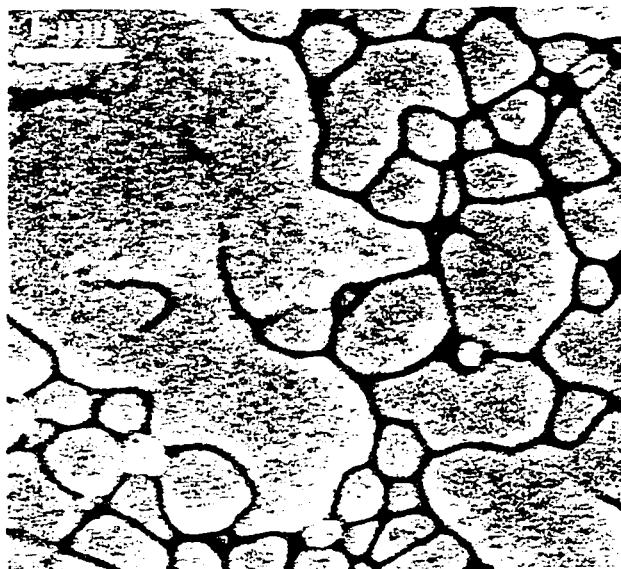
b) 1.8 mA/cm² (46at.% Sn – 90 min.)



c) 2.4 mA/cm² (48at.% Sn – 90 min.)

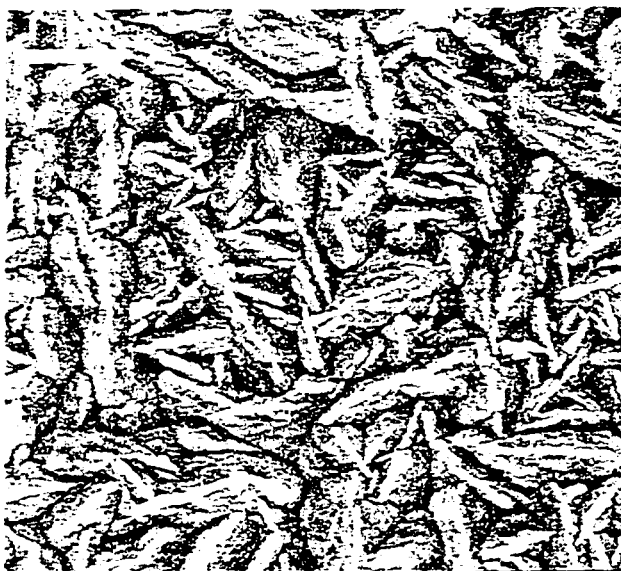
d) 3.2 mA/cm² (49at.% Sn – 60 min.)

Figure 6-15 SEM cross section images of samples plated from solutions containing 0.01-0.02 M ethylenediamine. (solution 5)



a) 1.2 mA/cm² (16at.% Sn – 180 min.)

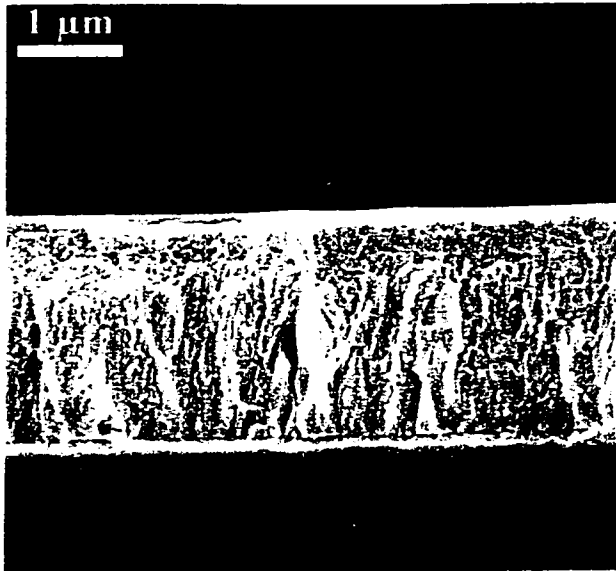
b) 1.8 mA/cm² (50at.%Sn – 90 min.)



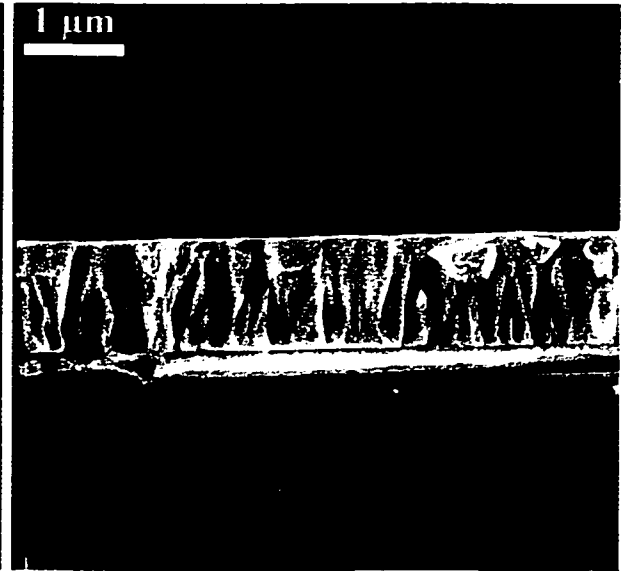
c) 2.4 mA/cm² (52at.% Sn – 90 min.)

d) 3.2 mA/cm² (?at.% Sn – 60 min.)

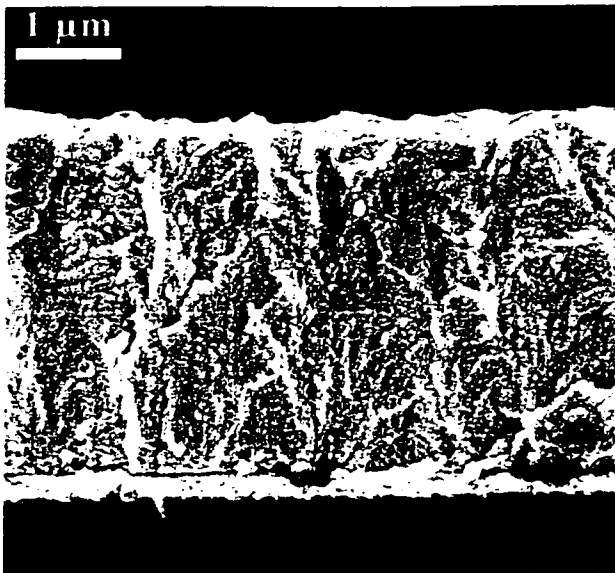
Figure 6-16 SEM plan view images of samples plated from solutions containing 0.05-0.06 M ethylenediamine. (solution 6)



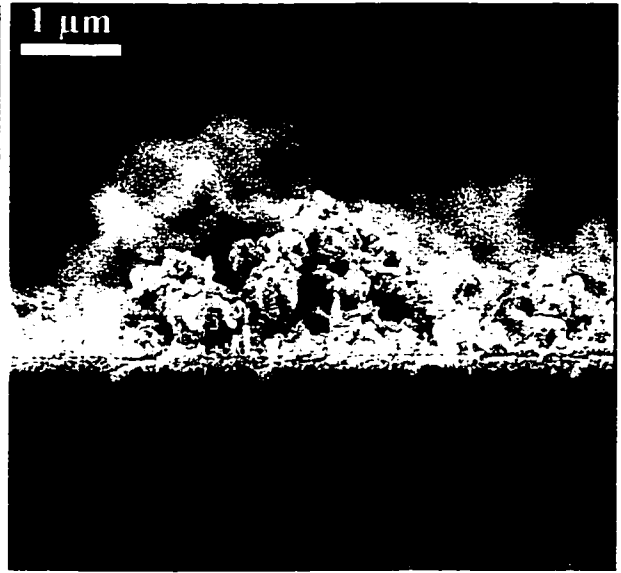
a) 1.2 mA/cm² (16at.% Sn – 180 min.)



b) 1.8 mA/cm² (50at.%Sn – 90 min.)

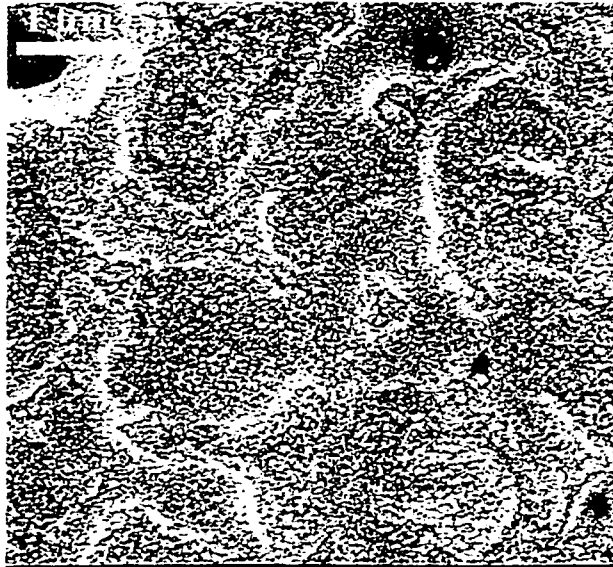


c) 2.4 mA/cm² (52at.% Sn – 90 min.)

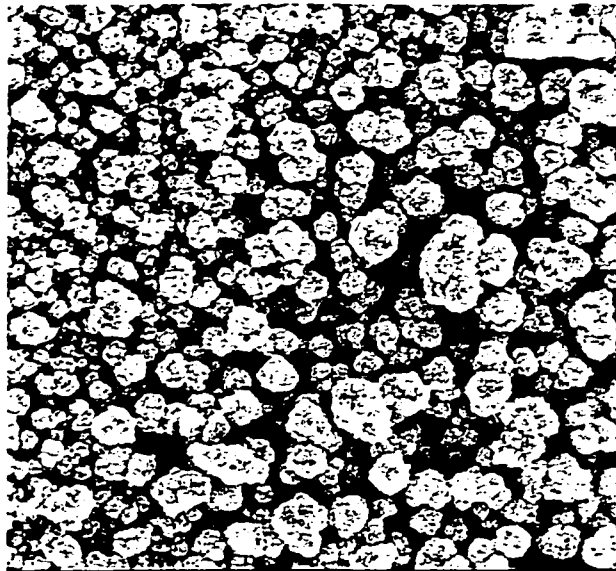


d) 3.2 mA/cm² (?at.% Sn – 60 min)

Figure 6-17 SEM cross section images of samples plated from solutions containing 0.05 - 0.06 M ethylenediamine. (solution 6)

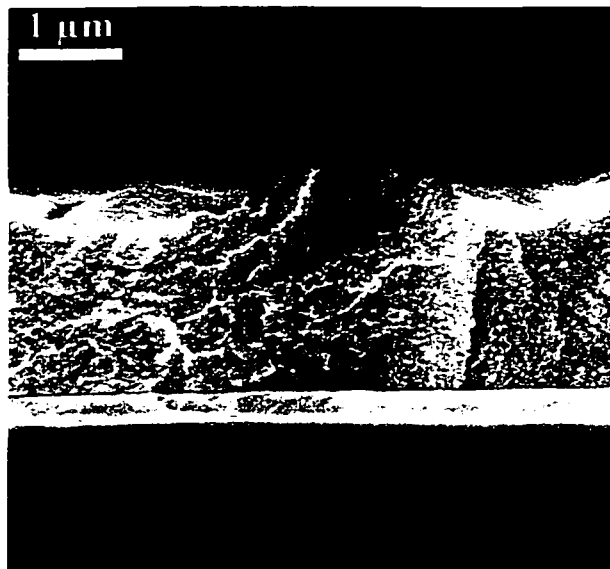


a) 1.2 mA/cm^2 (13at.% Sn – 90 min.)

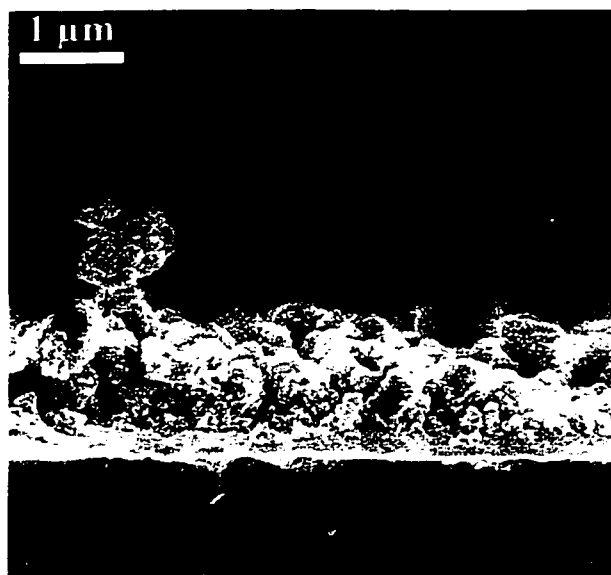


b) 2.4 mA/cm^2 (17at.% Sn – 90 min.)

Figure 6-18 SEM plan view images of samples plated from solutions containing 0.11 M ethylenediamine. (solution 3)

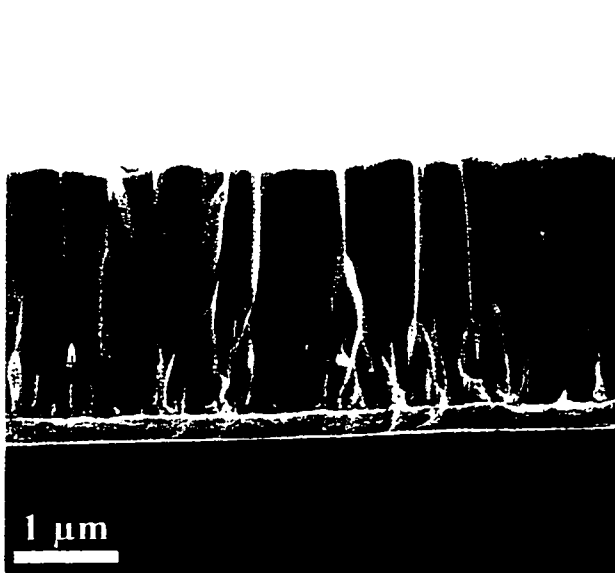


a) 1.2 mA/cm^2 (13at.% Sn – 90 min.)

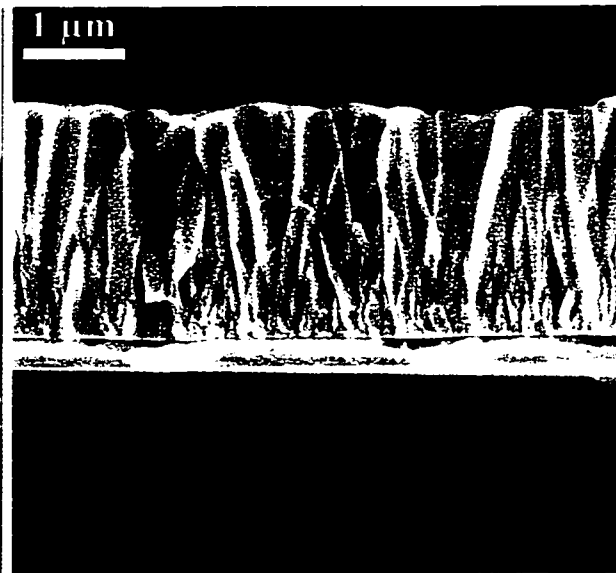


b) 2.4 mA/cm^2 (17at.% Sn – 90 min.)

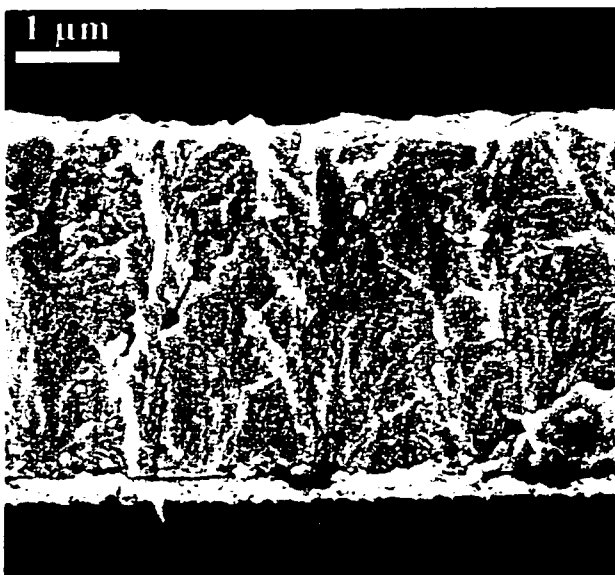
Figure 6-19 SEM cross section images of samples plated from solutions containing 0.11 M ethylenediamine. (solution 3)



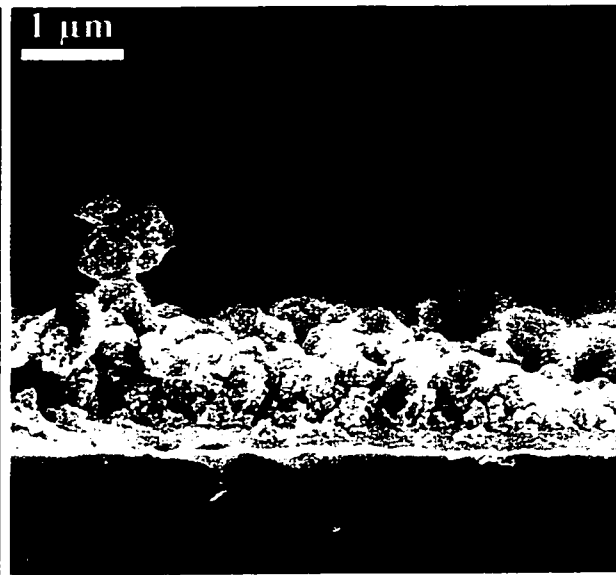
a) No ethylenediamine.
(49at.% Sn – 90 min.)



b) 0.01 - 0.02 M ethylenediamine.
(48at.% Sn – 90 min.)



c) 0.05 – 0.06 M ethylenediamine.
(52at.% Sn – 90 min.)



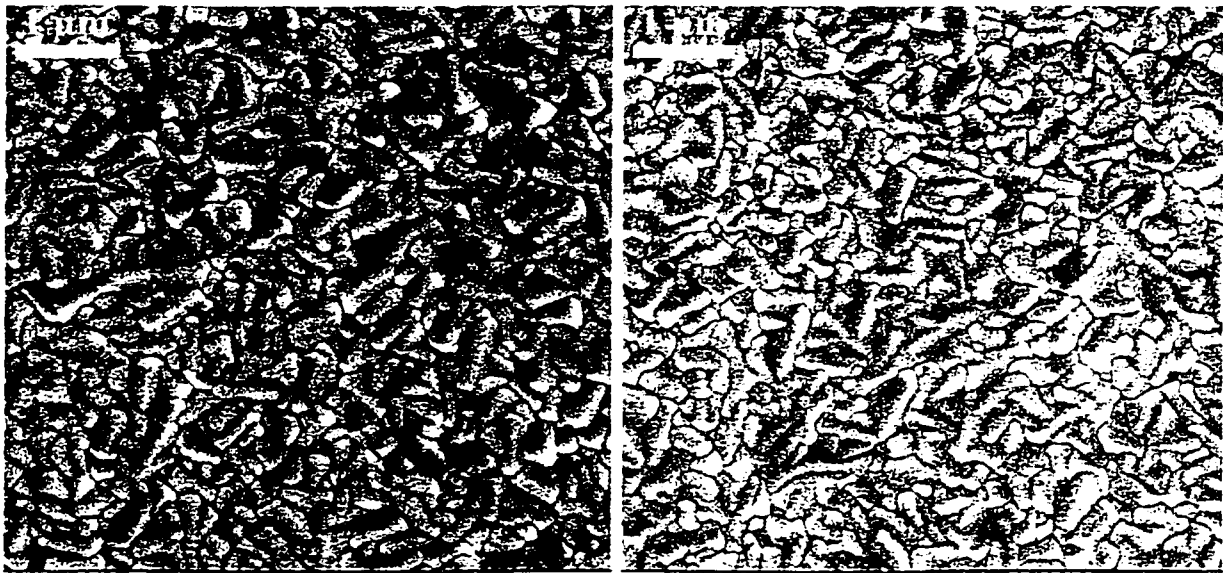
d) 0.11 M ethylenediamine.
(?at.% Sn – 60 min)

Figure 6-20 SEM cross section images of samples plated at 2.4 mA/cm^2 from solutions with varying ethylenediamine concentrations.

6.3.2 Plating With Reverse Pulse

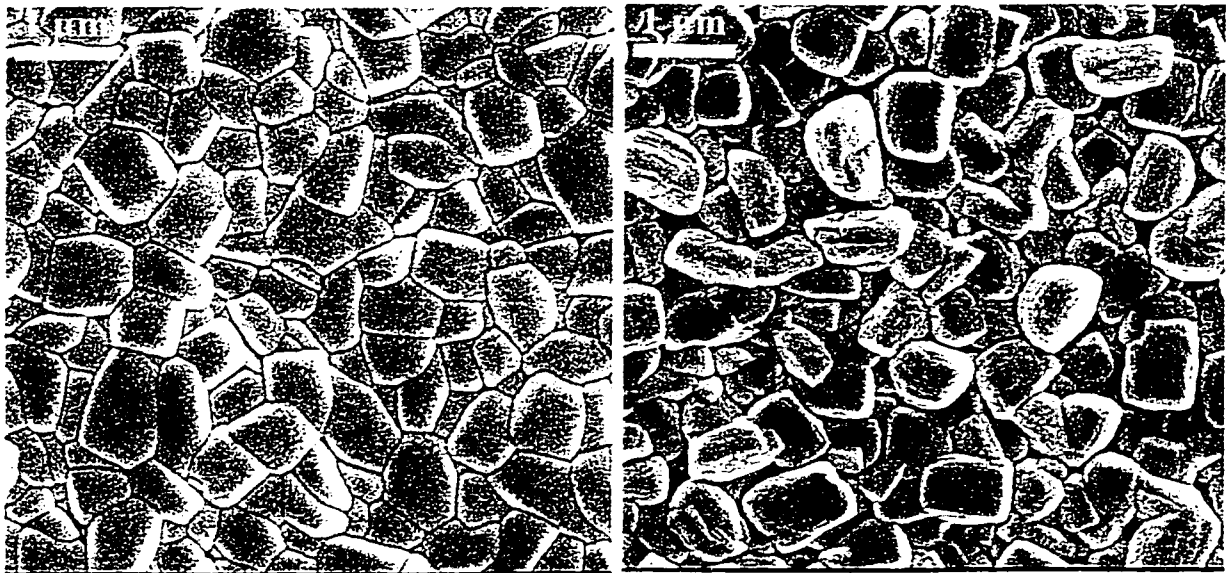
The effects on deposit structure of increasing the forward ON time and introducing a reverse pulse to the electroplating waveform are shown in Figures 6-21 and 6-22. Solution 5 (0.01-0.02 M ethylenediamine) was used for these experiments, and the structures deposited using an ON time of 2 ms and an OFF time of 8 ms are shown in Figures 6-14 and 6-15. The parameters used for the waveform including a reverse pulse were 2.4 ms forward ON time, 0.4 ms reverse ON time and 7.2 ms OFF.

The structure formed at a current density of 1.2 mA/cm^2 (Figure 6-22(a)) using the reverse pulse appears to have columnar (FT) structure with a few fine grained areas of BR type, whereas the structure formed using only a forward pulse (Figure 6-15(a)) is mostly a BR type structure. Both the forward pulse and forward + reverse pulse structures have a columnar FT structure at current densities between 1.8 and 2.4 mA/cm^2 . At a current density of 3.2 mA/cm^2 the deposit formed using a forward pulse (Figure 6-15(d)) is mostly a UD structure and the deposit formed using both a forward and reverse pulse (Figure 6-22(d)) is also a UD structure, but the grains appear larger. In general, for the reverse pulse parameters used, there seems to be little change in structure compared to the deposits using only a forward pulse. The larger grain size in the deposits formed using the forward and reverse pulse is most likely due to the increase in average forward current density and duty cycle, which is 20% higher than the average current density with the introduction of the reverse pulse.



a) 1.2 mA/cm² (13at.% Sn – 180 min.)

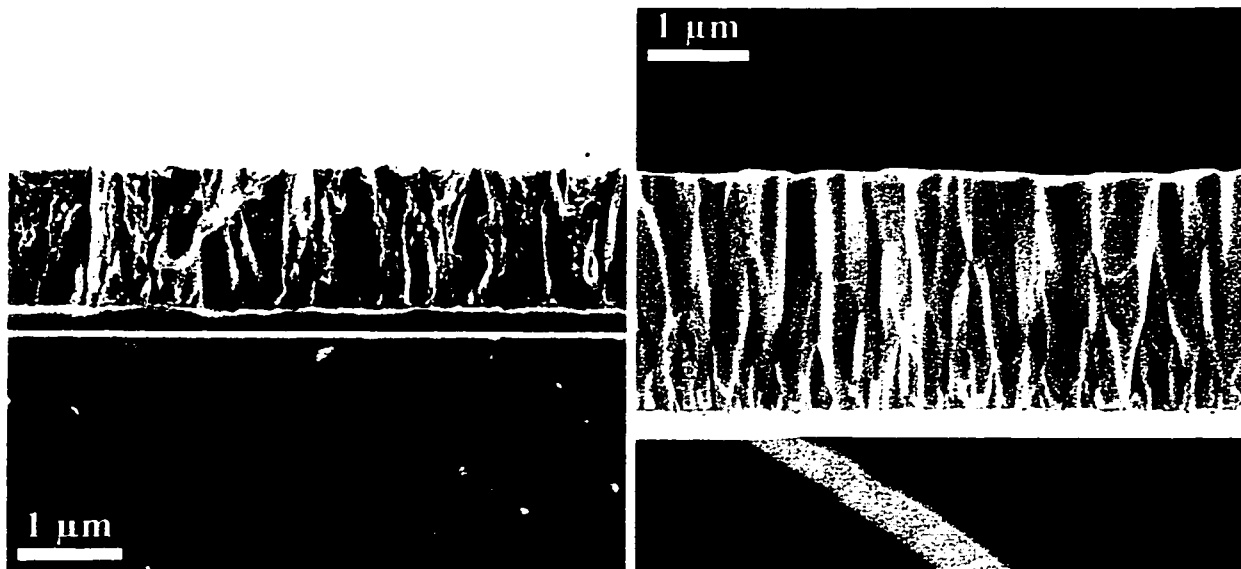
b) 1.8 mA/cm² (34at.%Sn – 90 min.)



c) 2.4 mA/cm² (48at.% Sn – 90 min.)

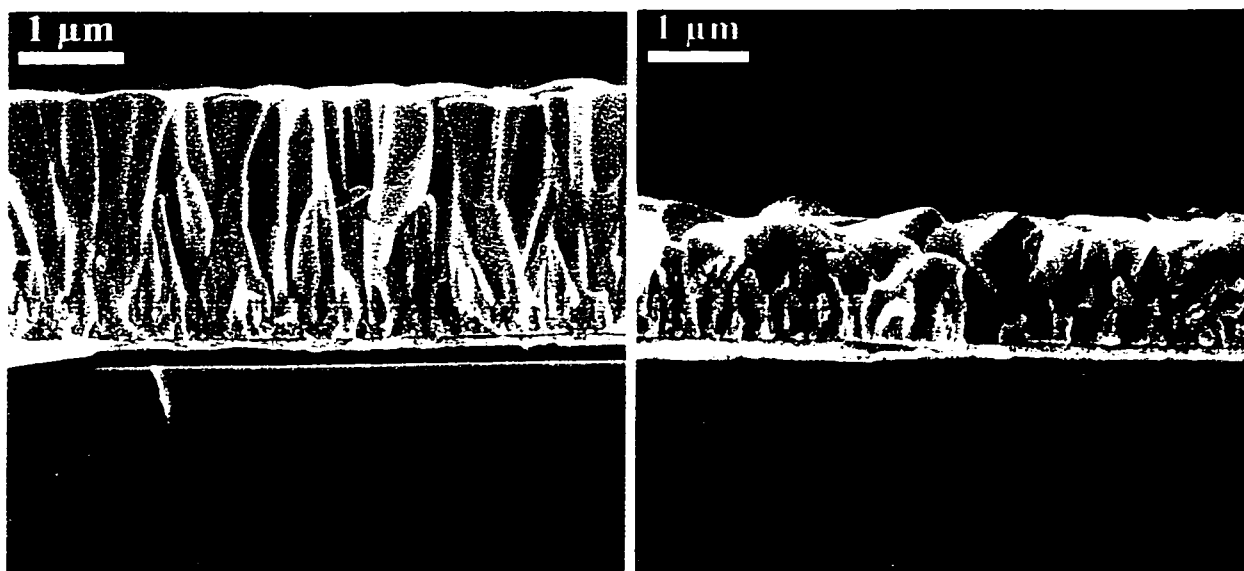
d) 3.2 mA/cm² (49at.% Sn 40 min.)

Figure 6-21 SEM plan view images of samples plated from solutions containing 0.01-0.02 M ethylenediamine, 2.4 ms Forw., 0.4 ms Rev., 7.2 ms OFF. (solution 5)



a) 1.2 mA/cm² (13at.% Sn – 180 min.)

b) 1.8 mA/cm² (34at.%Sn – 90 min.)



c) 2.4 mA/cm² (48at.% Sn – 90 min.)

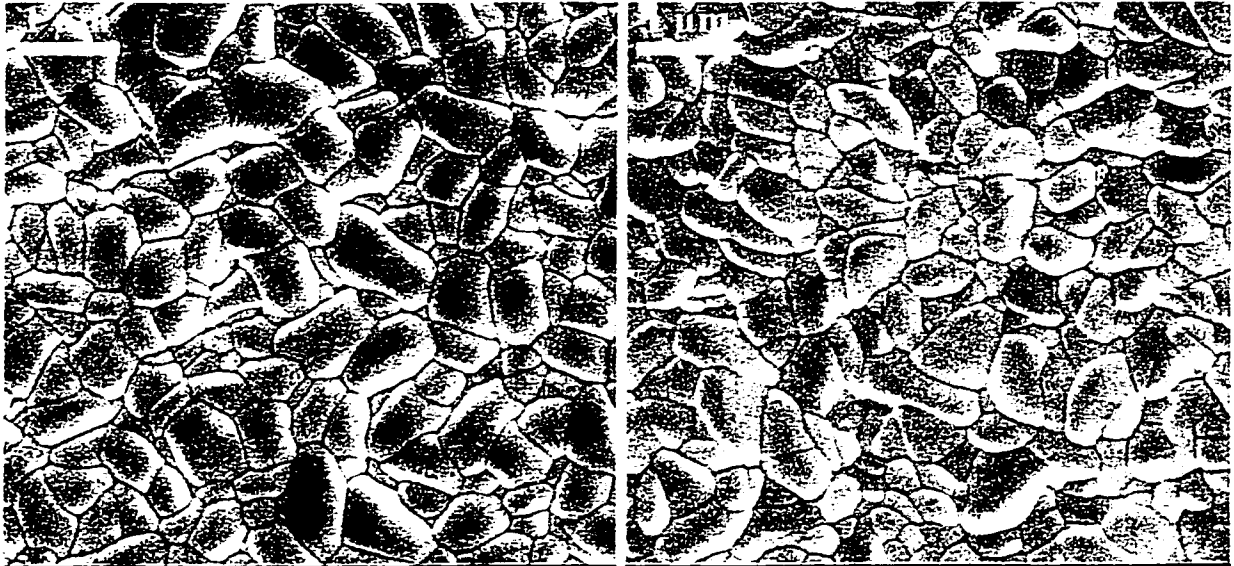
d) 3.2 mA/cm² (49at.% Sn – 40 min.)

Figure 6-22 SEM cross section images of samples plated from solutions containing 0.01-0.02 M ethylenediamine, 2.4 ms Forw., 0.4 ms Rev., 7.2 ms OFF. (solution 5)

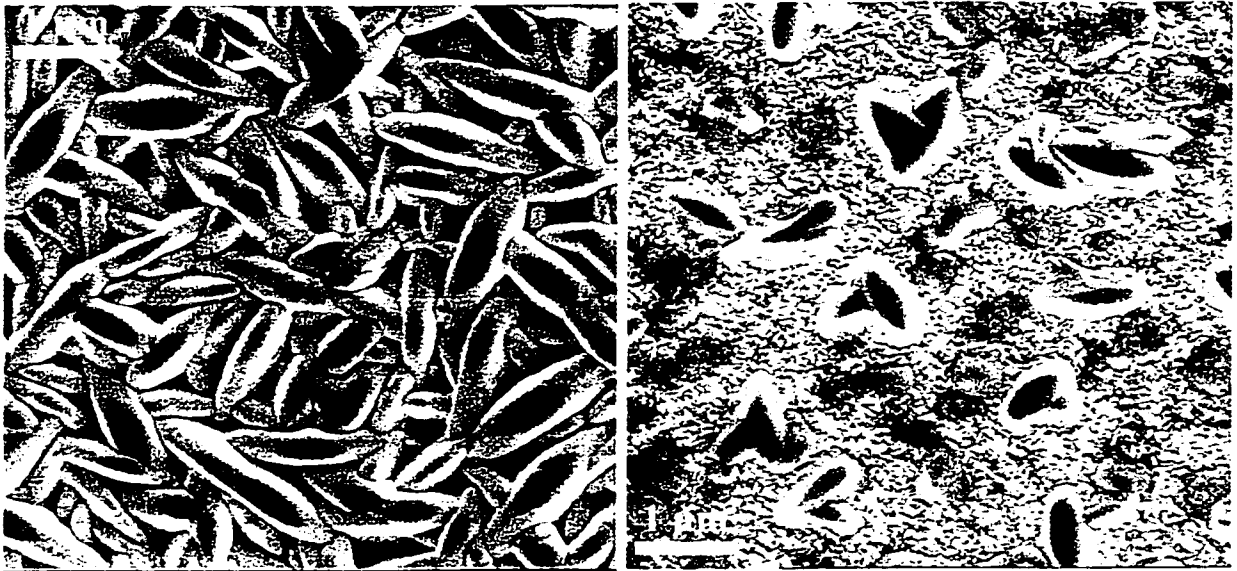
6.3.3 Varying SnCl₂-2H₂O Concentration

The structures plated at a current density of 2.4 mA/cm² from solutions where the ethylenediamine concentration was held constant at 0.01-0.02 M and the SnCl₂-2H₂O concentration was varied between 2 and 5 g/l are shown in Figures 6-23 and 6-24. As the SnCl₂-2H₂O concentration in the solution and the tin concentration in the deposit decrease, the structure becomes rougher. At a SnCl₂-2H₂O concentration of 5 g/l, the deposit structure is columnar and FT type. When the SnCl₂-2H₂O concentration is decreased to 4 g/l, the tin concentration in the deposit remains near 50 at.%, but the structure becomes a fine-grained UD type as the growth mechanism switches to three-dimensional nucleation.

As the SnCl₂-2H₂O concentration in the solution is reduced further, to 2 – 3 g/l, the structure of the deposit becomes increasingly rougher, with the initial growth being of UD type, which then leads to large fine-grained discs 2-3 μm in diameter. The reason for the formation of the discs is most probably due to the increase in local current density at the peaks of the original rough deposit combined with the depletion of Sn²⁺ ions at the cathode surface. The plating then continues at a higher rate on the peaks, leading to the formation of the protruding discs. From the structures observed, it can be seen that the decrease in the SnCl₂-2H₂O concentration in the solution increases the polarization and decreases the limiting current density. This is consistent with the observations of Sun [Sun99-2] who reported an increase in polarization with a decrease in the SnCl₂-2H₂O concentration in the solution between 5 and 10 g/l SnCl₂-2H₂O.

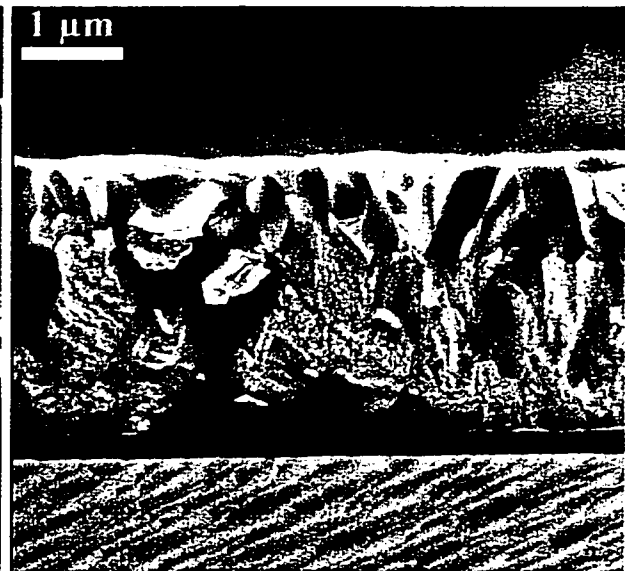
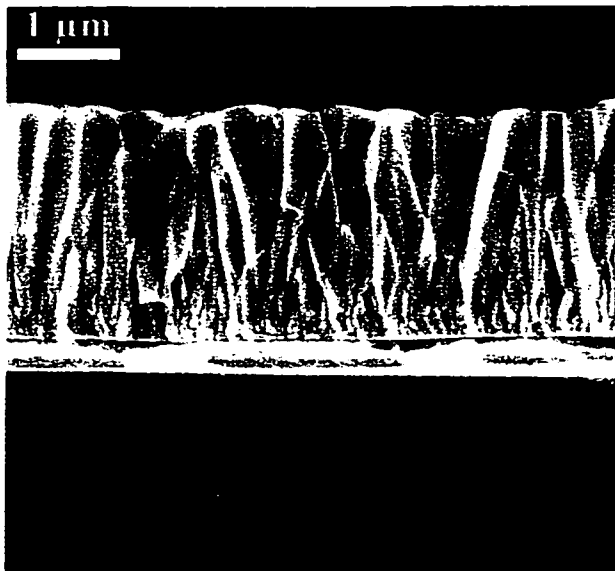


a) 5 g/l $\text{SnCl}_2 \cdot 2\text{H}_2\text{O}$ (48at.% Sn – 90 min.) b) 4 g/l $\text{SnCl}_2 \cdot 2\text{H}_2\text{O}$ (49at.% Sn – 90 min.)



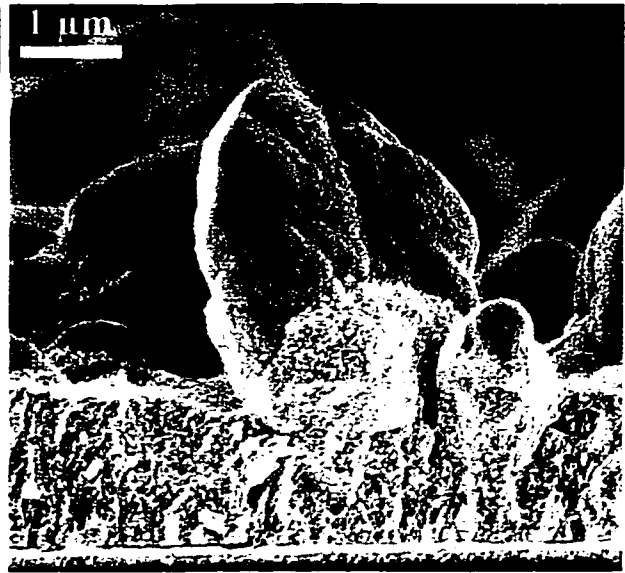
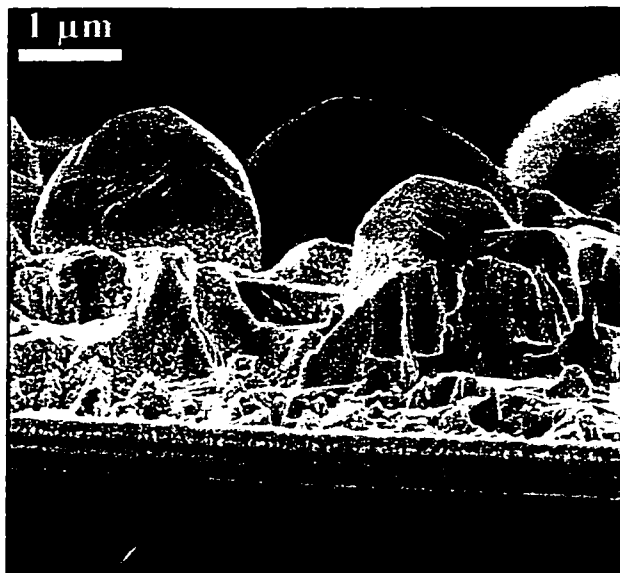
c) 3 g/l $\text{SnCl}_2 \cdot 2\text{H}_2\text{O}$ (43at.% Sn – 90 min.) d) 2 g/l $\text{SnCl}_2 \cdot 2\text{H}_2\text{O}$ (35at.% Sn – 90 min.)

Figure 6-23 SEM plan view images of samples plated from solutions containing 0.01-0.02 M ethylenediamine plated at 2.4 mA/cm^2 .



a) 5 g/l $\text{SnCl}_2 \cdot 2\text{H}_2\text{O}$ (48at.% Sn – 90 min.)

b) 4 g/l $\text{SnCl}_2 \cdot 2\text{H}_2\text{O}$ (49at.% Sn – 90 min.)



c) 3 g/l $\text{SnCl}_2 \cdot 2\text{H}_2\text{O}$ (43at.% Sn 90 min.)

d) 2 g/l $\text{SnCl}_2 \cdot 2\text{H}_2\text{O}$ (35at.% Sn – 90 min.)

Figure 6-24 SEM cross section images of samples plated from solutions containing 0.01-0.02 M ethylenediamine plated at 2.4 mA/cm^2 .

6.4 X-ray Diffraction

X-ray diffraction tests were made on the electroplated deposits in order to determine a relationship between the current density and structure with respect to preferred orientation. The x-ray diffraction runs were also used to determine the phases present in the deposit. In all the deposits, other than those which co-deposited nickel, either the ζ' (Au_5Sn) ordered phase, the δ (AuSn) phase or a combination of both phases was present. Atomic tin was not found in any deposit, and it is not fully known if atomic gold was present in any deposit, as there was always a gold peak from the substrate. X-ray diffraction analysis of a deposit plated on a platinum substrate showed no gold peak.

The intensities of each peak in a spectrum were measured, and then divided by the intensity of the most intense peak (area under the curve). The standard x-ray diffraction powder patterns for AuSn [Swanson57] and Au_5Sn [Osada74] were used. The three strongest peaks (relative intensities) for AuSn are $\{102\}$ (100%), $\{110\}$ (65%) and $\{100\}$ (51%). The three strongest peaks for Au_5Sn are $\{113\}$ (100%), $\{006\}$ (27%) and $\{110\}$ (25%). The resulting number was then divided by the intensity percentage found on the standard x-ray diffraction powder pattern, as the intensity reported in the powder pattern is for a random orientation. The two peaks with the highest normalized intensity were then chosen, and the most intense normalized peak intensity was divided by the next highest peak to obtain a ratio of intensity. If the crystallographic planes of the two normalized peaks chosen were parallel, then the most intense normalized peak was compared to the third most intense normalized peak. In this manner, a ratio of 1 would indicate a random orientation, and as the ratio becomes larger so does the amount of preferred orientation.

The x-ray diffraction results for deposits plated from solutions 1, 3, 5 and 6, containing varying amounts of ethylenediamine are given in Table 6-2, and the normalized peak intensity ratios for the AuSn phase are plotted in Figure 6-25. The deposits from solutions containing between 0 and 0.05-0.06 M ethylenediamine exhibit an AuSn $\{110\}$ preferred orientation with the AuSn $\{110\}$ planes parallel to the substrate

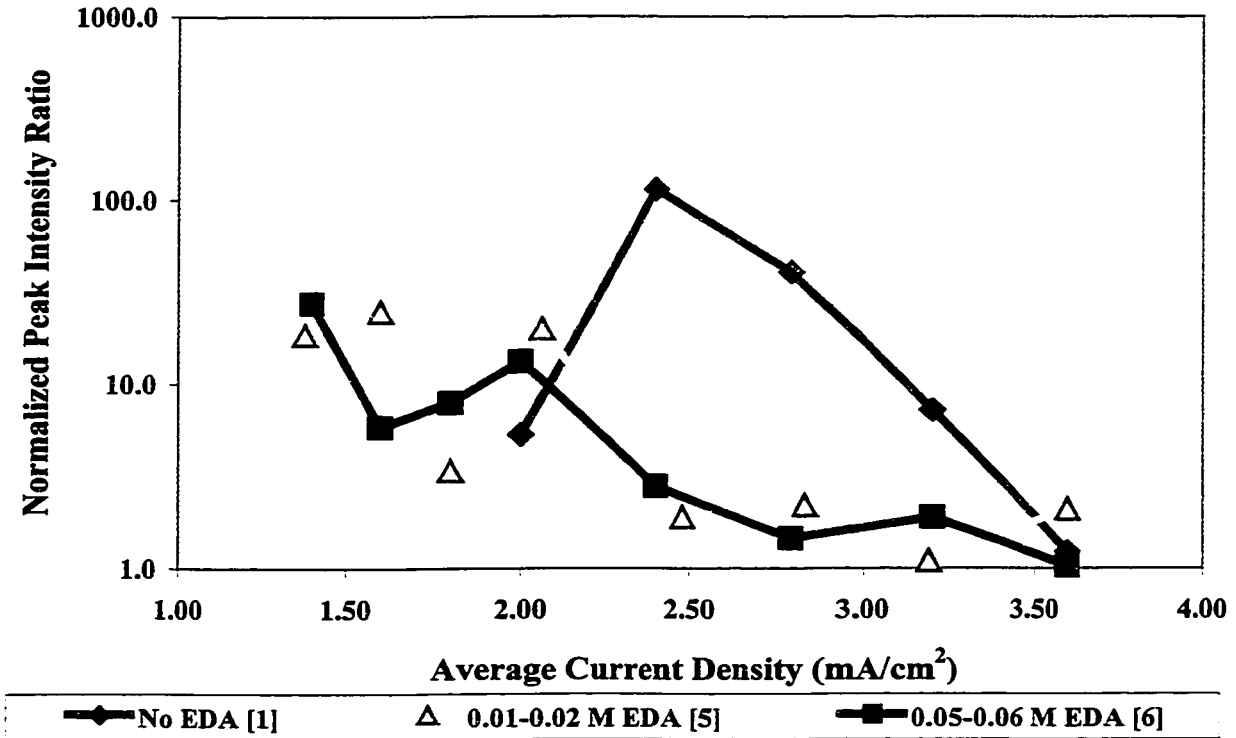
surface at current densities between 1.2 and 2.0 mA/cm². At current densities between 2.4 and 3.2 mA/cm², the deposits plated from solution 1 (no ethylenediamine) have a distinct preferred orientation, again with the AuSn {110} planes parallel to the substrate surface. The structures observed (Figure 6-13(b-d)) are all columnar FT type.

For the samples plated from solution 5 (0.01-0.02 M ethylenediamine) a fine-grained UD structure is observed at a current density of 3.2 mA/cm² (Figure 6-15(d)). The graph in Figure 6-25 shows no preferred orientation, which matches with the structure observed. The same is true for the structures observed at current densities of 2.4 and 3.2 mA/cm² for the deposits plated from solution 6 (0.05-0.06 M ethylenediamine) which are of UD type as well (Figure 6-17(c,d)) and show only a small AuSn {202} preferred orientation. As in the observed structures, the switch to three-dimensional nucleation and growth and the resulting loss of preferred orientation occurs at lower current densities as the concentration of ethylenediamine in the solution is increased. For all the solutions, the {110} planes are not dominant when preferred orientation is lost.

Table 6-2 Phases and orientation for deposits plated from solutions with varying ethylenediamine concentrations.

No Ethylenediamine				0.01 - 0.02 M Ethylenediamine				0.05 - 0.06 M Ethylenediamine				0.11 M Ethylenediamine			
Current Density (mA/cm ²)	Sn Content (at.%)	Phases and Orient.	Norm. Int. Ratio	Current Density (mA/cm ²)	Sn Content (at.%)	Phases and Orient.	Norm. Int. Ratio	Current Density (mA/cm ²)	Sn Content (at.%)	Phases and Orient.	Norm. Int. Ratio	Current Density (mA/cm ²)	Sn Content (at.%)	Phases and Orient.	Norm. Int. Ratio
1.2	13.6	Au ₃ Sn ₂₂₀ Au ₃ Sn ₀₀₆	5.7	1.24	12.2	Au ₃ Sn ₁₁₀ Au ₃ Sn ₀₀₆	1.9	1.2	16.1	Au ₃ Sn ₂₂₃ Au ₃ Sn ₂₂₀	1.1	1.2	12.6	Au ₃ Sn ₃₀₆ Au ₃ Sn ₁₁₃	5.9
1.4	15.5	Au ₃ Sn ₀₀₆ Au ₃ Sn ₂₂₃	17.7	1.38	23.3	Au ₃ Sn ₀₀₆ Au ₃ Sn ₁₁₃ Au ₃ Sn ₁₁₀ Au ₃ Sn ₂₁₀	2.4 18.5	1.4	49.6	Au ₃ Sn ₁₁₀ Au ₃ Sn ₂₁₀	27.4	1.4			
1.6	14.1	Au ₃ Sn ₀₀₆ Au ₃ Sn ₂₂₀	6.4	1.60	42.5	Au ₃ Sn ₁₁₀ Au ₃ Sn ₂₁₀ Au ₃ Sn ₀₀₆ Au ₃ Sn ₁₁₀	24.8 1.6	1.6	50.3	Au ₃ Sn ₁₁₀ Au ₃ Sn ₂₁₂	5.8	1.6			
1.8	16.9	Au ₃ Sn ₀₀₆ Au ₃ Sn ₁₁₃	1.7	1.80	46.6	Au ₃ Sn ₁₁₀ Au ₃ Sn ₂₁₀	3.4	1.8	49.9	Au ₃ Sn ₁₁₀ Au ₃ Sn ₂₁₀	7.9	1.8	18.6	Au ₃ Sn ₁₁₀ Au ₃ Sn ₁₁₃	1.1
2.0	37.9	Au ₃ Sn ₁₁₀ Au ₃ Sn ₂₁₁ Au ₃ Sn ₀₀₆ Au ₃ Sn ₁₁₃	5.3 3.2	2.06	45.4	Au ₃ Sn ₁₁₀ Au ₃ Sn ₂₁₀	20.0	2.0	50.0	Au ₃ Sn ₁₁₀ Au ₃ Sn ₂₁₀	13.3	2.0	18.7	Au ₃ Sn ₂₂₃ Au ₃ Sn ₁₁₀	1.2
2.4	49.3	Au ₃ Sn ₁₁₀ Au ₃ Sn ₂₁₀	114.8	2.48	47.9	Au ₃ Sn ₃₀₀ Au ₃ Sn ₁₁₀	1.9	2.4	51.9	Au ₃ Sn ₂₀₂ Au ₃ Sn ₂₁₂	2.8	2.4	16.5	Au ₃ Sn ₁₁₃ Au ₃ Sn ₂₂₃	1.4
2.8	47.1	Au ₃ Sn ₁₁₀ Au ₃ Sn ₂₁₀	40.6	2.84	50.3	Au ₃ Sn ₁₁₀ Au ₃ Sn ₂₁₂	2.2	2.8	53.1	Au ₃ Sn ₂₀₂ Au ₃ Sn ₂₁₂	1.5	2.8	7.0	Au ₃ Sn ₂₂₃ Au ₃ Sn ₁₁₃	5.3
3.2	50.0	Au ₃ Sn ₁₁₀ Au ₃ Sn ₂₁₀	7.2	3.19	48.9	Au ₃ Sn ₂₁₂ Au ₃ Sn ₁₁₀	1.1	3.2		Au ₃ Sn ₂₀₂ Au ₃ Sn ₁₀₀	1.9	3.2			
3.6	48.9	Au ₃ Sn ₂₀₂ Au ₃ Sn ₂₁₂	1.2	3.60	46.7	Au ₃ Sn ₁₀₀ Au ₃ Sn ₂₀₂	2.1	3.6	48.1	Au ₃ Sn ₂₁₂ Au ₃ Sn ₁₀₀	1.0	3.6			

Figure 6-25 Normalized intensity ratio of the AuSn phase versus current density for deposits electroplated from solutions with varying ethylenediamine content.

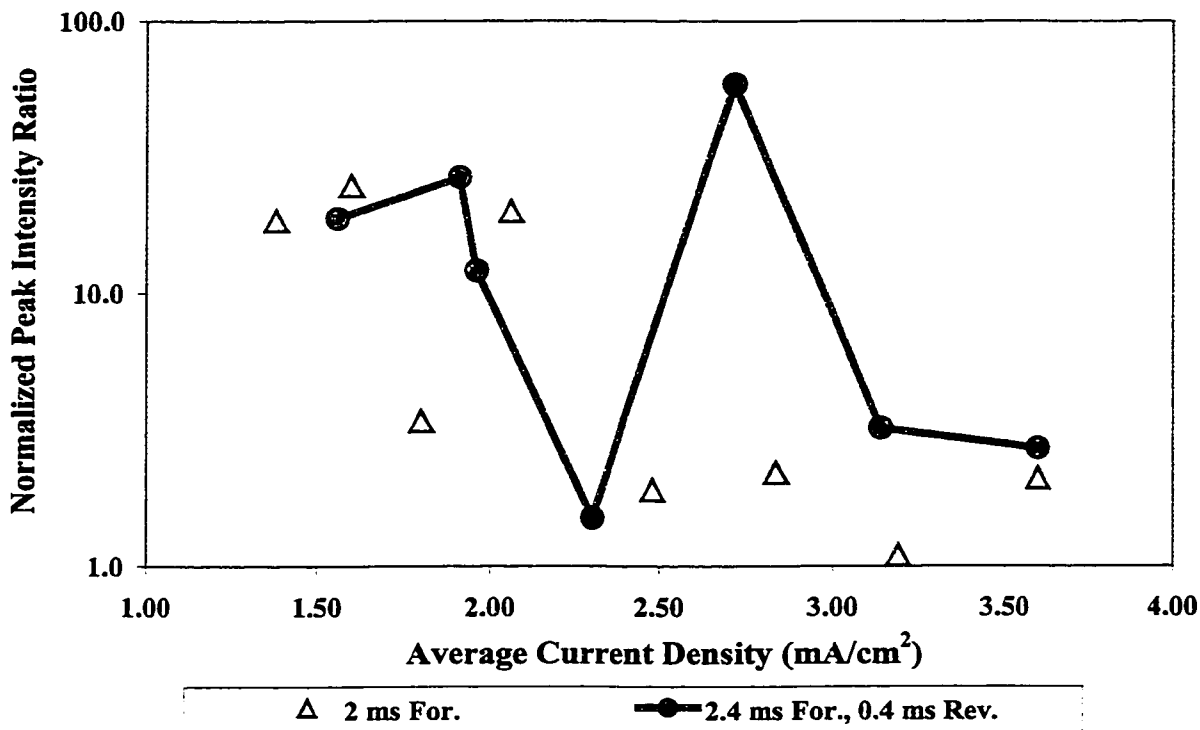


The x-ray diffraction data for solution 5 plated under two conditions, ie., with only a forward pulse versus a forward and reverse pulse is given in Table 6-3 and plotted in Figure 6-26. As with the observed structures (Figures 6-15 and 6-22), there is little difference in the preferred orientation, especially if the point at 2.8 mA/cm² for the forward + reverse pulse data is ignored.

Table 6-3 Phases and orientation for deposits plated from solution 5 (0.01-0.02 M ethylenediamine) using forward pulse and forward + reverse pulse.

2 ms For., 8 ms Off				2.4 ms For., 0.4 ms Rev., 7.2 ms Off			
Current Density (mA/cm ²)	Sn Content (at.%)	Phases and Orient.	Norm. Int. Ratio	Current Density (mA/cm ²)	Sn Content (at.%)	Phases and Orient.	Norm. Int. Ratio
1.24	12.2	Au ₅ Sn 110 Au ₅ Sn 006	1.9	1.27	13.3	Au ₅ Sn 113 Au ₅ Sn 220	2.1
1.38	23.3	Au ₅ Sn 006 Au ₅ Sn 113 AuSn 110 AuSn 210	2.4 18.5	1.46	15.0	Au ₅ Sn 113 Au ₅ Sn 006	1.1
1.60	42.5	AuSn 110 AuSn 210 Au ₅ Sn 006 Au ₅ Sn 110	24.8 1.6	1.56	44.1	AuSn 110 AuSn 210 Au ₅ Sn 006 Au ₅ Sn 110	18.8 2.2
1.80	46.6	AuSn 110 AuSn 210	3.4	1.91	34.3	AuSn 110 AuSn 210 Au ₅ Sn 006 Au ₅ Sn 110	26.6 2.1
2.06	45.4	AuSn 110 AuSn 210	20.0	1.96	47.5	AuSn 110 AuSn 210	12.1
2.48	47.9	AuSn 300 AuSn 110	1.9	2.30	47.8	AuSn 110 AuSn 300	1.5
2.84	50.3	AuSn 110 AuSn 212	2.2	2.72	47.2	AuSn 110 AuSn 210	58.8
3.19	48.9	AuSn 212 AuSn 110	1.1	3.14	49.2	AuSn 110 AuSn 112	3.2
3.60	46.7	AuSn 100 AuSn 202	2.1	3.60	49.2	AuSn 110 AuSn 300	2.7

Figure 6-26 Normalized intensity ratio of the AuSn phase versus current density for deposits electroplated from solution 5 (0.01-0.02 M ethylenediamine) using forward pulse and forward + reverse pulse.



The x-ray diffraction results for deposits plated from solutions 5, 7, 8 and 9, containing varying amounts of $\text{SnCl}_2 \cdot 2\text{H}_2\text{O}$ are given in Table 6-4, and the normalized peak intensity ratios for the AuSn phase are plotted in Figure 6-27. The general trend is for the decrease of preferred orientation with an increase in current density, which is consistent with the structures observed for all the solutions. The data is confusing when comparing the amount of preferred orientation at 2.4 mA/cm^2 with the structures observed in Figure 6-24. The deposit plated from the solution containing $3 \text{ g/l SnCl}_2 \cdot 2\text{H}_2\text{O}$ has the highest degree of preferred orientation, followed by the deposit plated from the solution containing $2 \text{ g/l SnCl}_2 \cdot 2\text{H}_2\text{O}$.

The structures observed (Figure 6-24(c,d)) show a UD three-dimensional nucleation type structure with large 2-3 μm diameter discs protruding from the deposit. It is possible that these protruding discs have a similar orientation even though they are made up of a large number of small grains, and this is affecting the preferred orientation. Figure 6-23(c,d) shows plan view images of the deposits in question, and it can be observed that there are a large number of closely packed discs making up the deposit plated from the solution containing 3 g/l $\text{SnCl}_2 \cdot 2\text{H}_2\text{O}$. There are relatively fewer discs protruding from the surface of the deposit plated from the solution containing 2 g/l $\text{SnCl}_2 \cdot 2\text{H}_2\text{O}$, matching the decrease in preferred orientation observed. The preferred orientation in the case of deposits formed from solutions with varying $\text{SnCl}_2 \cdot 2\text{H}_2\text{O}$ content cannot be used to predict the type of structure which forms, but only the amount of repetition within the structure type which does form.

Figure 6-27 Normalized intensity ratio of the AuSn phase versus current density for deposits electroplated from solutions with varying $\text{SnCl}_2 \cdot 2\text{H}_2\text{O}$ content.

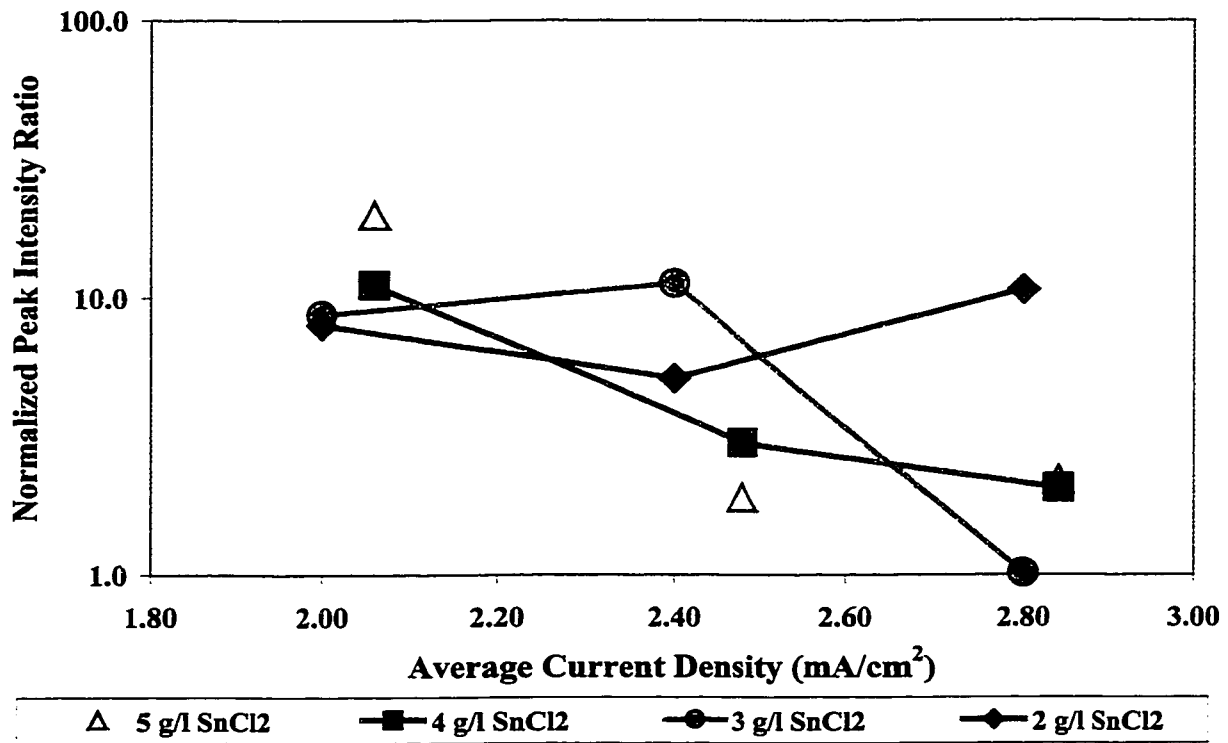


Table 6-4 Phases and orientation for deposits plated from solutions with varying SnCl₂-2H₂O concentrations.

5 g/l SnCl ₂				4 g/l SnCl ₂				3 g/l SnCl ₂				2 g/l SnCl ₂			
Current Density (mA/cm ²)	Sn Content (at.%)	Phases and Orient.	Norm. Int. Ratio	Current Density (mA/cm ²)	Sn Content (at.%)	Phases and Orient.	Norm. Int. Ratio	Current Density (mA/cm ²)	Sn Content (at.%)	Phases and Orient.	Norm. Int. Ratio	Current Density (mA/cm ²)	Sn Content (at.%)	Phases and Orient.	Norm. Int. Ratio
2.06	45.4	AuSn 110 AuSn 210	20.0	2.0	48.3	AuSn 110 AuSn 210	11.1	2.0	46.9	AuSn 110 AuSn 210	8.7	2.0	37.7	AuSn 110 AuSn 210 Au ₅ Sn 006 Au ₅ Sn 110	8.0
2.48	47.9	AuSn 300 AuSn 110	1.9	2.4	48.6	AuSn 112 AuSn 212	3.0	2.4	42.8	AuSn 110 AuSn 210 Au ₅ Sn 006 Au ₅ Sn 113	11.3	2.4	34.8	AuSn 110 AuSn 300 Au ₅ Sn 006 Au ₅ Sn 110	5.1
2.84	50.3	AuSn 110 AuSn 212	2.2	2.8	49.2	AuSn 212 AuSn 110	2.1	2.8	42.3	AuSn 110 AuSn 210 Au ₅ Sn 110 Au ₅ Sn 223	1.0	2.8	30.0	AuSn 110 AuSn 210 Au ₅ Sn 006 Au ₅ Sn 113	10.8
											1.56				2.3

6.5 Summary

The addition of ethylenediamine to the Au-Sn plating solution increases the stability of the plating solution as well as the plating rate, which is a step forward in the development of the current plating solution. The downside to this is that the roughness of the coating increases as the ethylenediamine concentration increases. At ethylenediamine concentrations of 0.11 M plating Au-Sn solder becomes unfeasible due to hydrogen reduction at the cathode. Decreasing the $\text{SnCl}_2 \cdot 2\text{H}_2\text{O}$ concentration in the plating solution leads to a decrease in the Sn concentration in the deposit. At a $\text{SnCl}_2 \cdot 2\text{H}_2\text{O}$ concentration of 2 g/l, the Sn concentration in the deposit is 30-35 at.%, which is the desired range if the deposit is to be soldered. Again, the reduction of $\text{SnCl}_2 \cdot 2\text{H}_2\text{O}$ concentration comes with the cost of increased coating roughness.

With an ethylenediamine concentration of 0.01-0.02 M, a $\text{SnCl}_2 \cdot 2\text{H}_2\text{O}$ of 2 g/l and a current density between 2.0 and 2.8 mA/cm^2 it is possible to produce near-eutectic composition deposits. Unfortunately the deposit produced has a roughness unsuitable for the application desired, so other plating parameters not studied in this thesis need to be changed in order to produce a more uniform deposit. The change in solution stability with the addition of 0.01-0.02 M ethylenediamine to the plating solution is small, with the bath life increasing from 15 to 17 days.

In order to produce uniform deposits using a more stable solution, the base solution should contain 0.05-0.06 M ethylenediamine, giving a solution stability of 22 days. Then the pulse parameters should be varied in order to give a smoother deposit without affecting the composition. A shorter ON time would most likely lead to a finer deposit without a great change in the deposit composition. The next parameters to vary would be solution agitation, as an increase in this value would lead to a smaller diffusion layer resulting in an increase in plating rate without a large sacrifice in roughness.

7 Conclusions and Recommendations

7.1 Conclusions

- i. The addition of ethylenediamine to the gold-tin alloy plating solution increases the stability of the solution by forming a complex ion with the existing gold-chloride or gold-sulfite complex in solution. The addition of up to 0.05-0.06 M ethylenediamine also increases the polarization for the reduction of tin at the cathode surface, decreasing the current density at which tin is deposited as well as decreasing the current density at which hydrogen reduction begins. There is then a trade-off between the stability of the solution and the range of current densities available for gold-tin alloy plating when ethylenediamine is added to the electroplating solution.
- ii. The addition of both NiCl_2 and ethylenediamine leads to the incorporation of nickel in the deposit, as ethylenediamine depolarizes the nickel reduction reaction into the range of gold and tin reduction.
- iii. As the concentration of ethylenediamine in the gold-tin plating solution increases, the resulting structure formed at a constant current density becomes rougher, as an increase in ethylenediamine concentration also results in an increase of the polarization and a reduction of the limiting current density promoting three-dimensional nucleation at a lowered current density.
- iv. A decrease in the $\text{SnCl}_2 \cdot 2\text{H}_2\text{O}$ concentration in the plating solution results in a coarser structure at a constant current density.
- v. The addition of ethylenediamine to the plating solution leads to a loss of preferred orientation in the deposit, matching the switch of the growth mechanism from two-dimensional to three-dimensional nucleation, which occurs near the limiting current density.

7.2 Recommendations for Future Research

The research of gold-tin alloy plating for this thesis project has answered some questions about the effects of the addition of ethylenediamine and tin concentration on the solution stability, electroplating parameters, composition and structure of the deposits. Upon the completion of this work, many more questions have been raised about gold-tin electroplating, which may serve as a basis for future experimentation.

7.2.1 Solution Development

- i. The stability and polarization of different gold complexes could be studied. The current complex is most likely gold-sulfite-ethylenediamine, which could be verified by changing the order of addition of the ethylenediamine and sulfite in the solution preparation. A gold-chloride-ethylenediamine complex could also be prepared by leaving sodium sulfite out of the solution.
- ii. The stability and polarization of solutions prepared using $\text{SnCl}_4 \cdot 5\text{H}_2\text{O}$ should be studied. The stability of the electroplating solution could increase by using tin(IV) instead of tin(II), as the oxidation of tin(II) to tin(IV) may be responsible for the reduction of the gold complex, which is currently the limiting factor in the solution stability. One drawback could be that gold-tin alloy plating may not be possible from a solution containing tin(IV).
- iii. Polarization tests should be carried out for the solutions which contain varying amounts of $\text{SnCl}_2 \cdot 2\text{H}_2\text{O}$, in order to see if a decrease in $\text{SnCl}_2 \cdot 2\text{H}_2\text{O}$ concentration results in increased polarization and lowered limiting current density.
- iv. Polarization and stability tests should be carried out on solutions containing higher gold and tin concentrations. If the stability is acceptable, the higher metal ion concentrations would most likely reduce the polarization, allowing for a higher plating rate and a larger range of current densities from which plating is possible. This would counter the decrease in polarization introduced by the ethylenediamine.

7.2.2 Deposit Composition and Structure

- i. A series of plating experiments could be made with the gold-tin plating solution and varying the age of the solution. The first test could be made on a solution immediately following preparation, the next test on a solution 1 day old, the next on a solution 2 days old and so on. The idea of this experiment would be to see if the tin concentration and plated thickness of the deposit decrease with time because of the oxidation of Sn^{2+} to Sn^{4+} .
- ii. In future work on preferred orientation, a number of x-ray diffraction tests should be done on each deposit in order to get more accurate results. More x-ray diffraction work needs to be done on the deposits plated from the solutions containing varied $\text{SnCl}_2 \cdot 2\text{H}_2\text{O}$ concentrations.
- iii. A series of plating runs should be made at current densities ranging between 0.2 and 3.6 mA/cm^2 , giving the full range of plating current densities. The advantage of this would be that the microstructures and the orientation for the low current densities ($0.2 - 1.2 \text{ mA/cm}^2$) could be studied in order to better understand the growth mechanisms for the Au_5Sn phase.
- iv. The effects of agitation and temperature on the microstructure of the deposit should be studied in order to confirm the effect of the ratio of the current density to the limiting current density on the microstructure produced.
- v. Transmission electron microscope (TEM) studies could be made to better understand the plated structures by studying the orientation of individual grains, especially in the deposits containing the protruding disc shapes plated from solutions containing 2-3 g/l $\text{SnCl}_2 \cdot 2\text{H}_2\text{O}$.
- vi. In order to obtain more consistent structures from the solutions containing 2-3 g/l $\text{SnCl}_2 \cdot 2\text{H}_2\text{O}$, the pulse parameters should be varied.

7.2.3 Miscellaneous

- i. With the possibility of being able to consistently plate only the AuSn phase, AuSn can be plated onto a gold substrate in order to create diffusion couples to study the gold-rich portion of the gold-tin phase diagram.

8 References

- [Avila86] A. J. Avila, 'Pulse Electrodeposition of Alloys', Chapter 11 in Theory and Practice of Pulse Plating, J.-C. Puipe & F. Leaman eds., American Electroplaters & Surface Finishers Society, Orlando (1986) pp. 189-208.
- [Barnes60] S. C. Barnes, G. G. Storey & H. J. Pick, 'The Structure of Electrodeposited Copper – III', *Electrochimica Acta*, **2** (1960), pp. 195-206.
- [Bradford93] S. A. Bradford, Corrosion Control, Van Nostrand Reinhold, New York (1993) pp. 33-46.
- [Brenner63] A. Brenner, Electrodeposition of Alloys, Principles and Practice, Academic Press, New York (1963) pp. 75-121.
- [Buene80] L. Buene, H. Falkenberg-Arell & J. Taftø, 'A Study of Evaporated Gold-Tin Films Using Transmission Electron Microscopy', *Thin Solid Films*, **65** (1980) p. 247-257.
- [Burton49] W. K. Burton, K. Cabera & F. C. Frank, 'Role of Dislocation in Crystal Growth', *Nature*, **163** (1949), pp. 398-399.
- [Catonne84] J. C. Catonne, J. D. Jehanno & J. Royon, 'Optimization of the Brillancy of Gold Silver Alloy Plating by Pulse Plating', *Proceedings of Interfinish 84, 11th World Congress on Metal Finishing*, Jerusalem, Israel (1984) pp. 191-196.
- [Chassaing89] E. Chassaing, K. Vu Quang & R. Wiat, 'Mechanism of Nickel-Molybdenum Alloy Electrodeposition in Citrate Electrolytes', *Journal of Applied Electrochemistry*, **19** (1989) pp. 839-843.
- [Cheh71] H. Y. Cheh, 'Electrodeposition of Gold by Pulsed Current', *Journal of the Electrochemical Society*, **118(4)** (1971) pp. 551-557.
- [Chen89] C. J. Chen & C. C. Wan, 'Crystal Orientation of Pb/Sn Alloy Deposit Under Pulse Current Condition', *Bulletin of Electrochemistry*, **5(1)** (1989), pp. 11-16.

- [Ciulik93] J. Ciulik & M. R. Notis, 'The Au-Sn Phase Diagram', *Journal of Alloys and Compounds*, **191** (1993) pp. 71-78.
- [Daebler91] D. H. Daebler, 'An Overview of Gold Intermetallics in Solder Joints', *Surface Mount Technology*, **6** (1991) pp 43-46.
- [Duffek73] E. F. Duffek, 'The State of Gold Plating in the Semiconductor and Microelectronics Industry', *Plating in the Electronic Industry, 4th Symposium*, Indianapolis (1973) pp. 194-208.
- [Fisher54] H. Fisher, Elektrolytische Abscheidung und Elektrokristallisation von Metallen, Springer Verlag, Berlin (1954).
- [Gabe78] D. R. Gabe, Principles of Metal Surface Treatment and Protection, 2nd edition, Pergamon Press, New York (1978) pp.29-79.
- [Holmbom98] G. Holmbom, J. A. Abys, H. K. Straschil & M. Sveinsson, 'Electrodeposition, Growth Morphology & Melting Characteristics of Gold-Tin Alloys', *Plating and Surface Finishing*, **85(4)** (1998), pp.66-73.
- [Ivey98] D. G. Ivey, 'Microstructural Characterization of Au/Sn Solder for Packaging in Optoelectronic Applications', *Micron and Microscopica Acta*, **29** (1998) pp. 281-287.
- [Jan63] J.-P. Jan, W. B. Pearson, A. Kjekshus & S. B. Woods, 'On the Structural, Thermal, Electrical and Magnetic Properties of AuSn', *Canadian Journal of Physics*, **41** (1963) pp. 2252-2266.
- [Kallmayer96] C. Kallmayer, H. Oppermann, G. Engelmann, E. Zakel & H. Reichl, 'Self-Aligning Flip-Chip Assembly Using Eutectic Gold/Tin Solder in Different Atmospheres', *1996 IEEE/CPMT Int'l Electronics Manufacturing Symposium*, (1996) pp. 18-25.
- [Katz94] A. Katz, C. H. Lee & K. L. Tai, 'Advanced Metallization Schemes for Bonding of InP-based Laser Devices to CVD-diamond Heatsinks', *Materials Chemistry and Physics*, **37** (1994) pp. 303-328.

- [Keshner89] T. D. Keshner, Yu. P. Khodyrev & S. I. Berezina, 'Composition and Properties of Zinc-Nickel Alloys from Ethylenediamine Electrolytes', *Protection of Metals*, **25(1)** (1989) pp. 129-132.
- [Kim96] J. H. Kim, M. S. Suh & H. S. Kwon, 'Effects of Plating Conditions on the Microstructure of 80Sn-20Pb Electrodeposits from an Organic Sulphonate Bath', *Surface and Coatings Technology*, **78** (1996), pp. 56-63.
- [Lainer70] V. I. Lainer, *Modern Electroplating*, Keter Press, Jerusalem (1970), pp. 3-56.
- [Landolt94] D. Landolt, 'Electrochemical and Materials Science Aspects of Alloy Deposition', *Electrochimica Acta*, **39** (1994) pp. 1075-1090.
- [Laude80] P. Laude, E. Marka & F. Zuntini, US Patent 4,192,723, Mar. 11, 1980.
- [Lee91] C. C. Lee, C. Y. Wang & G. S. Matijasevic, 'A New Bonding Technology Using Gold and Tin Multilayer Composite Structures', *IEEE Transactions Comp. Hybrids, Manufacturing Technology*, **14** (1991) pp. 407-412.
- [Lee94] Y. C. Lee & N. Basavanhally, 'Solder Engineering for Optoelectronic Packaging', *JOM*, **46(2)** (1994) pp. 46-48.
- [Leidheiser73] H. Leidheiser Jr. & A. R. P. Ghuman, 'Pulse Electroplating of Silver-Tin Alloys and the Formation of Ag₃Sn', *Journal of the Electrochemical Society*, **120(4)** (1973) pp. 484-487.
- [McMullen59] J. J. McMullen & N. Hackerman, 'Capacities of Solid Metal-Solution Interfaces', *Journal of the Electrochemical Society*, **106** (1959) pp. 341-346.
- [Matijasevic93] G. S. Matijasevic, C. C. Lee & C. Y. Wang, 'Au-Sn alloy phase diagram and properties related to its use as a bonding medium', *Thin Solid Films*, **223** (1993) pp. 276-287.
- [Matlosz93] M. Matlosz, 'Competitive Adsorption Effects in the Electrodeposition of Iron-Nickel Alloys', *Journal of the Electrochemical Society*, **140(8)** (1993) pp. 2272-2279.

- [Miller69] L. F. Miller, 'Controlled Collapse Reflow Chip Joining', *IBM Journal of Research and Development*, **13** (1969) pp. 239-250.
- [Morrissey94] R. J. Morrissey, US Patent 5,277,790, Jan. 11, 1994.
- [Natarajan84] S. R. Natarajan, R. M. Krishnan, S. Sriveeraraghavan & H. V. K. Udupa, 'Stripping of Nickel Deposits with Ethylene Diamine', *Metal Finishing*, **82(12)** (1984), pp. 49-53.
- [Okamoto84] H. Okamoto & T. B. Massalski, 'The Au-Sn (Gold-Tin) System', *Bulletin of Alloy Phase Diagrams*, **5(5)** (1984) pp. 492-503.
- [Okamoto93] H. Okamoto, 'Au-Sn(Gold-Tin)', *Journal of Phase Equilibria*, **14(6)** (1993) pp. 765-766.
- [O'Keefe78] T. J. O'Keefe & I. R. Hurst, 'The Effect of Antimony, Chloride Ion, and Glue on Copper Electrorefining', *Journal of Applied Electrochemistry*, **8** (1978), p. 109.
- [Osada74] K. Osada, S. Yamaguchi & M. Hirabayashi, 'An Ordered Structure of Au₅Sn', *Transactions of the Japan Institute of Metals*, **15** (1974), p. 256.
- [Pesco88] A. M. Pesco & H. Y. Cheh, 'Current and Composition Distributions during the Deposition of Tin-Lead Alloys on a Rotating Disk Electrode', *Journal of the Electrochemical Society*, **135(7)** (1988) pp. 1722-1726.
- [Pick55] H. J. Pick, *Nature*, **176** (1955), p. 693.
- [Pick60] H. J. Pick, G. G. Storey & T. B. Vaughan, 'The Structure of Electrodeposited Copper - I', *Electrochimica Acta*, **2** (1960), pp. 165-178.
- [Plumbridge96] W. J. Plumbridge, 'Solders in Electronics', *Journal of Materials Science*, **31** (1996), pp. 2501-2514.
- [Puiippe86] J.-C. Puiippe, 'Influence of Charge and Discharge of Electrical Double Layer in Pulse Plating', Chapter 4 in Theory and Practice of Pulse Plating, J.-C. Puiippe & F. Leaman eds., American Electroplaters & Surface Finishers Society, Orlando (1986) pp. 41-54.

- [Safranek88] W. H. Safranek, 'Deposit Disparities', *Plating & Surface Finishing*, **75(6)** (1988), p. 10.
- [Schalch76] E. Schalch, M. J. Nicol, J. W. Diggle, B. D. Charlton & J. P. H. Vaessen, 'The Cathodic Deposition of Gold', report 1848, National Institute for Metallurgy, Randburg South Africa, July 7, 1976, 41 pages.
- [Schubert59] K. Schubert, H. Breimer & R. Gohle, 'The Structures of the Systems Gold-Indium, Gold-Tin, Gold-Indium-Tin and Gold-Tin-Antimony', *Zeitschrift für Metallkunde*, **50(3)** (1959) pp. 146-153.
- [Seiter60] H. Seiter, H. Fisher & L. Albert, *Electrochimica Acta*, **2** (1960), p. 97.
- [Smith86] R. W. Smith, 'The α (Semiconductor) \leftrightarrow β (Metal) Transition in Tin', *Journal of the Less Common Metals*, **114** (1986) pp. 69-80.
- [Stanley87] G. G. Stanley, Chapter 15 in The Extractive Metallurgy of Gold in South Africa, Volume 2, The South African Institute of Mining and Metallurgy (1987) p. 842.
- [Swanson57] H. E. Swanson, N. T. Gilfrich & M. I. Cook, 'Standard X-ray Powder Diffraction Patterns', *National Bureau of Standards Circular 539*, **7** (1957), p. 19.
- [Sun99-1] W. Sun & D. G. Ivey, 'Microstructural Study of Co-electroplated Au/Sn Solder for Semiconductor Packaging Applications', *Journal of Materials Science*, submitted April 1999, 26 manuscript pages.
- [Sun99-2] W. Sun & D. G. Ivey, 'Development of an Electroplating Solution for Codepositing Au-Sn Alloys', *Materials Science and Engineering B*, in press (1999), 12 proof pages.
- [Tan93] A. C. Tan, Chapter 2 in Tin and Solder Plating in the Semiconductor Industry, Chapman & Hall, 1993, pp.21-63.
- [Thorpe50] J. F. Thorpe & M. A. Whiteley, Thorpe's Dictionary of Applied Chemistry, 4th edition, vol. VI, Longmans, Green & Co., New York, pp. 111-113.

- [Tsai91] R. Y. Tsai & S. T. Wu, 'Influence of Pulse Plating on the Crystal Structure and Orientation of Chromium', *Journal of the Electrochemical Society*, **138(9)** (1991), pp. 2622-2626.
- [Vaughan60] T. B. Vaughan & H. J. Pick, 'The Structure of Electrodeposited Copper – II', *Electrochimica Acta*, **2** (1960), pp. 179-194.
- [Wagner38] C. Wagner & W. Traud, *Zeitschrift für Elektrochem.*, **44** (1938), p. 391.
- [Winand75] R. Winand, 'Electrocrystallization of Copper', *Transactions of the Institution of Mining and Metallurgy*, **84** (1975), pp. C67-C75.
- [Winand94] R. Winand, 'Electrodeposition of Metals and Alloys – New Results and Perspectives', *Electrochimica Acta*, **39** (1994), pp. 1091-1105.
- [Ye92] X. Ye, M. De Bonte & J. R. Roos, 'Role of Overpotential on Texture, Morphology and Ductility of Electrodeposited Copper Foils for Printed Circuit Board Applications', *Journal of the Electrochemical Society*, **139(6)** (1992), pp. 1592-1600.
- [Ying88] R. Y. Ying, 'Electrodeposition of Copper-Nickel Alloys from Citrate Solutions on a Rotating Disk Electrode', *Journal of the Electrochemical Society*, **135(12)** (1988) pp. 2957-2964.
- [Yost90] F. G. Yost, M. M. Karnowski, W. D. Drotning & J. H. Gieske, 'Thermal Expansion and Elastic Properties of High Gold-Tin Alloys', *Metallurgical Transactions A*, **21A** (1980) pp. 1885-1889.
- [Zuntini74] F. Zuntini, G. Aliprandini, J-M. Gioria, A. Meyer & S. Losi, US Patent 3,787,463, Jan. 22, 1974.